

Extraction of *Curcuma longa* L. with supercritical CO₂

Dissertation

der Mathematisch-Naturwissenschaftlichen Fakultät
der Eberhard Karls Universität Tübingen
zur Erlangung des Grades eines
Doktors der Naturwissenschaften
(Dr. rer. nat.)

vorgelegt von
Ann-Kathrin Widmann
aus Herrenberg

Tübingen
2023

Gedruckt mit Genehmigung der Mathematisch-Naturwissenschaftlichen Fakultät der
Eberhard Karls Universität Tübingen.

Tag der mündlichen Qualifikation:

12.03.2024

Dekan:

Prof. Dr. Thilo Stehle

1. Berichterstatter/-in:

Prof. Dr. Rolf Daniels

2. Berichterstatter/-in:

Prof. Dr. Dominique Lunter

*„Aber sieh, Heidi, man muss nicht alles nur so
hinnehmen, was einem ein Peter sagt, man muss
es selbst probieren.“*

from „Heidis Lehr- und Wanderjahre“ by Johanna Spyri*

DANKSAGUNG

An dieser Stelle möchte ich mich bei allen bedanken, die mich auf meinem Weg zur Erstellung dieser Arbeit direkt oder indirekt unterstützt haben.

Mein besonderer Dank gilt dabei Herrn Prof. Dr. Rolf Daniels, der nach dem Tod von Herrn Wahl wie selbstverständlich die Betreuung meiner Arbeit übernommen und mir so die Fertigstellung ermöglicht hat, auch wenn das Thema außerhalb seines eigenen Forschungsgebietes liegt.

Außerdem möchte ich mich noch besonders bei Herrn apl. Prof. Dr. Dietmar R. Kammerer für das Übernehmen der Zweitbetreuung und die fachliche Unterstützung bedanken.

Für das Teilen seiner Expertise und die geduldige Anleitung zur Selbsthilfe danke ich von ganzem Herzen Klaus Weyhing.

Bei Beat Zehnder möchte ich mich für die zahlreichen Telefonate und hilfreichen Tipps zur CO₂-Extraktion im Allgemeinen und zu unserer Anlage im Besonderen bedanken.

Lysanne Salomon und Peter Lorenz danke ich für die fachkundige Anleitung und Hilfe zur LCMS und GCMS Analytik. Und dem Zentrallaboratorium Deutscher Apotheker e.V. danke ich für die Unterstützung mit der Karl-Fischer-Analytik.

Darüber hinaus möchte ich mich bei Gavin und Andrea Skillicorn und vor allem bei Birgit Friedmann für die unverhoffte Hilfe zum Schluss bedanken.

Ich danke meiner Familie und meinen Freunden für die moralische Unterstützung und insbesondere für den seelischen Beistand in schwierigen Episoden.

Zu guter Letzt möchte ich mich bei meinen lieben Kollegen für 4 ½ ereignisreiche Jahre mit fantastischen Mittagspausen und leidenschaftlichen Diskussionen bedanken.

Es war mir eine Freude!

PUBLICATIONS AND PRESENTATIONS

PUBLICATION

Ann-Kathrin Widmann, Martin A. Wahl, Dietmar R. Kammerer, Rolf Daniels

Supercritical fluid extraction with CO₂ of *Curcuma longa* L. in comparison to conventional solvent extraction

Pharmaceutics. 2022. 14 (9), page 1943 (17).

DOI: 10.3390/pharmaceutics14091943

[1]

Parts of this thesis have already been published in Pharmaceutics. 2022. 14 (9), page 1943 (17) [1] as an open access article distributed under the terms and conditions of the Creative Commons Attribution (CC BY) license by MDPI (Basel, Switzerland).

PERSONAL CONTRIBUTION

Ann-Kathrin Widmann: Conceptualisation, investigation, methodology, data curation, writing - original draft, visualization

Martin A. Wahl: Conceptualisation

Dietmar R. Kammerer: Writing – review and editing

Rolf Daniels: Conceptualisation, methodology, writing - review and editing, resources, supervision, project administration

POSTER PRESENTATION

Ann-Kathrin Widmann, Martin A. Wahl, Dietmar R. Kammerer, Rolf Daniels

Supercritical fluid extraction with CO₂ of *Curcuma longa* L. in comparison to solvent extracts

13th World Meeting on Pharmaceutics, Biopharmaceutics and Pharmaceutical Technology

28-31 March 2022 / Rotterdam

PERSONAL CONTRIBUTION

Ann-Kathrin Widmann: Conceptualisation, investigation, methodology, data curation, writing - original draft, visualization

Martin A. Wahl: Conceptualisation

Dietmar R. Kammerer: Writing – review and editing

Rolf Daniels: Conceptualisation, methodology, writing - review and editing, resources, supervision, project administration

SPECIAL NOTES

Legally protected trademarks are used without special identification.

SUMMARY

Curcuma longa L. is a traditional medicinal plant and spice containing a variety of lipophilic active substances with promising therapeutic properties [1]. For the purpose of this thesis, in a pressure and temperature range of 75–425 bar and 35–75 °C, the solvent properties of supercritical carbon dioxide were investigated when dried and milled *Curcuma longa* L. rhizomes were extracted [1]. The three main curcuminoids (curcumin, demethoxycurcumin, and bisdemethoxycurcumin) together with the three main constituents of the essential oil (α -turmerone, β -turmerone, and γ -turmerone) were analysed in the resulting extracts [1]. For statistical evaluation, experiments were performed employing a full factorial design, in which flow rate, extraction time, and drug load were kept constant [1]. Within the given conditions, the experimental design revealed an optimum yield of all aforementioned substances when supercritical carbon dioxide extraction was performed at 425 bar and 75 °C [1]. For comparison, solvent extracts using methanol and *n*-hexane were prepared and their main components were characterized using LC-MS and GC-MS [1]. The stability of the extracts was monitored during storage for 6 months at 22 and 40 °C under protection from light [1]. The decomposition of individual compounds was mainly observed in the presence of residual water in the extracts [1].

The second part of this thesis was the development of a stable hard capsule formulation with the resulting supercritical carbon dioxide extract of *Curcuma longa* L. with optimum yield at 425 bar and 75 °C. Freeze drying of the supercritical carbon dioxide extract was found to increase the compatibility of the extract with the hard gelatine capsule shell. 4 matrix formulations based on hard fat (with and without surface active additives), polyethylene glycol 4000, and mesoporous silica particles were loaded with the freeze-dried extract, and the extract loading capacity was determined. The mesoporous silica particle revealed the highest extract loading capacity (64%) followed by the polyethylene glycol matrix (57%) and the hard fat (19-25%). Storage trials of the developed hard capsule formulations, with extract concentrations 5% below these loading capacities were carried out for 3 months at 22 °C and at temperature cycle. A decrease in concentrations of individual extract compounds was noted especially in the hydrophilic matrix formulations based on polyethylene glycol 4000 and mesoporous silica.

ZUSAMMENFASSUNG

Curcuma longa L. ist eine traditionelle Heil- und Gewürzpflanze, die eine Vielzahl von lipophilen Wirkstoffen mit vielversprechenden therapeutischen Eigenschaften enthält [1]. In dieser Arbeit wurden die Lösungsmittleigenschaften von überkritischem Kohlenstoffdioxid in einem Druck- und Temperaturbereich von 75-425 bar und 35-75 °C bei der Extraktion von getrockneten und gemahlten *Curcuma longa* L.-Rhizomen untersucht [1]. Die resultierenden Extrakte wurden auf die drei Hauptcurcuminoide, nämlich Curcumin, Demethoxycurcumin und Bisdemethoxycurcumin zusammen mit den drei Hauptkomponenten des ätherischen Öls, d.h. α -Turmeron, β -Turmeron und γ -Turmeron hin analysiert [1]. Für die statistische Auswertung wurden Experimente unter Verwendung eines vollfaktoriellen Versuchsdesigns durchgeführt, bei dem Durchflussrate, Extraktionszeit und Drogenmenge konstant gehalten wurden [1]. Unter den gegebenen Bedingungen ergab das Versuchsdesign eine optimale Ausbeute aller oben genannten Substanzen, wenn die Extraktion mit überkritischem Kohlenstoffdioxid bei 425 bar und 75 °C durchgeführt wurde [1]. Zum Vergleich wurden Lösungsmittlextrakte mit Methanol und *n*-Hexan hergestellt und deren Hauptbestandteile mittels LC-MS und GC-MS charakterisiert [1]. Die Stabilität der Extrakte wurde nach 6-monatiger Lagerung bei 22 und 40 °C unter Lichtschutz überwacht [1]. Die Zersetzung der einzelnen Verbindungen wurde hauptsächlich in Anwesenheit von Restwasser in den Extrakten beobachtet [1].

Der zweite Teil der Arbeit war die Entwicklung einer stabilen Hartkapselformulierung mit dem erhaltenen überkritischen Kohlenstoffdioxid-Extrakt aus *Curcuma longa* L. mit optimaler Ausbeute bei 425 bar und 75 °C. Es wurde festgestellt, dass die Gefriertrocknung des überkritischen Kohlenstoffdioxid-Extrakts die Verträglichkeit des Extrakts mit der Hartgelatinekapselfülle erhöht. 4 Matrixformulierungen auf der Basis von Hartfett (mit und ohne oberflächenaktive Zusätze), Polyethylenglykol 4000 und mesoporösen Silikapartikeln wurden mit dem gefriergetrockneten Extrakt beladen und die Extrakt- Beladungskapazität wurde bestimmt. Die mesoporösen Silikapartikel wiesen mit 64 % die höchste Extrakt-Beladungskapazität auf, gefolgt von der Makrogolmatrix (57 %) und dem Hartfett (19-25 %). Lagerungsversuche der entwickelten Kapselformulierungen mit Extrakt-Konzentrationen, die 5% unter den gefundenen Beladungskapazitäten lagen, wurden für 3 Monate bei 22 °C und

Temperaturwechsel durchgeführt. Insbesondere in den hydrophilen Matrixformulierungen auf Basis von Polyethylenglykol 4000 und mesoporösem Siliciumdioxid wurde eine Abnahme der Konzentrationen der einzelnen Extrakt-Komponenten festgestellt.

TABLE OF CONTENTS

Danksagung.....	I
Publications and Presentations	II
Special Notes	III
Summary.....	IV
Zusammenfassung.....	V
Table of Contents.....	VII
Abbreviations.....	X
1. Introduction.....	1
1.1. Curcuma longa L.....	1
1.2. Supercritical CO ₂ (scCO ₂) Extraction.....	7
1.3. Capsule Formulations	13
1.3.1. Hard Capsules.....	15
1.3.2. Hard Fat.....	17
1.3.3. Polyethylene Glycol.....	20
1.3.4. Silica Carrier Systems	22
1.4. Aim	24
2. Material and Methods.....	25
2.1. Material	25
2.1.1. Chemicals	25
2.1.2. Consumables.....	26
2.1.3. Devices and Software	28
2.2. Methods.....	31
2.2.1. Preparation of Drug Material.....	31
2.2.2. Solvent Extraction	31
2.2.3. Supercritical Fluid Extraction	32
2.2.4. Experimental Design	34
2.2.5. Extract Stability Study	35

2.2.6.	Liquid Chromatography with Mass Spectrometric Detection (LC-MS).....	36
2.2.7.	High Performance Liquid Chromatography with Diode Array Detection (HPLC-DAD).....	37
2.2.8.	Gas Chromatography with Mass Spectrometric Detection (GC-MS)	38
2.2.9.	Karl Fischer Titration	39
2.2.10.	Freeze Drying of scCO ₂ Extracts.....	40
2.2.11.	Loading and Determination of Extract Loading Capacity	41
2.2.11.1.	Screening of the Extract Loading Capacity of Hard Fat and Macrogol	42
2.2.11.2.	Semi-Quantitative Determination of Extract Loading Capacity of Hard Fat and Macrogol	42
2.2.11.3.	Determination of Extract Loading Capacity of Aeroperl Carriers	43
2.2.12.	Polarization Microscopy	43
2.2.13.	Sample Preparation for Quantification via High Performance Liquid Chromatography	44
2.2.13.1.	Macrogol (Polyethylene Glycol 4000) Matrix Systems	44
2.2.13.2.	Hard Fat Matrix Systems	44
2.2.13.3.	Aeroperl 300 Carrier Systems	44
2.2.14.	Preparation of Capsule Formulations.....	45
2.2.14.1.	Macrogol (Polyethylene Glycol 4000) Matrix System	45
2.2.14.2.	Hard Fat Matrix Systems	45
2.2.14.3.	Aeroperl 300 Carrier System	45
2.2.15.	Stability Study of Capsule Formulations.....	47
2.2.16.	Uniformity of Dosage Units According to Ph. Eur. 2.9.40	48
2.2.16.1.	Mass Variation Test.....	48
2.2.16.2.	Content Uniformity Test	49
3.	Results and Discussion	50
3.1.	Phytochemical Characterization of Solvent Extracts of <i>Curcuma longa</i> L. ...	50

3.1.1.	Liquid Chromatography with Mass Spectrometric Detection (LC-MS)....	50
3.1.2.	Gas Chromatography with Mass Spectrometric Detection (GC-MS)	52
3.2.	Comparison of scCO ₂ Extraction and Conventional Solvent Extraction	54
3.2.1.	Loss of Extract in the Plant: Extraction of already scCO ₂ Extracted Drug with Methanol	54
3.2.2.	ScCO ₂ Extraction According to Experimental Design.....	57
3.2.3.	Comparison of scCO ₂ Extraction and Conventional Solvent Extraction .	61
3.2.4.	Water Content in Extracts.....	62
3.3.	Stability Study of Extracts	63
3.4.	Development of Capsule Formulations with scCO ₂ Curcuma Extract.....	72
3.4.1.	Compatibility of Components for Capsule Formulations	72
3.4.2.	Loading and Characterisation of Matrix Systems	73
3.4.3.	Microscopic Characterisation of Melt Matrix Systems	78
3.4.4.	Uniformity of Dosage Units According to Ph. Eur. 2.9.40	82
3.4.4.1.	Uniformity of Dosage Units: Mass variation	83
3.4.4.2.	Uniformity of Dosage Units: Content Uniformity	83
3.5.	Stability Study of Capsule Formulations with scCO ₂ Extract	85
4.	Summary and Conclusion	96
5.	Indices.....	98
5.1.	List of Figures	98
5.2.	List of Tables.....	101
5.3.	List of Equations.....	102
5.4.	References.....	103
6.	Appendix.....	124
6.1.	Supercritical Fluid Extraction According to Experimental Design	124
6.2.	Compositions of Capsule Formulations.....	125

ABBREVIATIONS

%	Percent
% r.h.	Percent relative Humidity
°C	Degree Celsius
Ø	Diameter
"	Inch
xg	Multiples of gravity
Å	Angstrom
Alu	Aluminium
AP	Atmospheric Pressure
APCI	Atmospheric Pressure Chemical Ionization
API	Active Pharmaceutical Ingredient
AV	Acceptance Value
bar	Bar
BDMC	Bisdemethoxycurcumin
c	concentration
CU	Content Uniformity
D	Density
DAC/NRF	Deutscher Arzneimittel-Codex/ Neues Rezeptur-Formularium
DAD	Diode Array Detector
DMC	Demethoxycurcumin
DoE	Design of Experiments
e.g.	Exempli gratia; for example
etc.	Et cetera; and other similar things
EMA	European Medicines Agency
eV	Electronvolt

FDA	Food and Drug Administration
g, kg, mg, μg	Gram, kilogram, milligram, microgram
GCMS	Gas Chromatography Mass Spectrometry
h	Hour
H	Enthalpy
HMPC	Committee on Herbal Medicinal Products
HPLC	High Performance Liquid Chromatography
i.e.	Id est; that means
IUPAC	International Union of Pure and Applied Chemistry
K	Kelvin
kcal	Kilocalories
kJ	Kilojoule
L, mL, μL	Litre, millilitre, microlitre
LCMS	Liquid Chromatography Mass Spectrometry
log	Decadic logarithm
m/z	Mass to Charge Ratio
m, mm, μm , nm	Metre, millimetre, micrometre, nanometre
min	Minute
mol	Mol
MS	Mass Spectrometry
MV	Mass Variation
n	Number of Experiments
no.	Number
p	Pressure
P_c	Critical Pressure
PE	Polyethylene
PEG	Polyethylene glycol, Macrogol

pH	Negative log of activity of hydrogen ions
Ph. Eur.	European Pharmacopoeia
psi	Pound-force per square inch (1 psi = 0.07 bar)
pulv. subt.	pulveratus subtilis, finely powdered
ref.	reference
RP	Reverse Phase
rpm	Revolutions per Minute
R _t	Retention Time
RT	Room Temperature
s	Seconds
S	Entropy
scCO ₂	Supercritical Carbon Dioxide
sd	Standard Deviation
SEM	Scanning Electron Microscopy
T	Temperature
TAG	Triacyl Glycerol
TC	Temperature Cycle
T _c	Critical Temperature
TIC	Total Ion Current
USP/NF	United States Pharmacopeia/ National Formulary
UV	Ultraviolet
v	Volume
w	Weight
WHO	World Health Organisation
\bar{w}	Mean weight
λ	Wavelength

1. INTRODUCTION

1.1. CURCUMA LONGA L.

Turmeric or *Curcuma longa* L. is a traditional medicinal plant and spice from southern and south-eastern Asia. Botanically it belongs to the family of Zingiberaceae and the mainly used parts of the plant are the rhizomes [2]. Figure 1 shows a drawing of the plant *Curcuma longa* L. [3], which exhibits wide phenotypic and genotypic variation [4,5]. The parts of interest, the rhizomes, are oblong, branched, and yellow to dark orange in colour. They contain many lipophilic active substances with promising therapeutic properties and before use or further processing, they are usually dried and ground but can be used fresh as well.



Figure 1 Schematic painting of *Curcuma longa* L. [3].

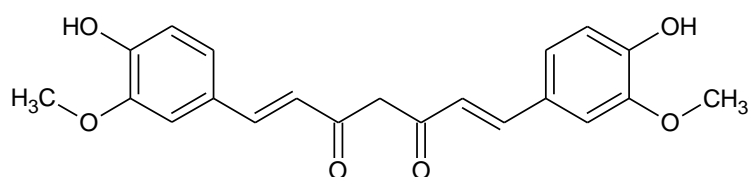
Initially, turmeric was used as a dye due to the bright yellow colour of the rhizomes, but later also found its way into religious ceremonies of Hinduism and Buddhism, medicine, cosmetics and food [5]. Besides being used today in nutrition and cosmetics [6], powdered turmeric continues to be a home remedy and traditional medicinal plant in south-east Asia [2,7]. Not only should it be part of the daily Asian diet, but considering the benefits every food should contain it [2,7]. Traditionally it is considered to be stimulating, carminative, blood purifying and aids if externally applied on stains, wounds and injuries [8]. Moreover, it is used against chest and abdominal distension, rheumatic disease, menstrual irregularities and as an anthelmintic and antiparasitic agent on the skin [8]. Turmeric plays an important role in Ayurveda, where it is believed to balance the three states of disease and therefore is applied in different formulas against inflammations, pain, indigestions, insect bites or stings, and hysteria [9]. Additionally, current traditional Indian medical practice applies it against biliary disorders, anorexia, cough, diabetic wounds, hepatic disorders, rheumatism and sinusitis [5]. In traditional Chinese medical practice, turmeric is considered to cure inflammations, gastrointestinal diseases and infections [6]. The European Medicines Agency (EMA) describes the use of the drug *Curcumae longae rhizoma* and different extracts based on ethanolic extraction of the drug against dyspeptic complaints due to biliary dysfunction, liver and stomach disorders [10].

More recent investigations show evidence of the choloretic effect of aqueous suspensions of *Curcumae longae rhizoma* in mouse model [11] and hint at the antidepressant effect in mouse model due to a reduction of the decrease of neurotransmitters and the serotonin turnover and due to additional reversal of induced serum corticotropin-releasing factor and cortisol level [12]. Moreover, the ethanolic extract of *Curcuma longa* L. showed phytotoxic and antifungal properties, weak antibiotic activity against *Staphylococcus aureus* and cytotoxicity in brine shrimp bioassay [13]. Other results indicate antioxidant activity in atherosclerosis in rabbit model [14], cardioprotection and functional recovery in ischemia and reperfusion model of myocardial injury [15], inhibition and reversal of aflatoxin-induced liver damage [16], and the anti-diabetic effect of ethanolic and *n*-hexane extracts of turmeric in type 2 diabetic mice due to adipocyte differentiation [17,18]. Remarkably, the ethanolic extract in these experiments appeared superior for separated *n*-hexane and ethanol extract fractions of the turmeric, which leads to the conclusion that the application of the full

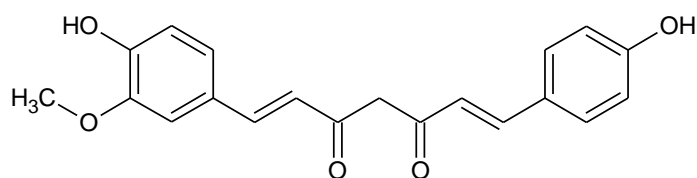
spectrum extract, in this case, acts in a superior way towards the separated compounds [18].

A closer examination of the compounds with pharmaceutical properties reveals two main groups of constituents: The curcuminoids and the essential oil. Figure 2 displays the molecular formula of curcuminoids with their three main representatives - curcumin, demethoxycurcumin (DMC) and bisdemethoxycurcumin (BDMC) [19]. The essential oil predominantly includes the terpenes α -turmerone, β -turmerone and γ -turmerone with their molecular formula shown in Figure 3 [19].

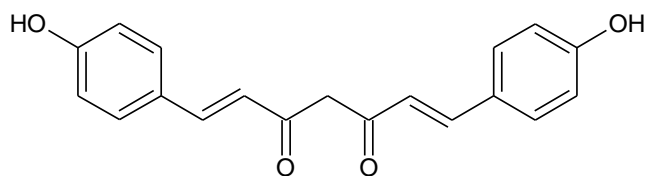
Apart from the curcuminoids and the essential oil, the rhizomes contain mostly carbohydrates and a little protein, fat and minerals [20].



curcumin



demethoxycurcumin DMC



bisdemethoxycurcumin BDMC

Figure 2 Molecular formula of the three main curcuminoids from *Curcuma longa* L.: curcumin, demethoxycurcumin (DMC), and bisdemethoxycurcumin (BDMC); drawn with ADC/ChemSketch.

Curcuminoids are often recovered by conventional solvent extraction [1,21] and are considered to be the most potent bioactive compounds in turmeric and therefore responsible for its biological functions [22]. They were discovered to give turmeric its intense yellow colour [23]. However, curcumin is poorly soluble in water with only approximately 8 µg/mL [23–25] and is remarkably sensitive to light [26,27]. Unfortunately, the bioavailability of curcumin after oral application is low [7,28] which is possibly due to its poor solubility in water, poor absorption, and rapid metabolism, followed by a fast systemic elimination [28].

Many pharmacological and technologically relevant effects of turmeric are related to the curcuminoids. Lipophilic extracts of turmeric have shown higher antioxidant properties than α-tocopherol when stabilizing perilla oil, which the authors attribute to the curcuminoids [29]. There is evidence of the *in vitro* anti-inflammatory activity of curcumin based on many different mechanisms such as inhibition of lipoxygenase, and of cyclo-oxygenase-2 expression, downregulation of chemokine expression, inhibition of lipopolysaccharide and nitric oxide production in macrophages, inhibition of phospholipase D activity and many more [30,31]. Furthermore, curcumin has shown inhibition of cell proliferation and apoptosis in rat and human lymphoid cells [32]. In human trials, anti-inflammatory activity was shown in patients with rheumatoid arthritis and against post-operative inflammation [30]. The previously postulated hepatoprotective activity of turmeric is attributed to different mechanisms of the curcuminoids, partially based on antioxidative, radical scavenging [33,34] and immunomodulating effects, but also on the decrease of phosphatase and transaminase activity, free fatty acid, cholesterol and phospholipid levels [35]. In addition, the anticancerogenic effects of curcumin are promising due to the inhibition of cell growth and angiogenesis [36–38], to the induction of apoptosis [37,39] among other mechanisms [40] and to its antimutagenic [41] properties. Curcumin also revealed antimicrobial effects on different bacteria and fungi [42].

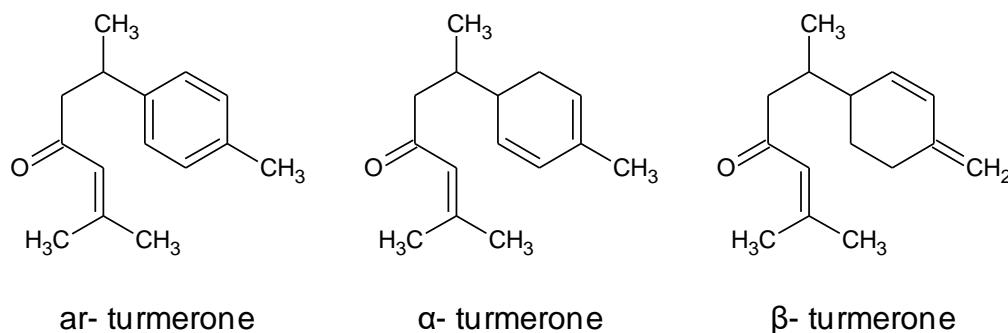


Figure 3 Molecular formula of the three main turmerones from *Curcuma longa* L.: α -turmerone, α -turmerone, and β -turmerone; drawn with ADC/ChemSketch.

The volatile oil of turmeric, containing mostly turmerones, has been demonstrated to have *in vivo* antifungal and anti-aflatoxicogenic properties [43], as well as antibacterial effects against various species [44]. Moreover, insect-repellent properties have been described [45]. In mice experiments, α -turmerone has shown antivenom activity against snakebites due to inhibition of proteolytic and haemorrhagic activities [46]. α -turmerone and the whole essential oil of turmeric revealed inhibition of platelet aggregation *ex vivo* and in rat model [47,48]. Anti-inflammatory effects of the essential oil were evident in mice after oral application [49] and *in vitro* immunomodulatory effects of the n-hexane extracted volatile oil of turmeric, by inhibition of cytotoxicity and proliferation of lymphocytes, have also been described [46]. Additionally, turmeric oil and especially α -turmerone has shown *in vitro* anticancer activity due to the induction of apoptosis in human leukaemia and lymphoma cell culture [49,50].

In rat studies, single oral doses of isolated curcumin induced no toxic effects even at doses of 1-5 g/kg [51]. Other experiments showed the oral tolerance of the essential turmeric oil in contrast to the toxic effects of the intraperitoneal injected essential oil [49]. Further studies in humans mostly reported no side effects [52–55] although some revealed slight irritative potential from daily use of turmeric, such as mild gastric irritation [56] or, in cases of topical use, allergic reactions on the skin [57–59]. According to the FDA notification from 2018, dietary dosages of turmeric and curcumin at 1000 mg/day for a 60 kg person are classified as ‘generally recognized as safe’ for human use [10].

Turmeric oils or oleoresins, which contain the essential oil and curcuminoids in different compositions depending on solvent and extraction method, are conventionally produced with hydro- or steam-distillation[60], Soxhlet extraction [61], microwave-, or

ultrasound-assisted extraction [62–65], but can also be obtained using supercritical fluid extraction as well [1,61,63,65,66]. Different extraction methods have been developed over the past years, either focused on the essential oil content or the curcuminoids. Whereas hydro- and aqueous steam-distillation, with the assistance of ultrasound or microwaves, result in high yields of extracted essential oil [64,65], the extraction of curcuminoids usually requires organic solvents such as ethanol, acetone, isopropanol or ethyl acetate [61,63].

More recently, a three-phase partitioning method for protein separation has been adopted for the extraction of oleoresin and curcuminoids from turmeric rhizomes [67–69]. In this process, the powdered rhizomes form a three-phased slurry with the addition of water, ammonium sulphate and *t*-butanol. Due to distribution equilibria, less polar substances accumulate in the upper organic phase, whereas more polar components are extracted in the aqueous phase. In direct comparison with ethanolic Soxhlet extraction (89 mg/g in 12 h) and ethanolic maceration (53 mg/g in 3 h), three-phase partitioning achieved a medium curcuminoid yield of 58 mg/g in the shortest process time of 2.5 h. Furthermore, the possibility of enzyme-assisted three-phase partitioning was found to speed up the extraction process threefold compared with conventional solvent extraction [68]. In this enzymatic extraction, the drug was pre-treated with amylases to break down the starch compounds and thus release the desired extractives.

Lateh et al describe a green extraction method based on microwave-assisted extraction with ethanol, propylene glycol, or macrogol 400 [70,71]. In their investigations ethanol appeared to generate the highest amount of extracted curcuminoids (5.7 mg/mL) followed by propylene glycol (4.2 mg/mL) and, to a lesser extent, macrogol 400 (3.4 mg/mL). To receive a curcumin-enriched extract, they perform a preparative column fractionation. Unfortunately, the separation of the extract from propylene glycol or macrogol 400 can be challenging and may thus require other organic solvents such as ethanol [70].

In the literature, the extraction of turmeric rhizomes with supercritical CO₂ (scCO₂) is often described either for extraction of volatile oil only [65,66] or, with the use of an organic cosolvent, for the extraction of more polar substances such as the curcuminoids [61,63,72].

1.2. SUPERCRITICAL CO₂ (scCO₂) EXTRACTION

ScCO₂ is an elegant alternative to conventional solvents, as it avoids the often laborious and expensive removal of potentially toxic solvent residues [1] since CO₂ itself only leaves residues that are harmless to health. Moreover, CO₂ is a non-flammable and non-explosive gas that can be recycled for extraction as a waste product from other processes [73].

The supercritical state is known as a state of aggregation at pressure and temperature settings above the critical point. The critical point differs for different substances, as displayed in Table 1, and was first discovered by Cagniard de la Tour in the early 19th century as being the pressure and temperature settings where the phase boundary between the liquid and gaseous state disappears [74]. For CO₂ the critical point is at 73.8 bar and 31.1 °C as shown in the phase diagram in Figure 4.

Table 1 Critical pressure and temperature for different substances for supercritical fluid extraction, data references [75–77].

Substance	Critical Pressure [bar]	Critical Temperature [°C]
CO₂	73.8	31.1
CCl₂F₂	40.7	111.8
ethane	48.3	32.4
N₂O	72.5	36.5
propane	42.4	96.8
water	217.7	374.1

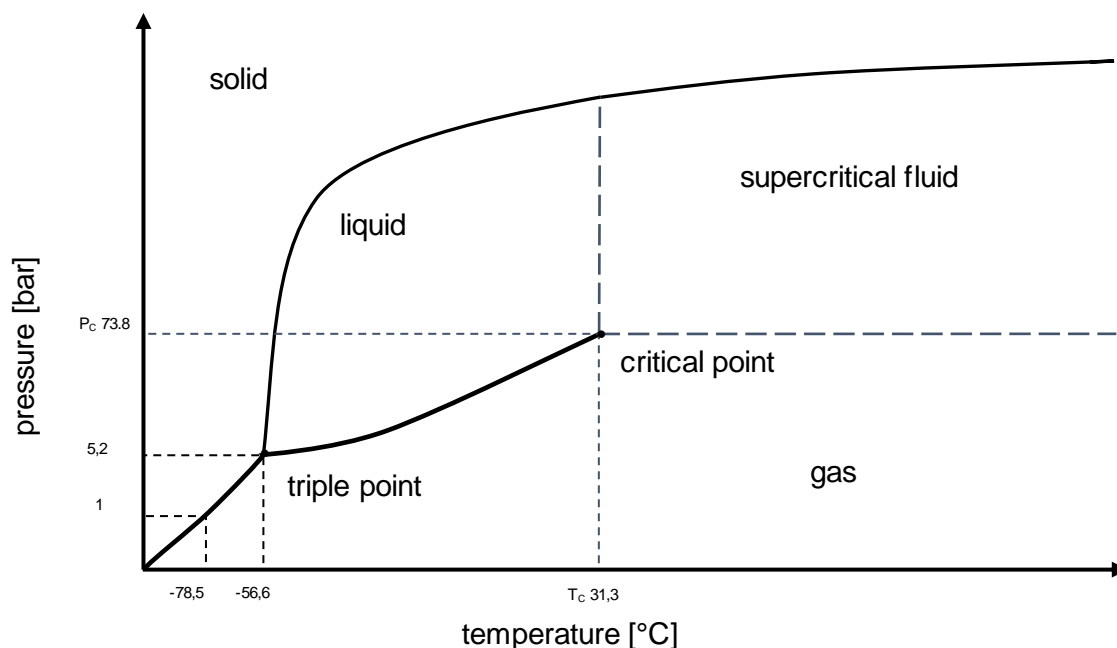


Figure 4 Phase diagram of CO₂, data reference [77].

The supercritical state provides favourable mass transport behaviour due to its properties between liquid and gaseous states, as displayed in Table 2. It has a significantly lower dynamic viscosity and only insignificantly lower density compared with liquid solvents [76,78,79], combined with a diffusion coefficient in-between gaseous and liquid states. Therefore, a supercritical solvent is often suitable as an alternative to conventional liquid solvents.

Table 2 properties of gas, supercritical fluid, and liquid of CO₂, data reference [75,80].

	Gas	Supercritical Fluid	Liquid
dynamic viscosity [Pa*s]	10 ⁻⁴	10 ⁻⁴	10 ⁻²
density [g/cm ³]	10 ⁻³	10 ⁻¹ - 1	1
diffusion coefficient [cm ² /s]	10 ⁻¹	10 ⁻³	10 ⁻⁵

In the case of supercritical fluid extraction with solvents, which like CO₂ are in a gaseous state at room temperature, the solvent can simply be removed from the resulting extract by pressure reduction and temperature change towards the gaseous

state. The typical set-up and technical aspects of the extraction and separation process are described in more detail in 2.2.3.

In the process of separation, the Joule-Thomson-Effect must be considered. Joule and Thomson described the cooling of an air-filled system under pressure during isenthalpic pressure release [81]. This decrease in temperature can be attributed to the expansion of the gas and therefore to the increase in the distance between the gas molecules which, requires energy in cases of mutual molecular attraction [82].

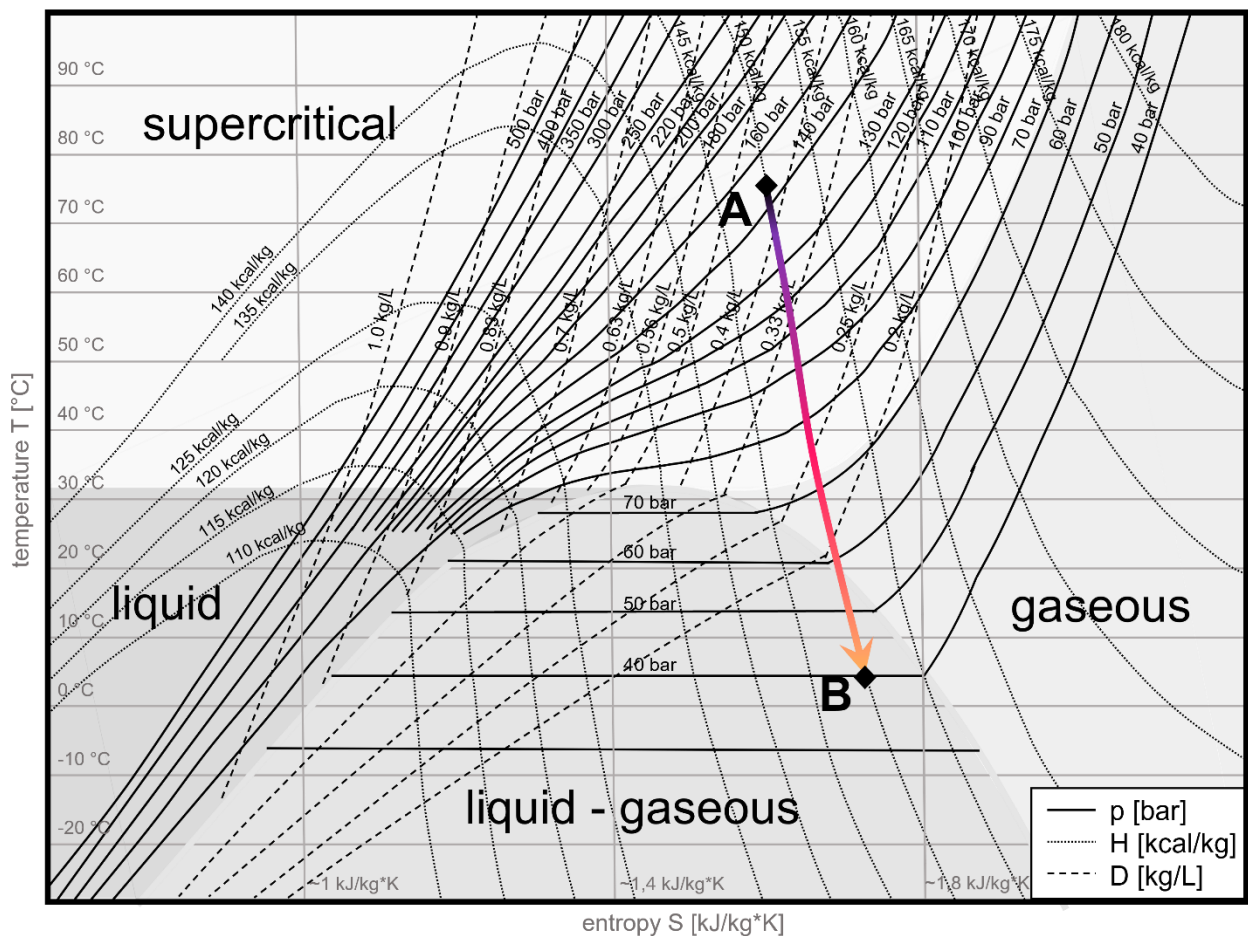


Figure 5 T,S-diagram of CO₂ with isotherms (T) in °C, isentropes (S) in KJ/kg*K, isobars (p) in bar, isenthalps (H) in kcal/kg, constant density (D) curves in kg/L, and aggregate states, data reference [83].

Figure 5 shows the TS-diagram of CO₂ which displays different states of aggregation: liquid, gaseous, supercritical state, and the biphasic area of liquid and gas. Isenthalpic pressure release from the supercritical state into the gaseous state, or into the mixed state of gas and liquid, results in cooling of the system according to the Joule-Thomson-Effect, depending on the pressure and temperature of the starting and target

conditions. As an example, this can be seen in Figure 5 in the isenthalpic pressure release from the supercritical state at A (75 °C and 150 bar) into the mixed state of gas and liquid at B (40 bar and 5 °C). The massive cooling of the system due to the Joule-Thompson-Effect results in condensation of the CO₂. To prevent the system from freezing during separation, the temperature must be controlled and sufficient energy must be supplied.

In 1910 Tyrer discovered the influence of solvent density above the critical temperature on the solubility of solutes, which increases as density increases [84]. As a consequence, the solubility of target compounds in a supercritical fluid can be modulated by influencing the density, which can be adjusted by simply varying pressure and temperature [85–87]. Figure 5 shows that the density of scCO₂ can be increased by either increasing the pressure or lowering the temperature. The development of models for predicting the solubility of different solvents and model substances, as a function of temperature and pressure or density in the supercritical state, is still under investigation [88–90]. Stahl et al summarize that, as a rule of thumb, solubility in scCO₂ decreases with increasing molar mass and polarity of the solute [91,92].

ScCO₂ is characterised by a relatively low solvent capacity but high selectivity when compared with conventional solvents [93]. This allows not only the possibility of selective extraction [93–96] but also the possibility of fractionation by varying the pressure and/ or temperature conditions [93,95,97,98].

ScCO₂ is a nondipolar solvent which, due to its low dielectric constant, was historically treated as a nonpolar solvent [76,99], which turned out to be an oversimplification of its properties [1,100]. More recent research shows that CO₂ still is a polar molecule and, therefore, it has been described as a quadrupolar solvent, since it has zero dipole moment but still significantly polar bonds, which balance each other due to molecular symmetry [101,102]. The partial negative charges on the oxygen atoms and the partial positive charge on the carbon atom result in Lewis base as well as Lewis acid properties [103]. This means it also can participate in Lewis acid-base interactions with e.g. carbonyl groups [104,105], or pyridine groups [106].

Moreover, solubility in the supercritical state can be modified by the addition of small amounts of liquid co-solvents like methanol, ethanol, water, or *n*-hexane [93,107,108].

These are mostly used to increase the solvent capacity, but reduce the solvents' selectivity compared with pure supercritical fluid [93].

The solubility of scCO₂ can be adjusted towards more polar substances, however the removal of the used co-solvents from the resulting product can be challenging [73] and offsets the advantage of the solvent-free process. Ethanol and water are, like CO₂, 'generally recognized as safe' according to the FDA [109,110] and are therefore often used as co-solvents in supercritical fluid extraction. Bitencourt et al describe the increase of solubility of ferulic acid in scCO₂ in the presence of ethanol or a mixture of ethanol and water (80:20) [109]. Regarding phenolic compounds such as ferulic acid, anthocyanins, or flavonoids, the literature shows that both co-solvents, water and ethanol, modify the yield and composition of the resulting scCO₂ extracts when used alone or in combination, depending on their proportion [109–111]. Iheozor-Ejiofor et al. investigated the extraction of rosavin from *Rhodiola rosea* L. with scCO₂ compared with conventional methanolic solvent extraction [112]. They found the scCO₂ extraction of rosavin with water as a co-solvent to be superior to all other tested methods, including the conventional solvent extraction with methanol and the scCO₂ extraction with the addition of ethanol and water [112]. The decaffeination of coffee beans has proven to be more efficient when the beans are pre-treated in water and/or extracted with humidified scCO₂ than completely dry with pure CO₂ [113]. It is suggested that the polar interactions, the increase of the bulk-density of the fluid mixture, and the softening and swelling of the plants' cellulose matrix are responsible for the extraction enhancement [112,114]. The literature describes that the addition of water and/or ethanol as co-solvent is likely to increase the solubility of target compounds such as polyphenols and can result in selectively enriched extracts compared with conventionally produced solvent extracts [96,109–112,114–116].

In scCO₂ extraction of plant material, it is crucial to consider the potential influence of water, as even dried plant material typically retains a residual amount of moisture. It is worth noting that the composition of the extracted substances may vary depending on the moisture content of the plant material and even minor amounts of residual water can substantially impact the extraction [117–119].

ScCO₂ extracts are predominantly used in nutritional supplements, flavours, spices, and cosmetics [96,120,121]. Pharmaceutically used extracts are currently primarily obtained by conventional solvent extraction.

In addition to extraction, scCO₂ can be implemented in various fields of application, a selection of which is displayed in Table 3.

Table 3 Examples of application of scCO₂ in research and industries.

Method	Examples	References
scCO₂ extraction	• Decaffeination of coffee or green tea	[96,113]
	• Extraction of essential oil or oleoresin from various plants like pepper, camomille, or hop	[92,94,95,120,122]
	• Extraction of <i>Cannabis sativa</i> L.	[123,124]
scCO₂ chromatography	• Extraction and chromatographic separation of fat- soluble vitamins	[125]
scCO₂ particle design	• Micronization of substances with poor aqueous solubility to enhance the dissolution rate by rapid expansion of supercritical solution (RESS):	[126–128] [129]
	• Essential oil-loaded particles from gas saturated solution (PGSS) to increase solubility and stability of the essential oil	[130]
	• Controlled precipitation by supercritical antisolvent (SAS) processing of polymer solutions for tissue engineering	[131,132]
Loading of carrier systems	• Loading of ibuprofen on powders, granules or tablet-like carriers from supercritical solution	[133–136]
	• Impregnation of cotton gaze surfaces with plant extract from <i>Melissa officinalis</i> L.	[137]

1.3. CAPSULE FORMULATIONS

When developing pharmaceutical preparations with plant extracts, the application route and the appearance of the extract need to be considered. In the case of scCO₂ extracts from turmeric, oral application seems to be a rational approach. Herbal scCO₂ extracts are often semi-solid or liquid. For improved standardization of dosage, compliance and masking of the extracts' taste, the development of a solid single dose preparation seems appropriate. The development of a tablet formulation in the case of semi-solid or liquid extracts can be challenging since the extract must be bound into a compressible powder mixture or granule. In contrast to tablet formulations, capsule formulations can carry high amounts of semi-solid or liquid fillings depending on the type of capsule (hard or soft capsule) once compatibility with the capsule shell material has been confirmed. The properties of the content can be adjusted to the capsule shell's material by adding appropriate excipients.

Matrix formulations are often chosen for API that show poor water solubility and/or poor bioavailability according to the biopharmaceutics classification system (BCS). Looking at the constituents of *Curcuma longa*, at least curcumin has shown poor bioavailability and water solubility [7,28], and not much better can be expected for the other components of the lipophilic scCO₂ extract of turmeric. The matrix-forming excipients can be designed to enhance solubility in water in different ways such as structural disruption of crystal-forming substances [138–141], solubility enhancement by increasing surface area [142–145], or solubility enhancement by surface active additives [146–148]. In addition, bioavailability of lipophilic substances can be increased by lipid carriers that transport the dissolved substance and drag it along the gastrointestinal absorption route [149–151].

The formulation of nanoparticles has been described in the literature to enhance dispersibility and bioavailability through the increase of surface-to-volume ratio [145]. Self-nanoemulsifying drug delivery systems (SNEDDS) are described for lipophilic compounds, such as curcumin and piperine, in lipophilic matrices with surface active ingredients optionally solidified in a carrier system [148]. They spontaneously form emulsions with a large surface area after disintegration of the carrier and it has been described in the case of curcuminoids, that these emulsions increase the absorption of the incorporated API significantly compared with simply suspended API [147,148].

Many dietary supplements use micellar structures with emulsifiers such as polysorbate 80 to enhance bioavailability of curcumin [146,152–156].

The first thing to note is that there are no formulated medicines based on turmeric, but there are many dietary supplements and pseudo-medicinal products. Most available capsule formulations with turmeric compounds have been developed with a focus either on curcumin alone or on curcumin-enriched extracts whereas other components such as the essential oil receive only little attention [146,152–156]. The extract and the added curcumin or curcuminoids usually originate from conventional solvent extraction [157].

For the development of a capsule formulation using the whole scCO₂ extract, the preparation of the capsule filling ought to be free from organic solvents like the scCO₂ extraction process. Table 4 shows characteristics of the four matrix variants applied in this thesis: Witepsol S58, Witepsol W45, Polyethylene glycol 4000 and Aeroperl 300 Pharma, the use of which substances has already been described in the literature for capsule fillings [158–161]. For capsule shell material hard gelatine was chosen.

Table 4 Overview of capsule filling matrices: hard fat (Witepsol S58, Witepsol W45), polyethylene glycol (PEG 4000), and mesoporous silica particle (Aeroperl 300 Pharma).

Matrix [ref.]	Melting point [°C]	Solubility in Water pH Value	Molecular Properties
Witepsol S58 [162]	32 – 33	practically insoluble 6 (no information on method)	hydroxyl value 60-70 hard fat + polyoxyethylene (25) cetyl stearyl ether + (stabilized) glyceryl ricinoleate
Witepsol W45 [163]	33 – 36	practically insoluble -	hydroxyl value 40-50 meets the requirements of Ph. Eur. monograph 'Hard Fat'
PEG 4000 [164]	50 – 58	500 g/L 4 - 7 (100 g/L; 20 °C)	Polyethylene glycol meets the requirements of Ph. Eur. monograph 'Macrogols'
Aeroperl 300 Pharma [165]	> 2000	> 1 mg/L 3.5 -5.5 (40 g/L; 40 °C)	mesoporous silicon dioxide specific surface area 260-320 m ² /g

1.3.1. HARD CAPSULES

Hard capsule shells come in a variety of colours and sizes with gelatine from different animal origins being the most commonly used shell material, followed by plant-based alternatives such as Hypromellose or pullulan [166,167].

Gelatine is a composition of protein chains modified from animal collagen and is easily dissolved in water and hydrolytically degraded depending on the pH value [168]. Due to the many functional groups of amino acids forming the gelatine proteins, many interactions can be assumed and observed e.g., ionic interactions or cross-linking [168].

The moisture inside the capsule shell is in constant equilibrium with the moisture of the environment and the capsule filling, therefore storage conditions of 35 to 65% r.h. are recommended for hard gelatine capsules. Deviations in humidity will result in either brittleness or, stickiness and deformation of the gelatine [166,169]. High humidity, heat and UV light can also cause cross-linking of the amino acids, altering the dissolution profile of the capsule [170]. In addition to the requirements for the storage conditions, the capsule filling needs to fulfil certain conditions. In particular, cross-linking catalysed by moisture or aldehydes from the capsule content can cause incompatibilities [171]. Obviously, fillings that dissolve or soften the capsule shell are also unsuitable for use.

Hard gelatine capsules are usually filled with powders, sugar spheres, solidified melted fat or polyethylene glycol [167,172], but other solid fillings such as small tablets or granules are also used. Liquid or semi-solid substances are more commonly encapsulated in soft gelatine capsules, but can be formulated in hard gelatine capsule shells as well through the addition of a sealing step, achieved by banding or dipping in a sealing solution and subsequent drying [172,173].

Comparing soft and hard gelatine capsules, hard gelatine capsules are manufactured without non-volatile plasticisers, but a with higher amount of moisture (13-16%) for flexibility of the material. Soft gelatine capsules, on the other hand, contain less water, but a certain amount (approximately 30%) of plasticisers such as glycerol. This high amount of plasticisers in soft gelatine capsules increases the permeability of the capsule shell to oxygen from the outside and to substances, such as active ingredients, from the inside [174,175]. This is an obstacle to storage stability, however plasticisers can also have a positive effect on the dissolution behaviour of poorly soluble substances after application of the capsule [158,174]. Although there is a certain

tendency, for both hard and soft gelatine capsules, for the active ingredients in the capsule filling to interact with the shell material, it should be noted that the potential for migration and thus interaction increases with the hydrophilicity of the substances in the filling, depending on the partition coefficient between filling and shell [158,170,172,174]. The encapsulation processes of hard and soft gelatine capsules differ significantly. For soft gelatine capsules, not only can the manufacturing of the capsule shell and filling not be separated, but the manufacturing process involves many highly humidity-sensitive steps in which the filling can get in contact with water from the gelatine shell [158,172]. In addition, the manufacturing of soft gelatine capsules has special machinery requirements [158,172].

Both hard and soft gelatine capsules can be used for lipophilic herbal extracts and preparations. The filling has to match the capsule shell and is therefore adjusted via pre-treatments (like drying or granulation) or the addition of other excipients [158]. Several capsule formulations with herbal components are available, such as GeloMyrtol [176], curcumin-Loges [146], or Sedariston [177].

1.3.2. HARD FAT

Fat in general is a mixture of mono-, di-, and triacylglycerols. Both the degree of saturation and the length of the fatty acids determine the properties of the lipid such as solid fat content, solubility or crystallization behaviour. The fatty acids in hard fat usually are completely hydrogenated with a chain length of 12-18 carbon atoms [178]. An important characteristic for hard fat is the hydroxyl value which reaches from 3 to 50 (without additives) and that determines the number of free hydroxyl groups, the respective ratio of di- and monoacylglycerols and therefore also potential hydrophilic or amphiphilic interactions [178,179]. Both hard fat variations in this thesis (Witepsol S58 and Witepsol W45) have high hydroxyl values of 60-70 and 40-50 (Table 4) in order to enhance the incorporation of extract substances by amphiphilic interactions.

Triacylglycerols (TAG) comprise a birefringent inner crystal structure that can incorporate liquids and solid substances [180–182]. This solid crystal network of lamellar structures, that build nanoplatelets which then aggregate to bigger microstructures, is incorporated by various mechanisms [180,183,184]. For different fully hydrogenated oils, the exclusion of liquid oil is described in the literature as a consequence of crystal size on nanoscale [185,186]. The composition of the TAGs and possible additives, as well as the solid-to-liquid fat ratio, affect the crystal structure as well as external variables. External variables are all parameters of the production process e.g., cooling and crystallisation processes and the shear rate applied [180,184,185].

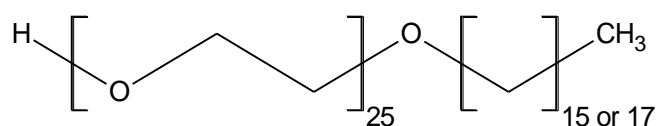
The triacylglycerols are known to be strongly affected by polymorphism i.e., different crystallization temperatures and cooling rates lead to different crystal structures and sizes at the molecular scale [182,184,187–189]. These polymorphic states differ energetically and shift from the energetically higher level α to the lower, more stable state β' and β . These shifts depend on the crystallization and recrystallization parameters (temperature, cooling rate, shear stress), the actual energy of the states and the fatty acid composition of the triacylglycerol. As a consequence of the different energy levels of the polymorphic state, they differ in their physical properties, such as the melting point [187–189] which can be pharmaceutically relevant in terms of dissolution and release of the API. There is evidence that fully hydrogenated hard fat tends to form the stable low energetic states β' and β without the shift from the α state

[190]. However, the polymorphism known for TAGs seems not inevitably related to its oil-binding capacity [180,184,186,191].

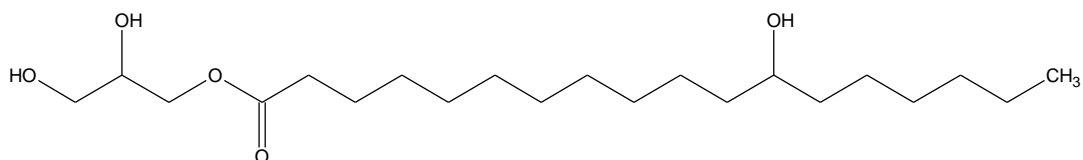
Acevedo and Marangoni explain the correlation between crystal growth and viscosity of the solidifying melt [192]. A low viscosity of the melt due to a low solid mass fraction promotes mobility of the TAGs and thus crystal growth towards larger nanoplatelets. Interesterification and the production process thereby do not affect the morphology of the nanoplatelets.

Marty and Marangoni have shown significant correlations between the oil migration rate, the solid fat content and the amount of mono- and diunsaturated TAGs for cocoa butter of different origins, as well as the relationship between a microstructure containing a large number of small crystals and a low oil permeability [193]. This indicates that the accumulation of small crystals promotes oil binding, whereas influences that coarsen the crystal structure have the opposite effect. Moreover, MacDougall et al. suggest that oil-binding capacity depends on the compatibility of the liquid oil phase and the surface of the solid crystallised nanoplatelets. High compatibility leads to strong adhesion to the surface and thus to high oil-binding capacity [194].

In addition to plain hard fat, the European Pharmacopoeia describes hard fat with additives i.e., excipients like lecithin, beeswax, and surfactants [178,195]. These additives change or extend molecular interactions of the hard fat which leads to changes in nano- and microstructure (i.e., changes of physical properties) and to more interactions with structural different substances (e.g., improvement of emulsification of the melted hard fat in the surrounding water after application, or improved incorporation of hydrophilic/amphiphilic liquids or API) [184,191]. The hard fat Witepsol S58 used in this thesis comes with the surface active additives polyoxyethylene (25) cetyl-stearyl ether and stabilized glyceryl ricinoleate, as displayed in Figure 6 [196].



polyoxyethylene (25) cetyl stearyl ether



stabilized glyceryl ricinoleate

Figure 6 Surface active additives contained in Witepsol S58; drawn with ADC/ChemSketch.

In pharmaceutical preparations, hard fat is used as a base for suppositories or in oral formulations. Dronabinol capsules monographed in DAC/NRF are a current example of a hard fat-based preparation filled into hard gelatine capsules [181]. Dronabinol as a lipophilic API, is dissolved in the hard fat that melts after application in the gastrointestinal tract. The solubilised formulation avoids the limitations of the solvation of the API from solid state and so enhances drug solubility in the gastrointestinal liquid by solute-solvent interactions [149,151]. Solubilised lipids and lipophilic API follow the physiological lipid absorption route forming micellar structures with bile secretion [149,151]. The micellar drug delivery is also the principle behind many turmeric supplements and home remedies, such as golden milk [197]. In fact, many dietary supplements skip the lipid formulation and focus directly on micellar structures with emulsifiers such as polysorbate 80 [146,152–156].

1.3.3. POLYETHYLENE GLYCOL

Polyethylene glycol (PEG) is a water-soluble polymer that is often used in pharmaceutical preparations [198]. Liquid and semi-solid PEG with a molecular weight below 600 g/mol is often part of semi-solid formulations or used as a plasticiser, co-solvent, or solubilizer [199,200]. In tablets, capsules, suppositories or coating materials, solid PEG is used [201,202]. Thalidomide capsules are a current example of oral formulations based on PEG 4000 (molecular weight 4000 g/mol) in hard gelatine capsules according to DAC/NRF [203]. Here the melted PEG reduces toxic dust from the API during the preparation of the capsules in comparison with common powder-filled capsule formulations.

The molecular weight of the polymer molecules determines its properties such as melting point, solubility, crystal structure and hygroscopicity [199,200]. PEG of lower molecular weight (e.g., 200 or 300 g/mol) has a lower melting point and a higher ratio of free hydroxyl groups in relation to the entire molecule. This results in a higher hygroscopicity. Due to the liquid state of the lower molecular PEGs, they have a higher tendency for autoxidative degradation and cross-linking reactions of gelatine than solid PEG, although both reaction tendencies are increasing with increasing molecular weight [168,170,204–206].

The high melting point of PEG with a molecular weight over 3350 g/mol (>50 °C) makes it an alternative for hard fat base in tropical climates since it withstands high temperatures well and releases its API by dissolving in surrounding water [207]. Obviously, the hygroscopicity of the PEG in tropical environments requires waterproof primary packaging.

From different animal experiments, the WHO has evidence of the toxicity of orally applied PEG in doses over 10 g/kg body weight. The toxicity along with the absorption thereby decreases with increasing molecular weight [208]. This toxicity can be related to the irritating and sensitizing potential and to the disruption of barrier functions due to lower molecular PEG [209]. However, the expectation of toxic effects is greatly reduced by the low doses of high molecular weight PEG associated with the pharmaceutical use of capsule formulations. Ultimately, the application of PEG remains a case-by-case decision.

For APIs in PEG matrix systems, different incorporation mechanisms are known. Crystallization as well as amorphous conditions have been observed depending on the

incorporated substance and the molecular mass of the PEG [210,211]. Vasa et al. describe the binding of different APIs in PEG 4000 in 3:1 (m/m) API:polymer ratios that were mixed above the APIs melting temperature and afterwards cooled to room temperature [211]. They observed very complex solidification behaviour for the mixtures and classified them as fully or partially dispersed, or fully phase-separated depending on the used API. The incorporation of essential oil in PEG matrix systems has been described in the literature for cumin oil in vaginal suppositories [212], the encapsulation of essential oil from lavender in PEG 6000 and from lime in PEG 4000 as particles from gas saturated solutions (PGSS) with the help of scCO₂ [130,213], and nanoformulations of essential oil in PEG 6000 [214–216]. Alkolade et al. described the CO₂-assisted encapsulation of lime oil in PEG 4000 and mixtures of PEG 4000 and lauric acid as PGSS formulations [130]. They observed an increase in oil loading capacity for the mixture of PEG 4000 and lauric acid (4:1) compared with PEG 4000 alone, which they attributed to specific interactions with increased hydrophobicity and to the lower crystallinity of the mixture compared with pure PEG 4000. The incorporation of whole plant extracts, as in this thesis, could potentially combine the mechanisms described above.

For several poorly soluble APIs, an increase in dissolution rate has been described as an effect of solid dispersion in PEG [212,217–219]. This may be encouraging for matrix formulations with *Curcuma longa*, as at least curcumin is known to have a poor bioavailability [7,28].

1.3.4. SILICA CARRIER SYSTEMS

Silica, respectively silicon dioxide (SiO_2), is available in different forms with varying properties for different purposes [220,221]. It is either manufactured by precipitation, thermal or flame hydrolysis of SiCl_4 , the latter also referred to as fumed or pyrogenic silica [222–225]. For carrier systems especially, granulated fumed silica particle are suitable. They are defined by their specific surface area (in m^2/g), pore and particle size. A pore size between 2 and 50 nm is referred to as mesoporous, below 2 nm it is microporous and above 50 nm it is macroporous [221,226]. Figure 7 shows plain spheric mesoporous silica particle (Aeroperl 300 Pharma) at 500x and 5000x magnification.

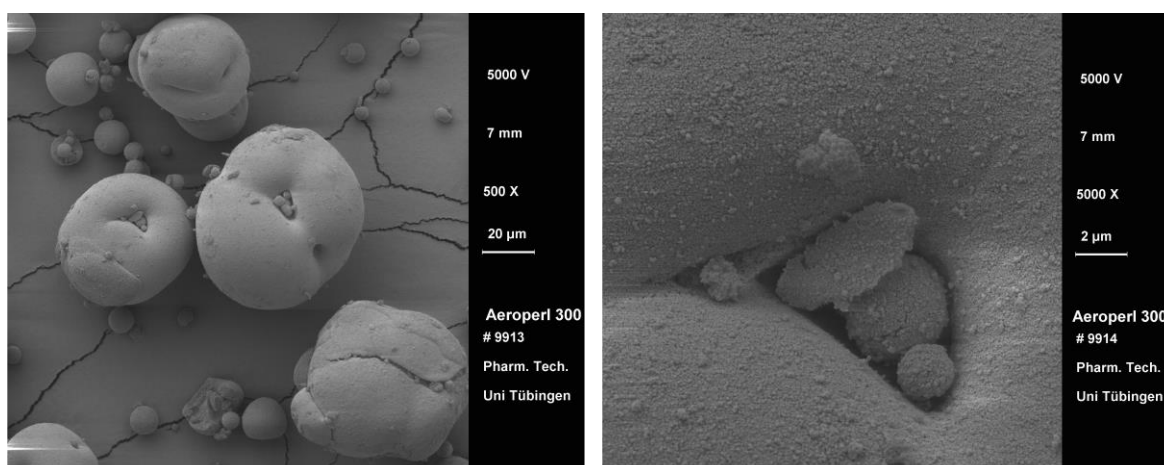


Figure 7 SEM images of Aeroperl 300 Pharma at 500x magnification (left) and 5000x magnification (right), published by Söpper [227].

The large surface area of the particle is an advantage when using mesoporous silica as a carrier system, since active substances adsorb onto the surface in and outside the pores [220]. The loading mechanism and the loaded substance thereby determine the incorporation and also the release from the carrier system. Loading mechanisms can be divided into solvent-based and solvent-free methods [220,221,228]. The solvent-based methods mostly target the amorphization of the loaded substances on the surface of the silica particle due to dissolving and solvent evaporation. Since loading is mostly processed with organic solvents, complete removal of the solvent is a prerequisite for these methods. scCO_2 can be used as a solvent for loading mesoporous silica particle as well, but the solubility and loading mechanism of scCO_2

is very complex and cannot be easily predicted. The solvent-free loading methods aim at the amorphization of the active substances by melting, milling or physical mixture [220,221,228]. Similar to the loading capacity the release of the active substances (solid or liquid) from the carrier system can be modified [229]. In the case of liquids loaded onto silica particle, it is attributed to solidified liquids or liquisolids [230–234]. The liquid is absorbed into the pores and inner structures of the particle according to its liquid-retention potential. Once the liquid-retention potential is exceeded the liquid is adsorbed onto the external surface of the particles. Spireas et al. described the flowable liquid-retention potential as dependant on the specific surface and porosity [230] in addition to the polarity, viscosity and the chemistry of the liquid which also affect the adsorption capacity [231]. The oil loading capacity of the mixture, until it changes from a free-flowing to a paste-like powder, was described by Choudhari et al. as 73 to 75% for oils from eucalyptus, peppermint and lemongrass in Aeroperl 300 [234] and by Shah et al. as up to 60% for citronella oil, whilst strictly limiting the adsorption to the internal specific surface respectively capillary stage of oil adsorption [233]. Since the API in this thesis is a liquid scCO₂ extract of turmeric, an incorporation of the liquid components in the carriers' pores could be expected as well as an adsorption of crystallized components on the internal and external surfaces.

Apart from its pharmaceutical use, mesoporous silica particles are used as a food additive, in cosmetics and are 'generally recognized as safe' according to the FDA [235].

1.4. AIM

This thesis aimed to evaluate the influence of pressure and temperature on the scCO₂ extraction and thus the compound pattern of the extracts from *Curcuma longa* L. Furthermore, the comparability of the received scCO₂ extracts with conventional solvent extracts was investigated. To this end, the thesis focused mainly on the change in solvent properties of pure scCO₂ when evaluating curcumin, demethoxycurcumin (DMC) and bisdemethoxycurcumin (BDMC), as well as ar-turmerone, α -turmerone, and β -turmerone recovery over a defined pressure and temperature range of 75–425 bar and 35–75 °C, deliberately without the addition of any co-solvents [1]. The obtained scCO₂ extracts were compared with conventionally produced *n*-hexane and methanol extracts to cover a wide range of polarity for organic solvent extraction. Different extraction patterns were expected, due to the different polarities of the solvents, representing the full range of extractables from turmeric [1]. The aim of this study was to compare the quantitative composition of conventional methanol (polar) and *n*-hexane (non-polar) extracts with scCO₂ extracts with respect to the aforementioned marker substances [1]. Moreover, scCO₂ extracts were studied for their stability during storage for 6 months at 22 and 40 °C, respectively, under protection from light [1].

In addition to the investigation of the scCO₂ extraction, the second aim was the development of a stable capsule formulation with the resulting scCO₂ extract. Currently, there are no turmeric capsules on the German pharmaceutical market, and only a few dietary supplements, containing the whole unmodified extract of turmeric. In this thesis, different hard gelatine capsule formulations were developed using whole turmeric extract with the highest yield of active compounds and four different matrix systems to bind the extract. The influence of plasticisers and the preparation process is enormous for soft gelatine capsules. Soft gelatine capsules were therefore excluded in this thesis in order to focus on the properties of the capsule filling. For the matrix, two different hard fat components (Witepsol W45 and Witepsol S58), polyethylene glycol 4000, and mesoporous silica carriers (Aeroperl 300 Pharma) were chosen. The maximum extract loading capacity for each matrix system was determined and stability of the capsule formulations with extract concentration of 5% below maximum loading capacity was studied during 3 months of storage at 22 °C and also in a temperature cycle (-5 to 40 °C), all under light protection.

2. MATERIAL AND METHODS

2.1. MATERIAL

2.1.1. CHEMICALS

Product	Company
α -turmerone	Toronto Research Chemicals (Toronto, Canada)
Acetonitrile (HPLC- grade)	Honeywell Riedel-de-Haën AG (Seelze, Germany)
Acetonitrile (LCMS- grade)	Sigma-Aldrich GmbH (Steinheim, Germany)
Aeroperl 300 Pharma	Evonik Industries AG (Hanau, Germany)
α -turmerone (analytical standard)	Sigma- Aldrich Chemie GmbH (Taufkirchen, Germany)
Carbon dioxide ($\geq 99.5\%$, technical grade)	Westfalen AG (Muenster, Germany)
Capsule shells (gelatine, size 1, transparent)	WEPA Apothekenbedarf GmbH & Co. KG (Hillscheid, Germany)
Chloroform (GC- grade)	Sigma Aldrich Chemie GmbH (Taufkirchen, Germany)
Curcumae longae rhizomae pulv. subt.	Heinrich Klenk GmbH & Co. KG (Schwebheim, Germany)
Curcumin (analytical standard)	Sigma Aldrich Chemie GmbH (Taufkirchen, Germany)
Formic acid (HPLC- grade)	Carl Roth GmbH + Co. KG (Karlsruhe, Germany)
Formic acid (98%, LCMS- grade)	Sigma- Aldrich GmbH (Steinheim, Germany)
HYDRANAL- Composite 5 (I ₂ , SO ₂ , imidazole, 2-methylimidazol all dissolved in diethylene glycol-monoethyl ether), Honeywell Fluka	Honeywell International Inc. (Charlotte, NC, USA)).

HYDRANAL- Methanol, dry for Karl-Fischer titration, Honeywell Fluka	Honeywell International Inc. (Charlotte, NC, USA)).
Isopropyl alcohol	Fisher Scientific GmbH (Schwerte, Germany)
Methanol (HPLC- grade)	Sigma- Aldrich Chemie GmbH (Taufkirchen, Germany)
N-hexane (HPLC- grade)	Sigma- Aldrich Chemie GmbH (Taufkirchen, Germany)
Polyethylene glycol 4000	Caesar & Loretz GmbH (Karlsruhe, Germany)
Potassium carbonate	Honeywell International Inc. (Charlotte, NC, USA)).
Water (highly purified, HPLC- grade)	In-house production in a Purelab Option Q7, Elga LabWater, Veolia Water Technologies Deutschland GmbH (Celle, Germany)
Witepsol W45	IOI Oleo GmbH (Witten, Germany)
Witepsol S58	IOI Oleo GmbH (Witten, Germany)

2.1.2. CONSUMABLES

Product	Company
aluminium foil, Toppits	Cofresco Frischhalteprodukte GmbH & Co. KG (Minden, Germany)
Alu- PE- pouch sealers	Coma Packaging GmbH (Wiesbaden, Germany)
Beaker 100 mL	Commonly available
Blades, surgically sterile, BAYHA	C Bruno Bayha GmbH (Tuttlingen, Germany)
Cannula Sterican 0.8 x 120 mm BL/LB, 21 G x 4¾", sterile	B. Braun GmbH & Co. KG (Melsungen, Germany)

Cannula Sterican 0.9 x 40 mm BL/LB, 20 G x 1½", sterile	B. Braun GmbH & Co. KG (Melsungen, Germany)
Cromafil Xtra H-PTFE-20/25	Macherey-Nagel GmbH & Co. KG (Dueren, Germany)
Eppendorf combi-tips advanced 1 mL	Eppendorf SE (Hamburg, Germany)
Eppendorf tubes 1.5 mL	Eppendorf SE (Hamburg, Germany)
Eppendorf tubes 2 mL	Eppendorf SE (Hamburg, Germany)
Filter paper 460 x 570 mm	VWR International GmbH (Leuven, Belgium)
Flare cap 20 mm	Zscheile & Klinger GmbH (Hamburg, Germany)
Glass plate 30 x 20 cm	Workshop University of Tuebingen (Tuebingen, Germany)
HPLC vials 1.5 mL with N11 crimps	Macherey-Nagel GmbH & Co. KG (Dueren, Germany)
HPLC vials 0.9 mL with N11 crimps	Macherey-Nagel GmbH & Co. KG (Dueren, Germany)
Injection vial 20 mL	Zscheile & Klinger GmbH (Hamburg, Germany)
Magnetic stir bar 10 mm, 30mm	Commonly available
Microscope slides and coverslips	VWR International GmbH (Leuven, Belgium)
Nucleosil 100-5 C8CC/3	Macherey-Nagel GmbH & Co. KG (Dueren, Germany)
Parafilm "M" Laboratory Film	Bemis Company Inc. (Neenah, WI, USA)
Pasteur pipettes (glas)	Glasshop University of Tuebingen (Tuebingen, Germany)
pH measuring strips, Pehanon 4.0 – 9.0	Macherey-Nagel GmbH & Co. KG (Dueren, Germany)
Pipette tips epT.I.P.S. 2- 200 µL	Eppendorf SE (Hamburg, Germany)
Pipette tips epT.I.P.S. 50- 1000 µL	Eppendorf SE (Hamburg, Germany)
Pipette caps, silicone, transparent	Commonly available

Rubber stopper for injection vials	Zscheile & Klinger GmbH (Hamburg, Germany)
Schott Duran glasses 100 mL, 250 mL, 500 mL (brown and white glass)	Schott AG (Mainz, Germany)
Silicone oil for melting point and boiling point apparatus	Sigma- Aldrich Chemie GmbH (Taufkirchen, Germany)
SpeedMixer vessels	Hausschild & Co. KG (Hamm, Germany)
Spreader card for powder filling	WEPA Apothekenbedarf (Hillscheid, Germany)
SunFire C18 column 100 Å, 5 µm, 4.6 µmm x 250 mm	Waters GmbH (Eschorn Germany)
Syringe, Omnifix 2 mL, 10 mL	B. Braun GmbH & Co. KG (Melsungen, Germany)
Zebtron ZB 5 ms capillary column (60 m x 0.25 mm ID x 0.25 µm film thickness, 5% phenylpolysiloxane + 95% diphenylpolysiloxane coating)	Phenomenex (Torrance, CA, USA)

2.1.3. DEVICES AND SOFTWARE

Product	Company
ADC/ChemSketch (Freeware) 2018.2.5	Advanced Chemistry Development Inc. (Toronto, Canada)
Analytical balance XPE 205DR	Mettler Toledo GmbH (Gießen, Germany)
Balance Sartorius excellence	Sartorius AG (Göttingen, Germany)
Capsule filler, Aponorm, for 30 capsules	WEPA Apothekenbedarf (Hillscheid, Germany)
Centrifuge Mini Spin	Eppendorf SE (Hamburg, Germany)
Climate control cabinet, type CB150	BINDER GmbH (Tuttlingen, Germany)
Freeze dryer Epsilon 2-4 LSCplus Software: LSCplus program 1.5.13.2	Martin Christ Gefriertrocknungsanlagen GmbH (Osterode am Harz, Germany)

Freezer (-28 °C)	Liebherr GmbH (Ochsenhausen, Germany)
GCMS Perkin Elmer Clarus 500, split injection Electron ionization Software: Turbomass version 5.4.2 Database: NIST MS database	PerkinElmer Inc. (Waltham, MA, USA) NIST Mass Spectral Library NIST2011, V 2.0, PerkinElmer Inc. (Waltham, MA, USA)
GraphPadPrism 8.2.1	GraphPad Software Inc.
Hand sealing tongs	Coma Packaging GmbH (Wiesbaden, Germany)
Hot air oven TU 60/60	W.C. Heraeus GmbH (Hanau, Germany)
HPLC LC-40D Degasser DGU-405 Autosampler SIL-40C Column oven CTO-40S Diode array detector SPC-M49 Software: LabSolutions	Shimadzu Europa GmbH (Duisburg, Germany)
JMP 15.2.0	SAS Institute Inc. (Cary, NC, USA)
LCMS HPLC Agilent 1200 Vacuum degasser G1379B Binary pump G1312A Autosampler G1329A Thermostatic column compartment G1316A Diode array detector G1315B Software: Agilent Chemstation (Rev. B.01.03 SR1)	Agilent (Waldbronn, Germany)
HCT ultra ion trap MS detector with APCI ion source Software: Bruker Daltonik esquire control (version 6.1)	Bruker Daltonik GmbH (Bremen, Germany)
Magnetic Stirring hotplate MR 3001K	Heidolph Instruments GmbH & Co. KG (Schwabach, Germany)
Mendeley Desktop 1.19.8	Elsevier Inc. (New York, NY, USA)

Microscope Axio Imager Z1 AxioCam MRm Software: Axio Vision v 4.6 ZEN 2.6 pro (blue edition)	Carl Zeiss Microscopy GmbH (Oberkochen, Germany)
Microsoft Office	Microsoft Corporation (Redmond, WA, USA)
Pipette Eppendorf research 100 µL (10-100 µL)	Eppendorf SE (Hamburg, Germany)
Pipette Eppendorf research 200 µL (20-200 µL)	Eppendorf SE (Hamburg, Germany)
Pipette Eppendorf research 1000 µL (100-1000 µL)	Eppendorf SE (Hamburg, Germany)
Rotary evaporator R-210 Vacuum controller V-850 Heating bath B-491	Büchi Labortechnik AG (Flawil, Switzerland)
Unichiller (-20- 40 °C) UC006	Peter Huber Kältemaschinenbau GmbH (Offenburg, Germany)
Schaukelschrank type 3401	Rubarth Apparate GmbH (Laatzen, Germany)
scCO₂ extraction pilot plant (custom-made)	Sietec- Sieber Engineering AG (Maur, Switzerland)
Software: VisiDAQ Runtime 3.11	Advantech Co., LTD (Leinfelden-Echterdingen, Germany)
Titrimo, 751 GPD	Deutsche METROHM GmbH & Co. KG (Filderstadt, Germany),
Vortex 2	IKA- Werke GmbH & Co. KG (Staufen, Germany)
Water bath	Daglef Patz KG, Chem.-Technische Spezialgeräte (Wankendorf, Germany)

2.2. METHODS

2.2.1. PREPARATION OF DRUG MATERIAL

The powdered drug was purchased in 1 kg packages from Heinrich Klenk GmbH & Co. KG (Schwebheim, Germany), repacked in three portions of approximately 300 g in aluminium-polyethylene pouches, heat sealed and then stored at -28 °C over the entire experimental work period.

As the influence of water, as a possible cosolvent in scCO₂ extraction, has already been confirmed [91], the drug material was preconditioned prior to extraction for 7 days at 42-43% r.h. over saturated K₂CO₃ solution [1,236].

2.2.2. SOLVENT EXTRACTION

Conventional solvent extraction was carried out as a two-step maceration by mixing 1 part of drug with 2.5 parts of solvent (methanol and *n*-hexane, respectively; *m/m*) [1]. Maceration was carried out under the exclusion of light by covering with aluminium foil and storing in a laboratory cupboard [1]. After 24 h the suspension was filtered through a commercial cellulose paper filter and 2.5 parts of the respective solvent were again added to the remaining insolubles [1]. After a further 24 h, both filtrates were combined and the solvent was removed with a rotary evaporator (Büchi, Labortechnik AG, Flawil, Switzerland) [1].

2.2.3. SUPERCRITICAL FLUID EXTRACTION

Supercritical fluid extraction was performed in a scCO₂ Sietec-Sieber pilot plant unit (Sietec-Sieber, Maur, Switzerland) with dried, powdered turmeric. Figure 8 illustrates the layout of the scCO₂ pilot plant unit [1]. All experiments were performed using a constant drug load of 150 g for the design of experiments and 300 g in the stability study and production of extract for the capsule formulations [1]. The extraction was conducted at a flow rate of 5.0 kg/h for 1 h [1].

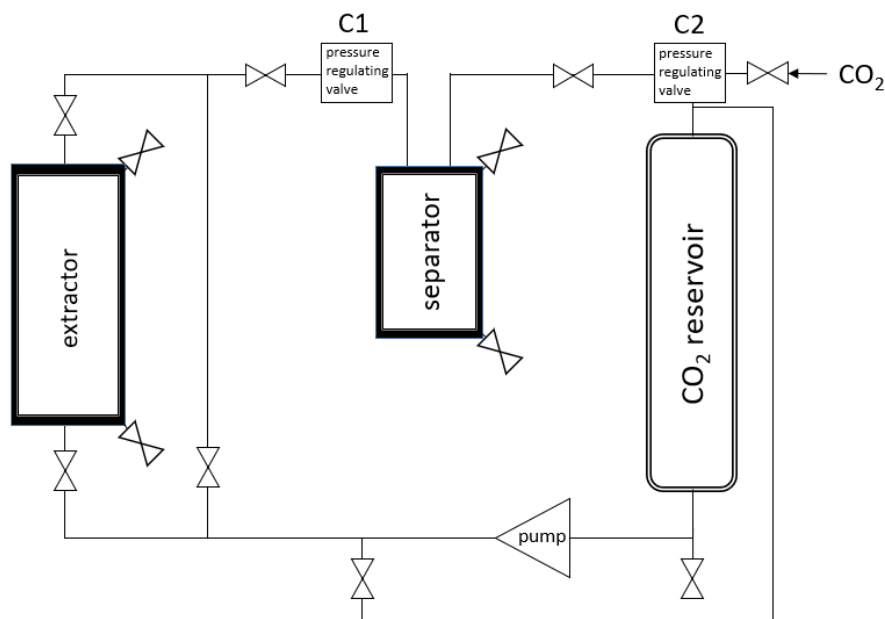


Figure 8 Simplified schematic depiction of the scCO₂ pilot plant unit [1].

Dissolved substances followed the stream of scCO₂, which was pumped out of the CO₂ reservoir, where it was stored in liquid state at 3 °C and 40 bar, into the extractor and afterwards into the separator [1]. Extracted components were separated from the scCO₂ due to a sudden pressure release behind the pressure-regulating valve C1 in the separator at 40 bar and 30 °C [1]. This allowed the transition of scCO₂ first into the liquid and subsequently into the gaseous state [1], as highlighted in Figure 9 in purple as an isenthalpic pressure release from extraction conditions B to separator conditions in the biphasic liquid and gaseous area. This two-stage process prevented the extract from becoming a non-separable aerosol [1]. The extraction conditions marked with E in Figure 9 would show a gaseous-only phase separation after an isenthalpic release to the separator pressure of 40 bar (red curve in Figure 9) according to the T,S-diagram and therefore create a non-separable aerosol. Significant cooling of the separator

could lead to biphasic separation from these extraction conditions, but since this was not an option all extraction conditions that would result in separation outside the liquid-gaseous biphasic condition were excluded. The circular system allowed recycling of the CO₂ [1].

The pressure and temperature of the extraction process were varied in a range of 75-425 bar and 35-75 °C, respectively, according to a statistical design of experiments (Table 5), depending on the requirements for the extract to be obtained[1].

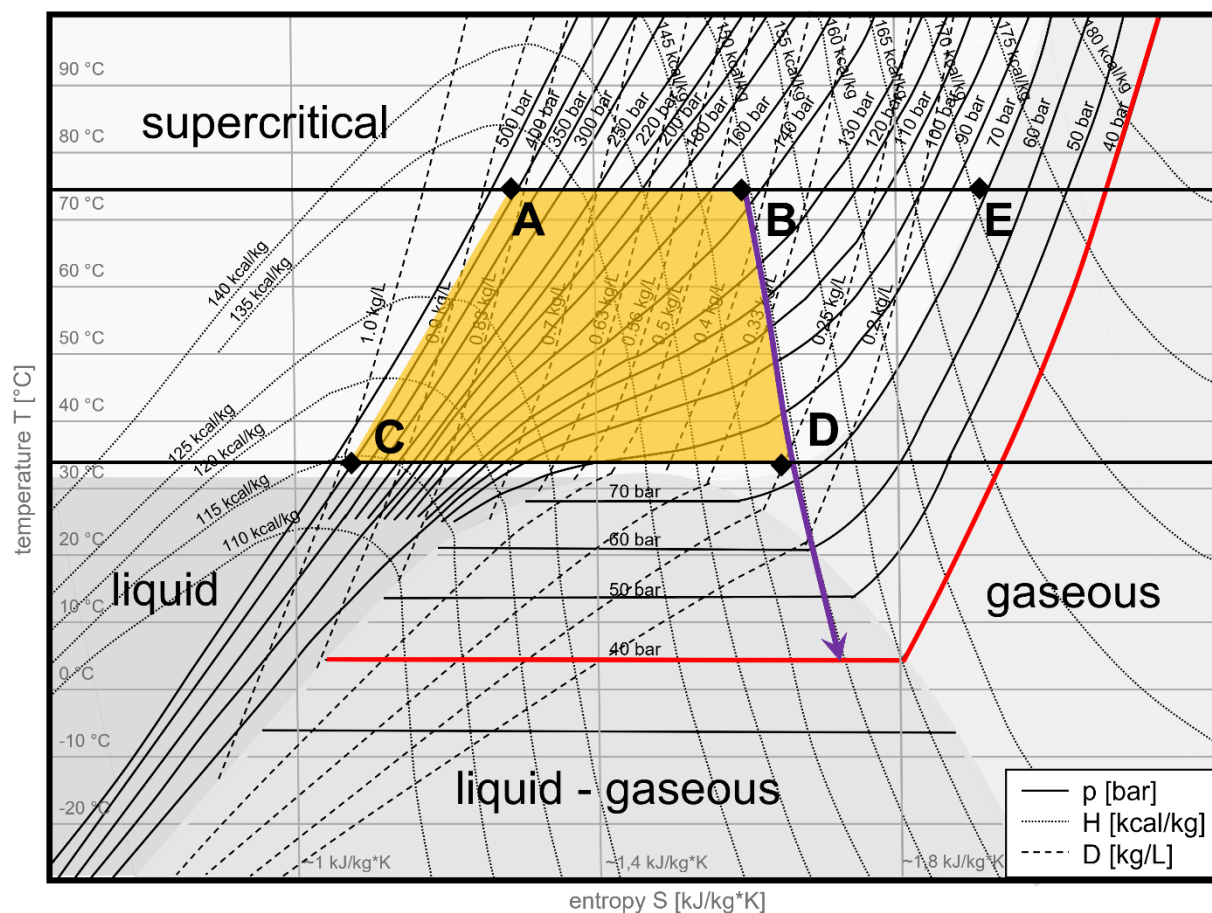


Figure 9 T,S-diagram of CO₂ with isotherms in °C, isentropes in KJ/kg*K, isobars in bar, isenthalps in kcal/kg, and aggregate states, data reference [83]. The red isobar marks the separation pressure during the scCO₂ extractions. The points A to D mark the most extreme extraction conditions: A 425 bar and 75 °C, B 150 bar and 75 °C with isenthalpic pressure relief to separation (purple), C 425 bar and 35 °C, D 75 bar and 35 °C framing the whole range of pressure and temperature conditions investigated (displayed in yellow). Point E (75 bar and 75 °C) marks a combination of extraction conditions that cannot be realized with the current pilot plant.

2.2.4. EXPERIMENTAL DESIGN

For screening over the full scCO₂ range that was to be covered by the pilot plant unit used in the present study, a full factorial design was chosen, and the data were assessed using JMP 15.2 software (SAS Institute Inc., Cary, NC, USA) for experimental design and statistics [1]. All experiments were performed in triplicate and 6 additional centre points were included, which led to 33 experiments in total as specified in Table 5 [1]. The extracted substances were dissolved in methanol to allow complete withdrawal from the pilot plant unit [1]. The methanolic solutions were assayed using HPLC-DAD [1]. The extract yield was determined after the removal of methanol by rotary evaporation (Büchi, Labortechnik AG, Flawil, Switzerland) [1].

Table 5 Experimental conditions according to a full factorial design in the correct experimental order [1].

Experiment	Pressure [bar]	Temperature [°C]
1	75	35
2	250	35
3	425	35
4	250	55
5	125	55
6	425	55
7	425	75
8	250	75
9	150	75
10	125	55
11	425	35
12	425	75
13	250	35
14	250	75
15	425	55
16	75	35
17	150	75
18	250	55
19	425	35
20	250	55
21	250	35
22	250	75
23	75	35
24	150	75
25	425	75
26	425	55
27	125	55
28	250	55
29	250	55
30	250	55
31	250	55
32	250	55
33	250	55

2.2.5. EXTRACT STABILITY STUDY

For evaluating extract stability, only scCO₂ extracts obtained under maximum pressure conditions (425 bar) were analysed [1]. To investigate the influence of dissolved CO₂ during storage, the extracts were withdrawn from the separator using a syringe without adding a solvent [1]. For comparison, conventional methanol and *n*-hexane extracts were examined and a scCO₂ extract, withdrawn from the separator as a methanolic solution, with subsequent removal of the solvent using a rotary evaporator (Büchi, Labortechnik AG, Flawil, Switzerland), as shown in Table 6 [1]. All extracts were prepared in triplicate and aliquots of 500 mg each were stored in 0.9 mL glass vials with a flare cap closure [1]. Samples were stored at 22 and 40 °C and protected from light. Samples were taken at 1, 28, 84, and 168 days after production for quantifying individual compounds using HPLC-DAD after dissolving the extracts in methanol [1].

Table 6 Characteristics of the extracts monitored in the stability study [1].

Extract	Extraction Parameters	
methanol	methanol	solvent extract
<i>n</i> -hexane	<i>n</i> -hexane	solvent extract
42535	scCO ₂ ; 425 bar; 35 °C	direct removal
42555	scCO ₂ ; 425 bar; 55 °C	direct removal
42575	scCO ₂ ; 425 bar; 75 °C	direct removal
42575R	scCO ₂ ; 425 bar; 75 °C	removed as methanolic solution

2.2.6. LIQUID CHROMATOGRAPHY WITH MASS SPECTROMETRIC DETECTION (LC-MS)

LC-MS measurements were carried out only for characterization of the main components measuring conventional solvent extracts in concentrations of 2-4 mg/mL dissolved in methanol [1]. An Agilent 1200 HPLC (Agilent, Waldbronn, Germany) system equipped with a vacuum degasser (G1379B), a binary pump (G1312A), an autosampler (G1329A), a thermostatic column compartment (G1316A) and a diode array detector (G1315B) was used for chromatographic separation [1]. A binary gradient eluent system (mobile phases A: 0.1% formic acid (v/v); B: acetonitrile) was applied using a SunFire C18 column 100 Å, 5 µm, 4.6 mm × 250 mm (Waters GmbH, Eschborn, Germany) in combination with a Nucleosil 100-5 EC 4/3 precolumn (Macherey-Nagel GmbH and Co. KG, Dueren, Germany) at a flow rate of 1.0 mL/min with the following gradient: 0–11 min, 35% B; 11–25 min, 35–70% B; 25–35 min, 70–100% B; 35–40 min, 100% B; 40–45 min, 100–35% B [1]. The column oven was set at 25 °C and the injection volume was set at 20 µL [1]. For detection, the wavelengths were set at 250, 265 and 425 nm [1]. Mass spectrometric analyses were performed with an HCT ultra ion trap MS detector with an APCI ion source (Bruker Daltonik, Bremen, Germany) [1]. The device parameters were applied as follows: dry gas flow rate (N₂), 4 l/min; nebulizer pressure, 50 psi; and capillary temperature, 325 °C; MS spectra were generated in the positive ionization mode with a compound stability and trap drive level of 100% in a range of *m/z* 50-1500 [1]. For data acquisition and processing the software Agilent Chemstation (Rev. B.01.03 SR1) (Agilent, Waldbronn, Germany) and Bruker Daltonik Esquire Control (version 6.1) (Bruker Daltonik GmbH, Bremen, Germany) were used [1].

2.2.7. HIGH PERFORMANCE LIQUID CHROMATOGRAPHY WITH DIODE ARRAY DETECTION (HPLC-DAD)

Quantification of all extracts included in the experimental design, the stability study and the capsule formulations was carried out with HPLC-DAD [1]. All samples were assayed with HPLC using a Shimadzu HPLC system (Shimadzu Europa GmbH, Duisburg, Germany) equipped with a degassing unit (DGU-405), a solvent delivery module (LC-40D), an autosampler (SIL-40C), a column oven (CTO-40S) and a photo diode array detector (SPC-M49) [1]. A binary gradient eluent system (mobile phases A: 0.1% formic acid (v/v); B acetonitrile) was applied using a SunFire C18 column 100 Å, 5 µm, 4.6 mm × 250 mm (Waters GmbH, Eschborn, Germany) in combination with a Nucleosil 100-5 C8CC/3 precolumn (Macherey-Nagel GmbH and Co. KG, Dueren, Germany) at a flow rate of 1.0 mL/min with the following gradient: 0-20 min, 40-75% B; 20-25 min, 75-80% B; 25-28 min, 80-90% B; 28-31 min, 90% B; 31-32 min, 90-40% B; 32-36 min; 40% B [1]. The column oven was set at 30 °C and the injection volume was set at 10 µL [1].

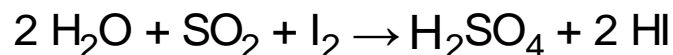
Curcumin standard was detected at 425 nm with a retention time of 13.6 min, ar-turmerone at 250 nm after 23.8 min and α -turmerone at 250 nm after 27.5 min [1]. Curcumin was used for the quantification of all three curcuminoids and ar-turmerone for the three turmerones in question [1]. Substances were quantified as curcumin or ar-turmerone equivalent using peak height values [1]. To this end, equivalents to extract concentrations of 3.0-4.0 mg/mL for scCO₂ extracts, 1.0-1.5 mg/mL for *n*-hexane extracts, and 0.3–0.5 mg/mL for methanol extracts were measured dissolved in methanol [1].

2.2.8. GAS CHROMATOGRAPHY WITH MASS SPECTROMETRIC DETECTION (GC-MS)

Gas chromatographic measurements were performed according to Lorenz et al. [237] with a PerkinElmer Clarus 500 gas chromatograph (PerkinElmer Inc., MA, USA) using split injection (split ratio: 30:1, injection volume: 1.0 μL) equipped with a mass detector. A Zebron ZB 5 ms capillary column was used with 60 m \times 0.25 mm inner diameter, 0.25 μm film thickness, and 5% phenylpolysiloxane and 95% dimethylpolysiloxane coating (Phenomenex, Torrance, CA, USA). As carrier gas, helium was used at a flow rate of 1 mL/min. The oven temperature followed a heating rate of 4 $^{\circ}\text{C}/\text{min}$ from 100 to 320 $^{\circ}\text{C}$ with a final hold time of 45 min. Electron ionization mode (70 eV) was used for the mass spectrometric detection. Peak characterisation was performed with the help of NIST Mass Spectral Library NIST2011, V 2.0, PerkinElmer Inc. (Waltham, MA, USA). For separation of the volatile components, the methanolic solvent extract was dissolved in methanol (3.0 g in 200 mL) and fractionated with *n*-hexane in a separatory funnel (3 times with 200 mL *n*-hexane each for 2 min). The *n*-hexane phase was dried in a rotary evaporator (Büchi, Labortechnik AG, Flawil, Switzerland). Afterwards, the dried extract fraction was dissolved in chloroform (5 mg/mL) for measurement in the gas chromatograph.

2.2.9. KARL FISCHER TITRATION

Water content was determined according to Ph. Eur 2.5.12 'water: semi-micro determination' [238] based on the reaction of water with iodine (I₂) and sulfur dioxide (SO₂) as shown in following Equation 1 [1].



Equation 1 Simplified reaction principle of Karl Fischer's titration of water with iodine (I₂) and sulfur dioxide (SO₂) [1].

The analysis was performed in a 751 GPD Titrino (Deutsche METROHM GmbH & Co. KG, Filderstadt, Germany) and, for the required anhydrous surrounding and solvent for the samples, Hydranal Methanol dry was used [1]. The titrant applied was Hydranal Composite 5, containing the necessary reagents iodine and sulfur dioxide as well as imidazole and 2-methylimidazole as basic components, all dissolved in diethylene glycol- monoethyl ether [1]. In accordance with Ph. Eur., at first standardisation was completed with pure water. Afterwards, suitability was tested with the scCO₂ extract produced at 425 bar and 75 °C, taken from the plant as a methanolic solution with subsequent removal of the solvent and therefore considered to be water-free (Table 6, 42575R) [1]. The mean percentage recovery for the extract was 100.5%. For water determination, the regression line was calculated with addition of water to the extract after Ph. Eur. and resulted in a slope of 1.004 and percentage errors of e₁ = 0.4% and e₂ = 0.0% [1]. All samples were measured in duplicate [1].

2.2.10. FREEZE DRYING OF scCO₂ EXTRACTS

Freeze drying was performed in an epsilon 2-4 LSCplus freeze dryer (Martin Christ Gefriertrocknungsanlagen GmbH, Osterode am Harz, Germany) in a 9-step program according to Table 7 for 53 h. The ice condenser was set at a temperature of -90 °C over the entire process. For drying, the extract was divided in 20 mL glass injection vials with flat, thin bottoms, 5 to 6 g each. Afterwards, the dried extract was pooled and stored in a brown Schott Duran glass flask at a maximum of 5 °C. This method was used only on scCO₂ extracts of *Curcuma longa* L. produced at 425 bar and 75 °C.

Table 7 Freeze drying method for scCO₂ extracts.

Step	Time [h]	Shelf Temperature [°C]	Pressure [mbar]
• Loading	0	RT	AP-
• Freezing	1	RT to -40	AP
• Drying	12	-40	AP to 0.01
• Drying	12	-40 to -20	0.01
• Drying	12	-20	0.01
• Drying	12	-20 to -10	0.01
• Drying	1	-10 to 0	0.01
• Post-drying	3	0 to 20	0.01
• Withdrawal	0	20 to RT	AP

RT = room temperature AP = atmospheric pressure

2.2.11. LOADING AND DETERMINATION OF EXTRACT LOADING CAPACITY

As mentioned in 3.2.1, maximizing compound recovery for curcuminoids and turmerones revealed optimum extraction conditions at 425 bar and 75 °C. Therefore, only these extracts were used for the development of capsule formulations. Prior to further processing, the scCO₂ extract was freeze-dried according to 2.2.10. Determination of maximum loading capacity was carried out in steps of 2.5%, calculated based on the hydrous raw scCO₂ extract and later recalculated for the dried scCO₂ extract as shown in Table 8. All data in the following text refer to the calculated content of freeze-dried extract. All experiments were carried out in triplicate.

Table 8 Extract concentration in capsule formulation calculated as raw extract and correspondingly calculated as dried extract, which is equivalent to 45% of the undried mass. Only the most interesting concentrations are displayed.

Extract Concentration [% (m/m)]	
scCO ₂ extract	scCO ₂ extract
raw	dried
30.0	16.1
32.5	17.7
35.0	19.4
37.5	21.2
40.0	23.0
42.5	24.9
45.0	26.8
75.0	57.3
77.5	60.6
80.0	64.2
82.5	67.8
85	71.7

2.2.11.1. SCREENING OF THE EXTRACT LOADING CAPACITY OF HARD FAT AND MACROGOL

Analogous to the determination of the oil factor according to Thoma et al. [239], the extract loading capacity is determined based on the fact that liquid components can escape from mixtures of solid and liquid components after some time if loading capacity is exceeded. The extract represents the liquid oily component and the respective matrix system forms the solid component. The scCO₂ extract concentrations to be analysed were weighed out at 500 mg in a 20 mL injection vial, a small magnetic stir bar was added and sealed with a rubber stopper. Then the mixtures were melted and mixed on a magnetic stirrer hotplate until it was visually homogeneous. For hard fat matrix systems, it was therefore heated up to 40 °C and for PEG 4000 up to 60 °C. The well-mixed samples were removed from the hotplate and left to cool and solidify completely. Small portions of the cooled samples were withdrawn from the vial, placed loosely on sheets of filter paper and covered to be protected from light. Due to capillary forces, liquid oily components are dragged into filter paper [240] and, in the case of the yellow scCO₂ extract, they leave easily visible stains. After 24 h, samples were checked for the formation of yellow stains on the filter paper due to extract leakage. Leakage of extract from the matrix was considered a failure and thus overloaded. The highest determined concentration without leakage was set maximum loading capacity.

2.2.11.2. SEMI-QUANTITATIVE DETERMINATION OF EXTRACT LOADING CAPACITY OF HARD FAT AND MACROGOL

The determination of the extract loading capacity of melted matrix substances with a standardised contact area was performed almost as described in 2.2.11.1. Extract and matrix were weighed in a 20 mL injection vial, sealed and heated while stirring until it all melted and was well mixed as described. The melt then was pipetted into small plastic cylinders, cut from the cannula cover of Cannula Sterican 0.8 x 120 mm BL/LB, 21 °G x 4³/₄" (B.Braun GmbH & Co. KG, Melsungen, Germany) in pieces of 5 mm with a surgical blade (C Bruno Bayha GmbH, Tuttlingen, Germany) and placed flat on a glass plate. This resulted in a standardised contact area of 18.9 mm². After complete solidification of the melt, the plastic cylinders were loosened carefully from the glass plate with the surgical blade without damaging the contact surface of the solidified melt to the glass plate. Then it was placed on a sheet of filter paper. The evaluation followed after 24 h under protection from light like described in 2.2.11.1.

2.2.11.3. DETERMINATION OF EXTRACT LOADING CAPACITY OF AEROPERL CARRIERS

The analysed concentration of scCO₂ extract in Aeroperl 300 was weighed in a 20 mL injection vial and a small magnetic stir bar was added before sealing it with a rubber stopper and placing it on a magnetic stirrer hotplate as described in 2.2.11.1. It was stirred at room temperature until it looked homogeneous and evenly coloured. A small portion of the mixture was placed loosely upon a sheet of filter paper. After 24 h under protection from light, the evaluation followed as described in 2.2.11.1.

2.2.12. POLARIZATION MICROSCOPY

The polarization microscopic images were captured with an Axio Imager Z1 microscope (Carl Zeiss, Jena, Germany) with crossed polarizers and a $\lambda/4$ wave plate. Samples were examined at a magnification of 20x or 40x. For microscopy, the freeze-dried extract was applied directly and thinly on a glass microscope slide, then a coverslip was placed upon it. The capsule-filling formulations with hard fat and polyethylene glycol were applied out of the melt onto a microscope slide, immediately covered with a coverslip and then left to cool briefly.

2.2.13. SAMPLE PREPARATION FOR QUANTIFICATION VIA HIGH PERFORMANCE LIQUID CHROMATOGRAPHY

2.2.13.1. MACROGOL (POLYETHYLENE GLYCOL 4000) MATRIX SYSTEMS

For HPLC analyses, a sample equivalent to approximately 30 mg extract was weighed and dissolved in 10 mL of methanol. The solution could be measured directly via HPLC according to 2.2.7.

2.2.13.2. HARD FAT MATRIX SYSTEMS

Sample preparation included a repetitive liquid-liquid phase distribution process. A sample equivalent to approximately 30 mg extract was weighed in a 2 mL Eppendorf Tube (Eppendorf SE, Hamburg, Germany). The extraction followed the steps shown in Figure 10.

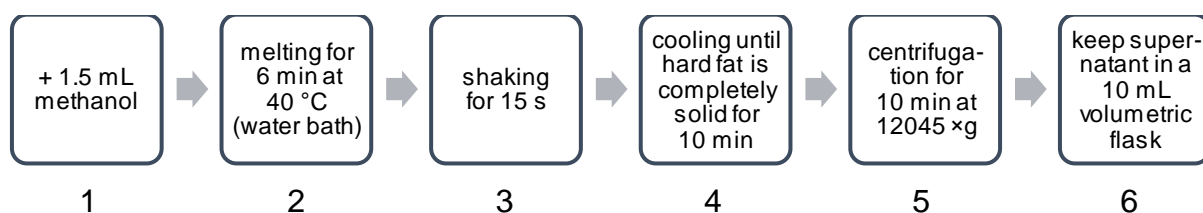


Figure 10 Extraction method for $scCO_2$ extract from hard fat matrix. The steps 1 to 6 were repeated 3 times with the same sample. Supernatants were united and filled up to 10 mL with methanol.

All steps 1 to 6 were repeated 3 times. Shaking was done on a Vortex 2 (IKA- Werke GmbH & Co. KG, Staufen, Germany) and centrifugation was performed in a MiniSpin (Eppendorf SE, Hamburg, Germany). The emerging supernatants were combined and supplemented to 10 mL with methanol. The solution was filtered with a Cromafil Xtra H-PTFE-20/25 filter (Macherey Nagel GmbH & Co. KG, Dueren, Germany) directly into an HPLC vial and measured according to 2.2.7.

2.2.13.3. AEROPERL 300 CARRIER SYSTEMS

A sample equivalent to approximately 30 mg extract was weighed and dissolved in 10 mL of methanol. The solution was filtered directly into an HPLC vial with a Cromafil Xtra H-PTFE-20/25 filter (Macherey Nagel GmbH & Co. KG, Dueren, Germany) and measured according to 2.2.7.

2.2.14. PREPARATION OF CAPSULE FORMULATIONS

2.2.14.1. MACROGOL (POLYETHYLENE GLYCOL 4000) MATRIX SYSTEM

For calculation of weights, a mass of 520 mg was assumed for capsule filling per capsule with PEG 4000 (assuming a density of 1.04 g/cm³, determined in preliminary experiments). A preparation overage of 4 capsules was added to compensate for unavoidable residues in the vessels. PEG 4000 and freeze-dried scCO₂ extract were weighed in a 100 mL beaker, covered with parafilm and subsequently placed in a silicon oil heating bath on a magnetic stirring hotplate MR 3001K (Heidolph Instruments GmbH & Co. KG Schwabach, Germany). The mixture was stirred with a magnetic stir bar at 100 rpm at 60 °C until it melted completely and then mixed homogeneously. In the meantime, the hard gelatine capsule shells were placed in a capsule filling machine and opened. The melt was inserted into the lower halves with a glass Pasteur pipette with silicone cap until they were filled evenly. After complete solidification of the melt, the capsules were sealed.

2.2.14.2. HARD FAT MATRIX SYSTEMS

The calculated mass of the capsules' hard fat-based fillings was 450 mg per capsule (assuming a density of 0.900 g/cm³, determined in preliminary experiments). A preparation overage of 4 capsules was added to compensate for unavoidable residues in the vessels. The hard fat component and the freeze-dried scCO₂ extract were weighed in a 100 mL beaker, covered with parafilm, and subsequently placed in a silicon oil heating bath on a magnetic stirring hotplate MR 3001K (Heidolph Instruments GmbH & Co. KG Schwabach, Germany). The mixture was stirred with a magnetic stir bar at 100 rpm at 40 °C until it melted completely and then mixed homogeneously. In the meantime, hard gelatine capsule shells were placed in a capsule filling machine and opened. The melt was inserted into the lower capsule halves with a glass Pasteur pipette with silicone cap until they were filled evenly. After complete solidification of the melt, the capsules were sealed.

2.2.14.3. AEROPERL 300 CARRIER SYSTEM

For Aeroperl 300, the filling mass per capsule had to be determined for different extract concentrations individually. For a concentration of 57.3% of freeze-dried scCO₂ extract of *Curcuma longa* L., the filling mass was determined as 240 mg per capsule. Before using, Aeroperl 300 was dried for 30 min at 120 °C in a hot air oven. After cooling, both

Aeroperl 300 and scCO₂ extract were weighed in a 10 mL beaker and covered with parafilm. On a magnetic stirring hotplate, Aeroperl and extract were mixed at room temperature by means of a magnetic stir bar. Stirring speed was initially set at 100 rpm, after 20 min it was increased to 250 rpm and after a further 25 min to 300 rpm until it was homogeneously mixed. The hard gelatine capsule shells were opened in a manual capsule filling machine and filled with the help of a spreader card without tapping the machine and sealed directly afterwards.

2.2.15. STABILITY STUDY OF CAPSULE FORMULATIONS

For evaluating capsule stability, only capsule preparations with high extract concentrations were analysed. To compare the influence of high extract loading on the capsule stability in different formulations, capsules were prepared according to 2.2.14 with freeze-dried scCO₂ extract of *Curcuma longa* L. in concentrations as shown in Table 9. All formulations were prepared in triplicate with 30 capsules for each batch. The capsules were stored in open SpeedMixer vessels (Hausschild & Co. KG, Hamm, Germany) that were lined with filter paper circles and protected from light. Relative humidity was set at 43% r.h. by a saturated K₂CO₃ solution. Storage temperatures were set at 22 °C and under a temperature cycle (TC) program over 24 h, as seen in Table 10. Samples were taken at 1, 7, 14, 28 and 84 days after production. All samples were visually checked for leakage visible as stains on the filter paper circles. Only those stored at 22 °C were analysed via HPLC according to 2.2.13.

Table 9 Concentration of extract loading in capsule formulations analysed in stability study. For the exact compositions of the tested capsule formulations refer to the appendix Table 19.

Matrix	Extract Concentration in %	Extract Concentration [mg per capsule]
Witepsol S58B	16.1	71
Witepsol W45	21.2	93
PEG 4000	21.2	109
Aeroperl 300 Pharma	57.3	127

Table 10 Course of Temperature during storage in the temperature cycling test (TC).

Time [hh:mm]	Temperature [°C]
00:00	-5
08:00	-5
10:00	40
20:00	40
22:00	-5
23:59	-5

2.2.16. UNIFORMITY OF DOSAGE UNITS ACCORDING TO PH. EUR. 2.9.40

According to the general monographs for pharmaceutical preparations and for capsules in Ph. Eur. [241,242], testing of uniformity of dosage units is not required for herbal drugs or herbal drug preparations. However, single dose preparations must follow uniformity of dosage units Ph. Eur. 2.9.40 [243] and therefore a Mass Variation (MV) test for hard capsules with doses ≥ 25 mg per capsule and $\geq 25\%$ of API per capsule and a Content Uniformity (CU) test for doses < 25 mg or $< 25\%$ of API per capsule are required. Respective MV and CU tests were carried out for qualitative evaluation of the production of the capsule formulations as required for non-herbal capsule formulations.

2.2.16.1. MASS VARIATION TEST

For MV test 10 respectively, 30 capsules of each batch were weighed and the mass of the capsule filling was calculated by subtracting the mass of the capsule shell. The total extract represents the API. Assuming that the concentration within the filling mass is uniform, the actual extract content was calculated from the exact weights for the melt. The A value i.e., the actual content of API in % of the intended content of API, was calculated according to Equation 2.

$$A = \frac{C_{actual}}{C_{target}} * 100$$

Equation 2 Calculation of the A value [%]; C_{actual} = actual concentration [%]; C_{target} = target concentration [%].

All sample contents were calculated as described in Equation 3 and calculation of the Acceptance Values (AV) was carried out after case 1 (reference value M for target content T per dosage form of $T \leq 101.5$) according to Equation 4 as described in Ph. Eur. 2.9.40.-2. [243].

$$x_i = w_i * \frac{A}{\bar{w}}$$

Equation 3 Individual determination of contents of each capsule; x = content of capsule [%]; w = weight of capsule [mg]; \bar{w} = mean weight of capsule filling [mg].

$$AV = |M - \bar{X}| * k\bar{s}$$

Equation 4 Calculation of Acceptance Value (AV) according to general formula (Ph. Eur. 2.9.40); M = reference value; \bar{X} = mean of individual contents ($x_1; \dots x_i$)[%]; k = acceptability constant (for 10 capsules k = 2.4, for 30 capsules k = 2.0); s = sample standard deviation.

Criteria for acceptance were chosen as recommended in the Ph. Eur. method; with a maximum allowed acceptance value (L1) of 15% and a maximum allowed range for deviation of each dosage unit (L2) of < 25%.

2.2.16.2. CONTENT UNIFORMITY TEST

For CU tests, the content of the capsules had to be determined using an appropriate analytical method. Since the scCO₂ extract used was a multi-component system it was decided to determine the individual contents of curcumin, demethoxycurcumin (DMC), bisdemethoxycurcumin (BDMC), ar-turmerone, α -turmerone and β -turmerone by HPLC-DAD measurements (sample preparation according to 2.2.13; HPLC-DAD measurements according to 2.2.7). The curcuminoids (curcumin, DMC, BDMC) and the turmerones (ar-, α -, and β -turmerone) were combined into these 2 groups of APIs and expressed as delivered doses.

The Acceptance Values (AV) were calculated according to Equation 4 and case 1 (Ph. Eur. 2.9.40.-2.). Criteria for acceptance were chosen like for MV.

3. RESULTS AND DISCUSSION

3.1. PHYTOCHEMICAL CHARACTERIZATION OF SOLVENT EXTRACTS OF *CURCUMA LONGA* L.

Conventional turmeric methanol and *n*-hexane extracts were analysed by LC-MS to identify their main constituents [1]. It was assumed that by covering both polar (methanol) and non-polar (*n*-hexane) extracts, it should be possible to find all major compounds at least in one of the extracts [1]. Extracts obtained with scCO₂ were expected to yield phytochemical profiles in between those of the aforementioned two extremes [1].

3.1.1. LIQUID CHROMATOGRAPHY WITH MASS SPECTROMETRIC DETECTION (LC-MS)

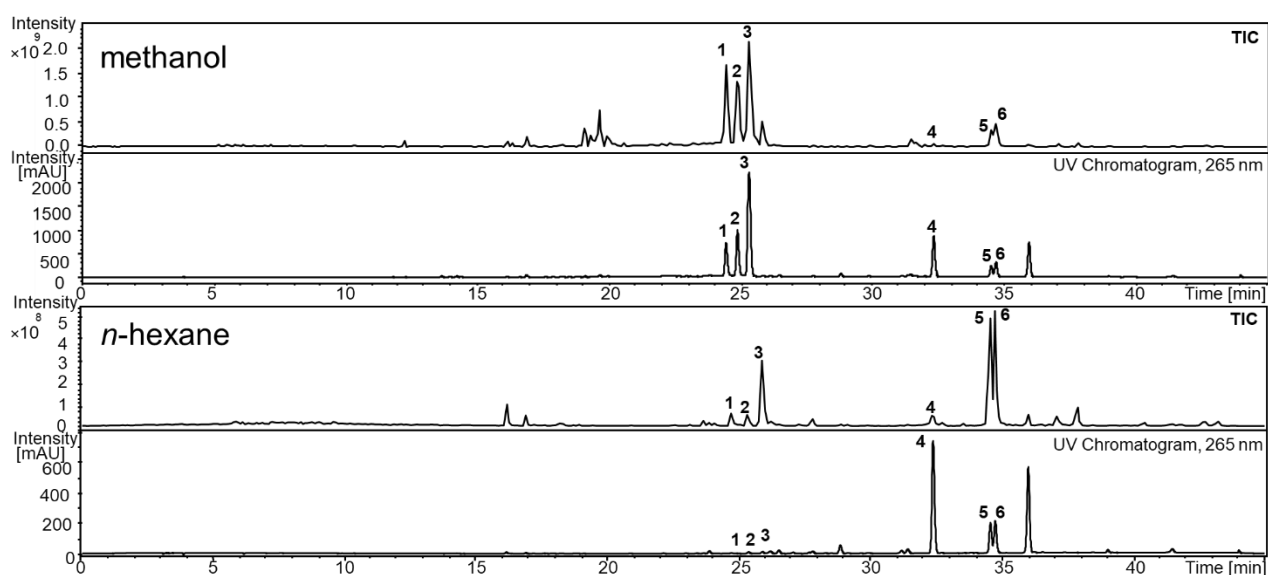


Figure 11 Total ion current (TIC) and UV chromatogram of methanol and *n*-hexane extracts; 1: bisdemethoxycurcumin (BDMC); 2: demethoxycurcumin (DMC); 3: curcumin; 4: *ar*-turmerone; 5: α -turmerone; 6: β -turmerone [1].

Figure 11 shows the ultraviolet (UV) chromatograms and total ion currents (TIC) of the methanol and *n*-hexane extracts [1]. Six major signals were number-coded and based on their UV and MS data further characterised and assigned (Table 11) [1]. Curcumin, *ar*-turmerone and α -turmerone were identified in comparison with respective reference

substances [1]. BDMC, DMC and β -turmerone were characterized using their MS spectra, which were compared with literature data [1].

Table 11 Retention times (R_t), UV- and mass spectrometric data of active substances of turmeric. Only the most intense m/z ratios of fragment ions are displayed. (P precursor ion) [1].

Peak no.	R_t [min]	Peak Assignment	UV λ_{max} [nm]	MS ⁿ Data [m/z]			References
				MS ^{1, P}	MS ^{2, P}	MS ³	
1	24.5	bisdemethoxycurcumin (BDMC)	425	309	225	147	[244], [245], [246]
2	24.9	demethoxycurcumin (DMC)	425	339	245	175	[244], [245], [246]
3	25.3 Ref.: 25.3	curcumin	425	369	245	175	reference standard, [244], [245], [246], [247]
4	32.3 Ref.: 32.4	α -turmerone	240	217	119	92	reference standard, [248]
5	34.5 Ref.: 34.6	α -turmerone	236	219	121	93	reference standard, [249], [250], [248]
6	34.7	β -turmerone	242	219	201	121	[249], [250], [248]

3.1.2. GAS CHROMATOGRAPHY WITH MASS SPECTROMETRIC DETECTION (GC-MS)

For GC measurements samples of the methanol extract had to be prepared as a highly volatile solution in chloroform. Therefore, the volatile *n*-hexane fraction of the methanolic extract had to be separated by liquid-liquid phase distribution according to 2.2.8.

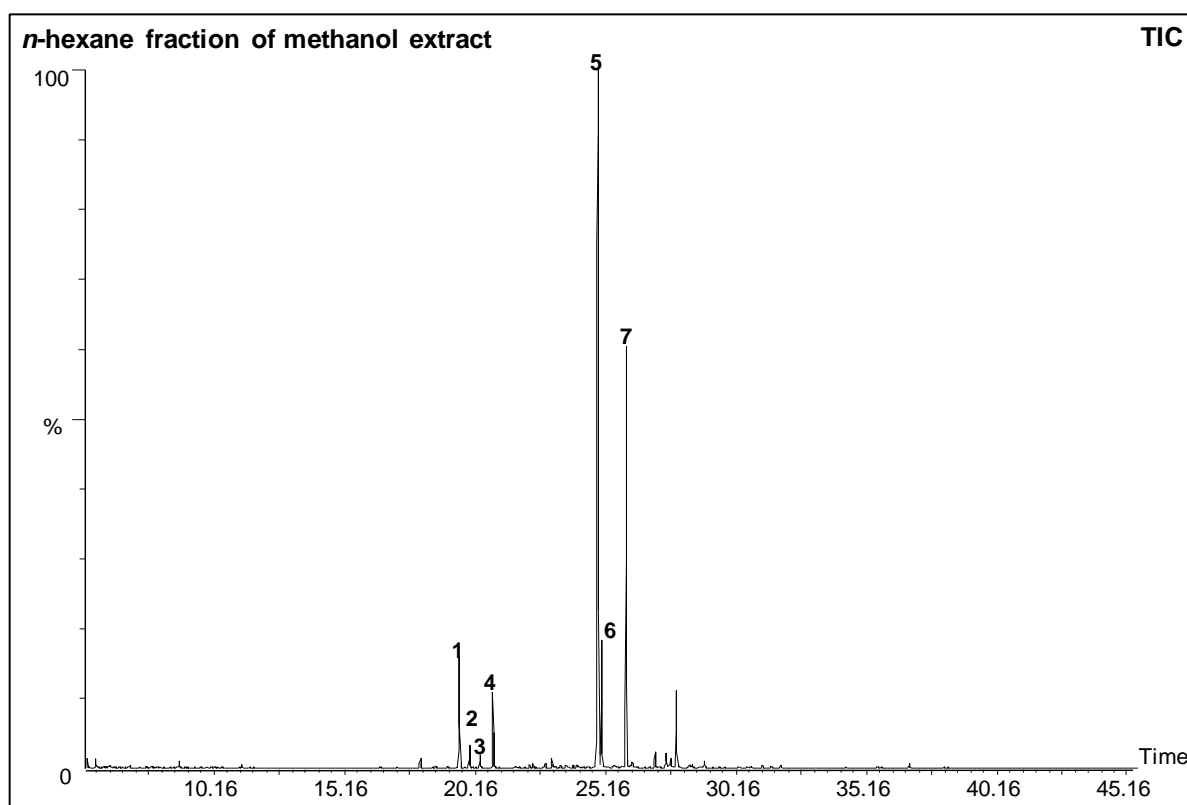


Figure 12 Total ion current (TIC) of *n*-hexane soluble fraction of methanol extract: 1: α -curcumene; 2: α -zingiberene; 3: β -bisabolene; 4: β -sesquiphellandrene; 5: α -turmerone; 6: α -turmerone; 7: β -turmerone.

The main components in the *n*-hexane soluble fraction of the methanol extract are displayed in the total ion current in Figure 12. Seven main peaks were characterised and identified via NIST MS database as shown in Table 12 based on their characteristic fragment profiles.

Table 12 Retention times (R_t), UV- and mass spectrometric data of active substances of *n*-hexane soluble fraction of methanolic extract from turmeric. Only the most intense m/z ratios of fragments are displayed in their relative intensity to the base peak (% bp).

Peak no.	R_t [min]	Peak Assignment	Main Fragments [m/z] (% bp)		
1	19.60	α -curcumene	119 (100)	132 (96.3)	105 (54.5)
2	19.98	α -zingiberene	119 (100)	93 (87.2)	69 (32.6)
3	20.37	β -bisabolene	69 (100)	93 (84.7)	67 (40.6)
4	20.98	β -sesquiphellandrene	69 (100)	91 (51.4)	93 (48.6)
5	24.92	ar-turmerone	83 (100)	119 (73.7)	216 (31.3)
6	25.04	α -turmerone	83 (100)	105 (63.3)	120 (39.1)
7	26.00	β -turmerone	120 (100)	83 (28.3)	105 (17.6)

The sesquiterpenoids found in the *n*-hexane fraction represent the main components of the essential turmeric oil [19]. According to the high lipophilicity and solubility in *n*-hexane reported in the literature [19], the *n*-hexane soluble fraction had captured the main components of the essential oil contained in the methanol extract very well.

Since the main components of the essential oil (ar-turmerone, α -turmerone, β -turmerone) shown via GC MS in Figure 12 could also be analysed by HPLC as well, (as seen in Figure 11 in the UV chromatogram) further experiments were only carried out by HPLC-DAD.

3.2. COMPARISON OF scCO₂ EXTRACTION AND CONVENTIONAL SOLVENT EXTRACTION

3.2.1. LOSS OF EXTRACT IN THE PLANT: EXTRACTION OF ALREADY scCO₂ EXTRACTED DRUG WITH METHANOL

For general investigation of the comparability between scCO₂ extraction and conventional solvent extraction, the loss of extract in the scCO₂ pilot plant was analysed. The loss of extractives in the pilot plant could affect the amount of curcuminoids and turmerones in scCO₂ extract and therefore result in incorrectly low values for contents compared with conventional solvent extracts. As a standard for comparison, the conventionally produced methanolic extract was chosen and assumed to represent an exhaustive extraction. To also achieve a complete extraction for the scCO₂ extraction process, re-extraction of the already scCO₂-extracted drug was performed with methanol according to 2.2.1. To this end, scCO₂ extraction was carried out under maximum extraction conditions (425 bar and 75 °C) and the scCO₂ extract was directly recovered from the separator.

Figure 13 and Figure 14 show the amount of curcuminoids (Figure 13) and turmerones (Figure 14) extracted with scCO₂. Furthermore, the results of the re-extraction of the remaining drug with methanol, as well as the sum of these two extraction steps, are shown. The latter representing assumably a full spectrum and complete extract. In comparison, a conventionally produced methanol extract is displayed.

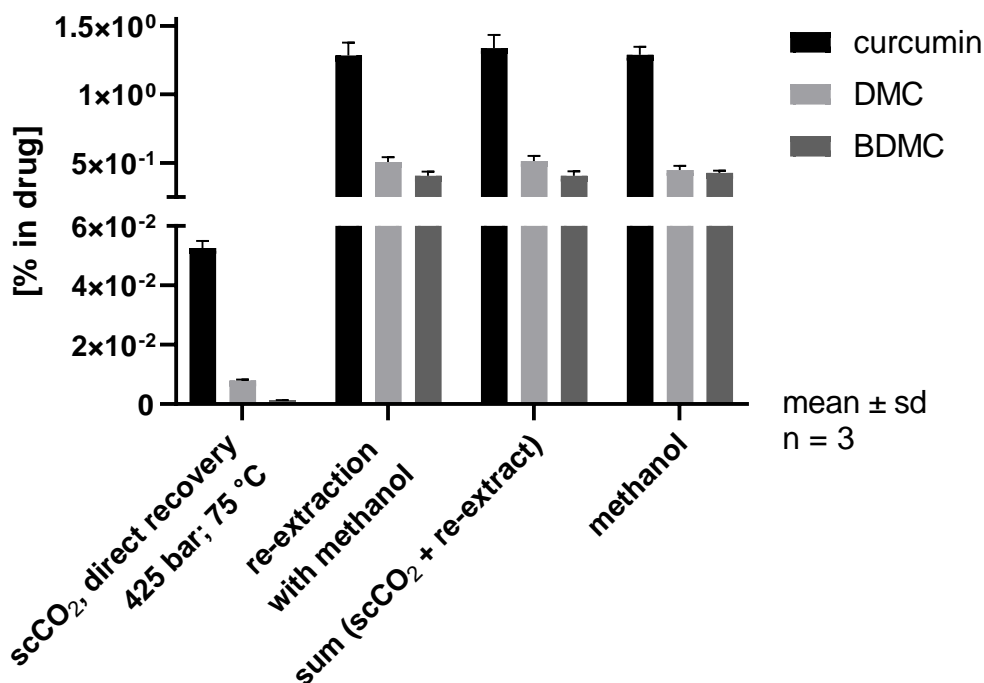


Figure 13 Comparison of curcuminoid content (curcumin, demethoxycurcumin DMC, bisdemethoxycurcumin BDMC) in: scCO₂ extract after direct recovery from the separator; extract resulting from the re-extraction of the remaining drug material from scCO₂ extraction; sum of extracted content in total form scCO₂ extraction and re-extraction; methanolic solvent extraction; all data related to drug before extraction.

For the curcuminoids i.e., curcumin, DMC and BDMC, contents extracted by scCO₂ stayed about 20 times below those of methanolic extraction. Extraction properties are described in more detail in 3.2.2. As shown in Figure 13, re-extraction with methanol seems to retrieve the remaining curcuminoids from the drug material. Moreover, the proportion of extracted curcuminoids by scCO₂ appears negligibly small compared with extracted curcuminoids from the methanolic extraction, since there is no significant difference between the sum of contents of the extraction and re-extraction and the re-extraction alone. The extracted curcuminoids from the re-extraction correspond to the curcuminoid contents of the conventional methanolic solvent extraction. Direct recovery of the scCO₂ extract from the pilot plant caused a certain loss in extract substance remaining in the separator, however this loss most likely has no major impact on the detected extracted amount of curcuminoids by scCO₂.

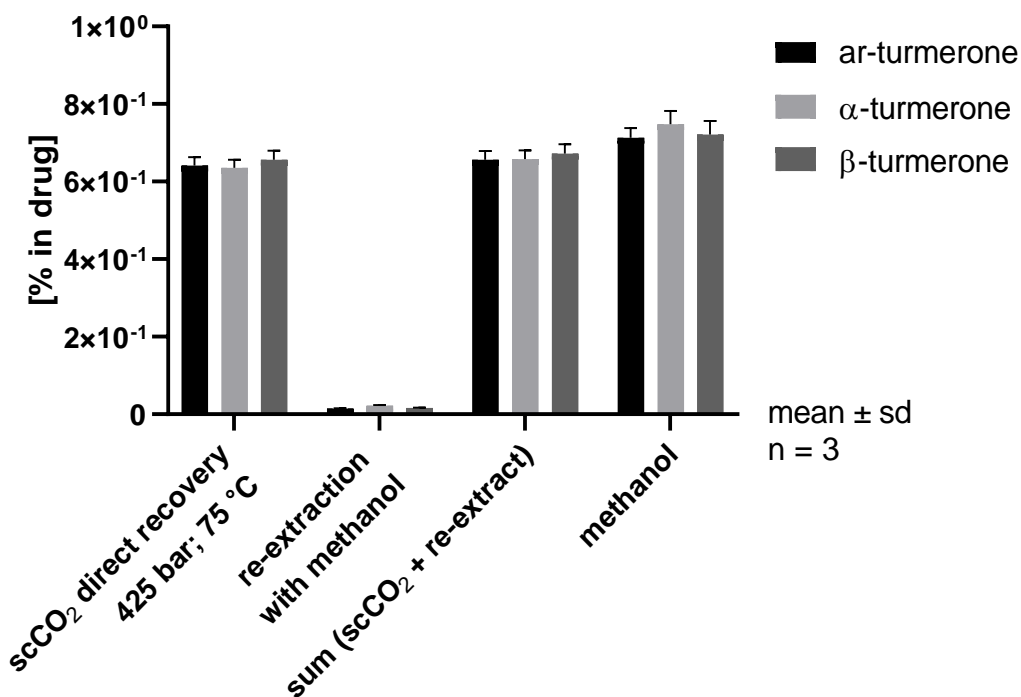


Figure 14 Comparison of turmerone content (ar-turmerone, α-turmerone, β-turmerone) in: scCO₂ extract after direct recovery from the separator; extract resulting from the re-extraction of the remaining drug material from scCO₂ extraction; sum of extracted content in total form scCO₂ extraction and re-extraction; methanolic solvent extraction; all data related to drug before extraction.

The extraction of turmerones, displayed in Figure 14 by the lead components ar-turmerone, α-turmerone and β-turmerone, shows that scCO₂ extraction enables almost complete extraction of these substances. Contents extracted by scCO₂ are up to 60 times higher than those of the methanolic re-extraction. The high solubility of turmerones in scCO₂ and therefore high extractability is consistent with previous publications [251,252]. For more detailed investigations of extraction properties, please refer to 3.2.2. Comparison of the sum of extraction and re-extraction with conventionally produced methanolic extract shows no significant difference in contents. This is similar to the extraction of curcuminoids, although in case of the turmerones the methanolic re-extraction seems negligible versus the scCO₂ extraction.

It was demonstrated that the results of scCO₂ extraction can be considered unaffected by losses in the pilot plant, since there were no significant differences between the sum of scCO₂ extraction and methanolic re-extraction and the conventional methanolic extraction for either curcuminoid or turmerone content.

3.2.2. ScCO₂ EXTRACTION ACCORDING TO EXPERIMENTAL DESIGN

To systematically study the influence of extraction conditions on the composition of turmeric scCO₂ extracts, a full factorial experimental design was used [1]. At this point, reference is made to the results of the individual experiments in the appendix in Table 18. Figure 15 illustrates the extract yield recovered from the extraction of 150 g powdered drug load [1]. It should be noted that the extract yields considered were obtained from methanolic solution and are therefore to be considered without co-extracted water [1]. The yield of water-free extract ranges between below 2.3% for extraction settings under 100 bar and 40 °C and above 3.1% for pressure settings above 300 bar, in combination with high-temperature settings above 60 °C [1].

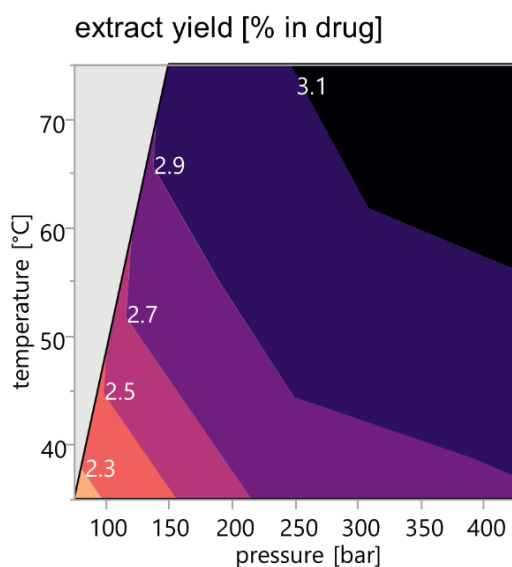


Figure 15 Response contour plot illustrating the extract yields depending on pressure and temperature; the area marked in grey represents combinations of pressure and temperature settings, which were not investigated; recovery rate related to the drug material in % (m/m) [1].

Figure 16 shows the response contour plots, which have been calculated from the quantitative data of the marker substances of the scCO₂ extracts [1]. Both temperature and pressure have a clear impact on the recovery rates of the six main compounds [1]. The curcumin and BDMC contents of the extracts were found to increase with increasing pressure and temperature, while the DMC content reached a maximum at maximum pressure and intermediate temperature settings [1]. Curcumin extraction thereby ranged between <0.02% for low-to-intermediate pressure and temperature settings (75–200 bar and 35–60 °C) and >0.12% for maximum pressure and temperature settings (425 bar and 75 °C) [1]. For BDMC the extraction varied between <0.0005% (settings below 200 bar and 55 °C) and >0.0035% (settings above 400 bar

and 70 °C), while DMC content ranged between <0.002% (settings below 125 bar and 50 °C) and >0.014% (settings of above 400 bar and 50–60 °C) [1].

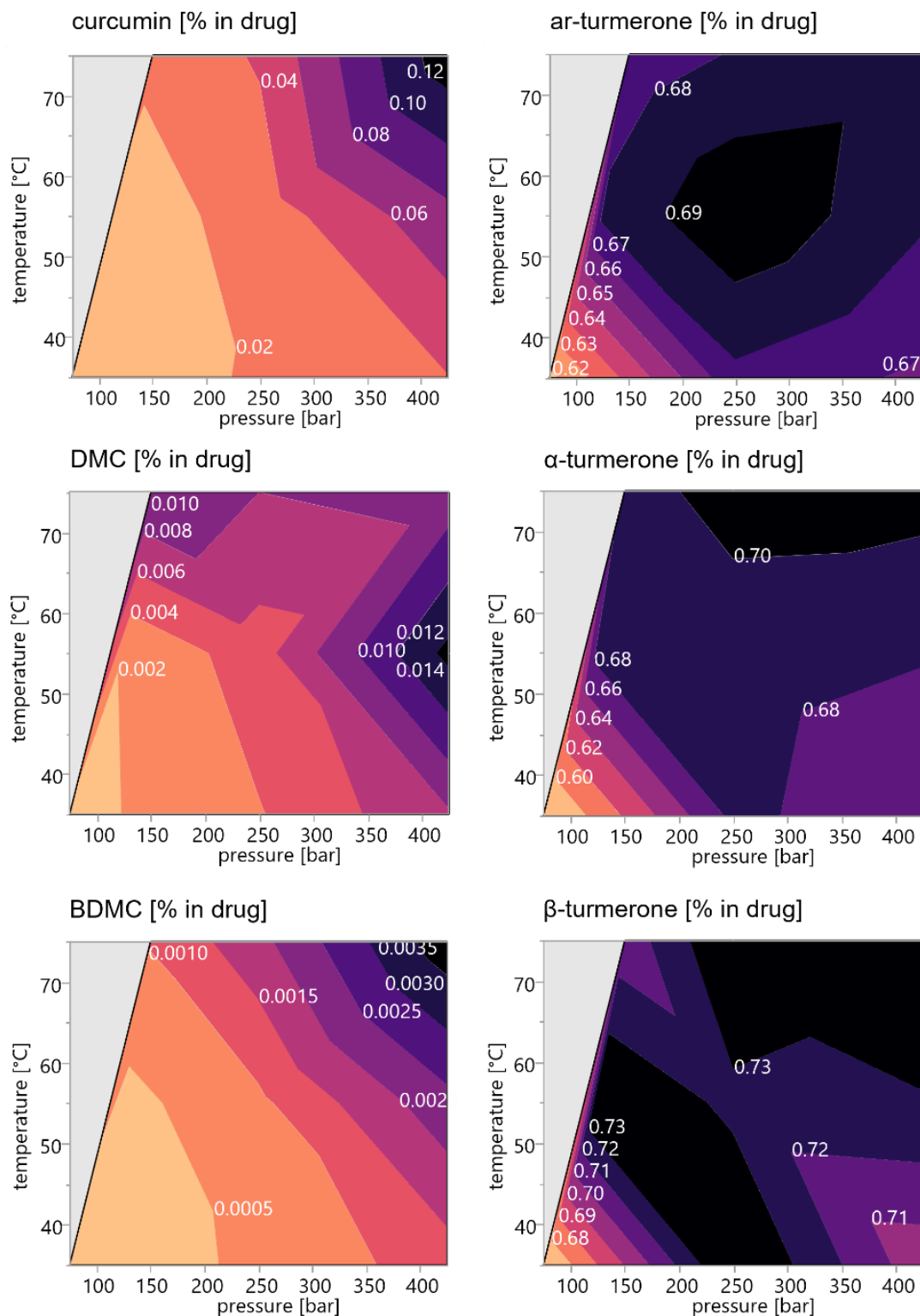


Figure 16 Response contour plots illustrating the recovery rates of all target compounds (curcumin, demethoxycurcumin (DMC), bisdemethoxycurcumin (BDMC), ar-turmerone, α-turmerone, β-turmerone) depending on pressure and temperature; the areas marked in grey represent combinations of pressure and temperature settings, which were not investigated; recovery rates are related to the drug material in % (m/m) [1].

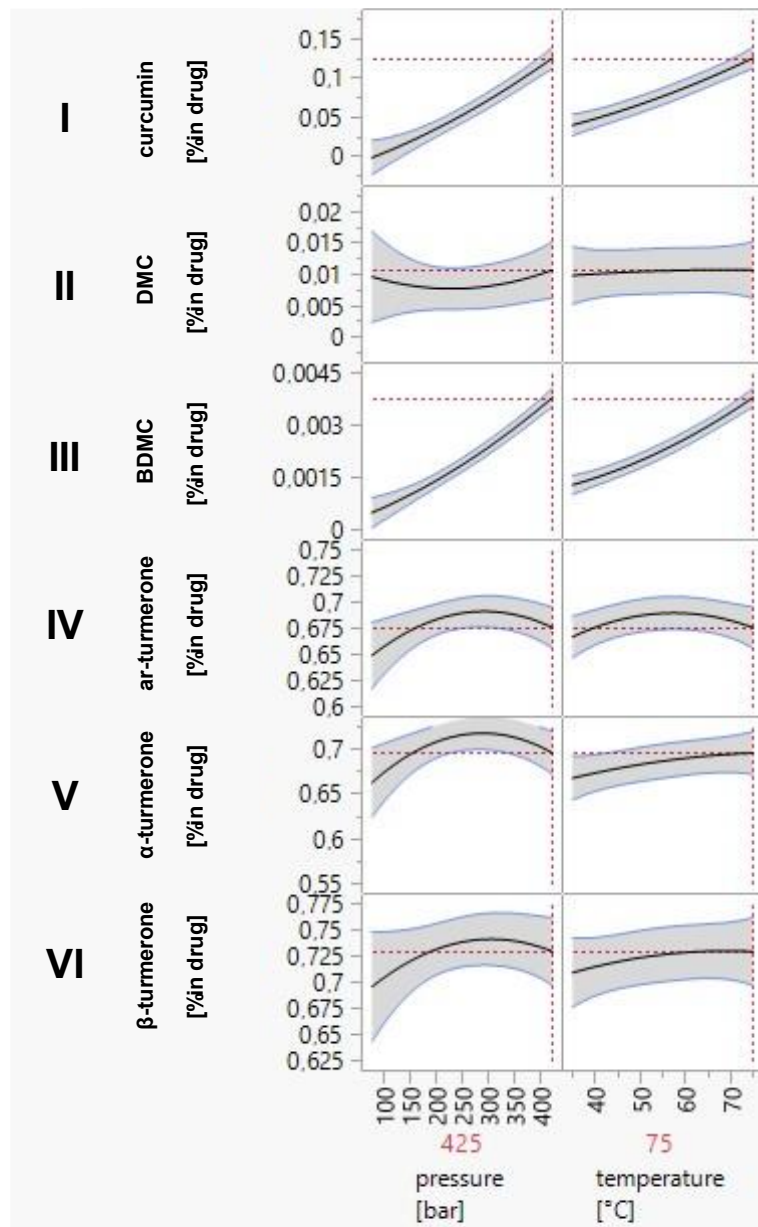


Figure 17 Prediction profiler diagrams with confidence intervals of significance level 0.05 show the separate influence of pressure and temperature on the recovery of all target compounds ((curcumin I, demethoxycurcumin II (DMC), bisdemethoxycurcumin III (BDMC), ar-turmerone IV, α -turmerone V, β -turmerone VI). The optimum extraction conditions for maximal compound recovery are marked with the red dotted lines: 425 bar and 75 °C [1].

The prediction profiler diagrams show the individual influence of temperature and pressure on extraction rates (Figure 17) [1]. A closer examination of the slopes and shapes of the curves in these diagrams reveals a much greater effect of temperature and/or pressure change on curcumin and BDMC recovery than on the yields of DMC and of the turmerones [1]. Due to the steeper slope upon changing the pressure, the influence of this latter parameter can be considered most significant (Figure 17 I-III) [1]. To optimize curcuminoid extraction would thus require maximum pressure conditions of 425 bar and intermediate to high temperature settings of 55 to 75 °C [1].

Turmerones generally have a better solubility in scCO₂ due to their rather non-polar sesquiterpene structure [1]. Nevertheless, they are considered to form part of the less-volatile essential oils [1,91,92]. They yielded maximal recoveries of <0.68–0.73% within a broad range of pressure and temperature settings (above 200 bar and 50 °C), with medium to high pressure and temperature being advantageous, as shown in Figure 16 [1]. The steeper slope of the pressure dependent prediction profiler graphs for the turmerones (Figure 17 IV-VI) indicates that pressure changes have a greater impact on their extraction rate than temperature changes [1]. Furthermore, an extraction process aiming at maximal turmerone recovery would be best performed at medium pressure and temperature settings (250 bar/55 °C) [1]. This is consistent with previous publications [1,251,252].

The extraction behaviour of turmerones and curcuminoids can be explained by their enhanced solubility in scCO₂ with increasing density, which is clearly visible even at small pressure changes above the critical point (73.8 bar; 31.0 °C) [1,85–87]. Furthermore, scCO₂ is described as a nondipolar, but it is also a quadrupolar solvent and a Lewis acid. This allows scCO₂ to dissolve turmerones as well as the more polar curcuminoids [1,105].

Maximizing compound recovery for both curcuminoids and turmerones reveals optimum extraction conditions at 425 bar and 75 °C based on the DoE [1]. If it would have been technically feasible to extend the design space to higher pressure and temperature conditions, it could be expected that the maximum would be found at more extreme conditions [1].

3.2.3. COMPARISON OF scCO₂ EXTRACTION AND CONVENTIONAL SOLVENT EXTRACTION

Comparing the optimized scCO₂ extract to *n*-hexane and methanol extracts reveals similar results for all three solvents when assessing turmerone recovery rates, yielding 0.66-0.86% (Figure 18) [1]. In contrast, curcuminoid extraction behaviour differed significantly, with methanol yielding by far the highest curcuminoid concentrations of approximately 1.5% for curcumin, 0.57% for DMC and 0.48% for BDMC, and with *n*-hexane yielding the lowest amounts of < 0.0026% for curcumin, 0.0013% for DMC and 0.0013% for BDMC [1]. The scCO₂ extract showed intermediate curcuminoid concentrations of approximately 0.11% for curcumin, 0.02% for DMC and 0.004% for BDMC, which is in line with expectations considering its polarity as a quadrupolar solvent and a Lewis acid [1,105]. This allows scCO₂ to interact with the hydroxy and ether groups of the curcuminoids, which goes along with a solubility of these compounds ranging between the nonpolar *n*-hexane and the highly polar methanol [1]. Without the use of potentially toxic solvents, both turmerones and curcuminoids can be extracted with scCO₂ [1]. Thereby, the composition pattern can be varied using pressure and temperature settings [1].

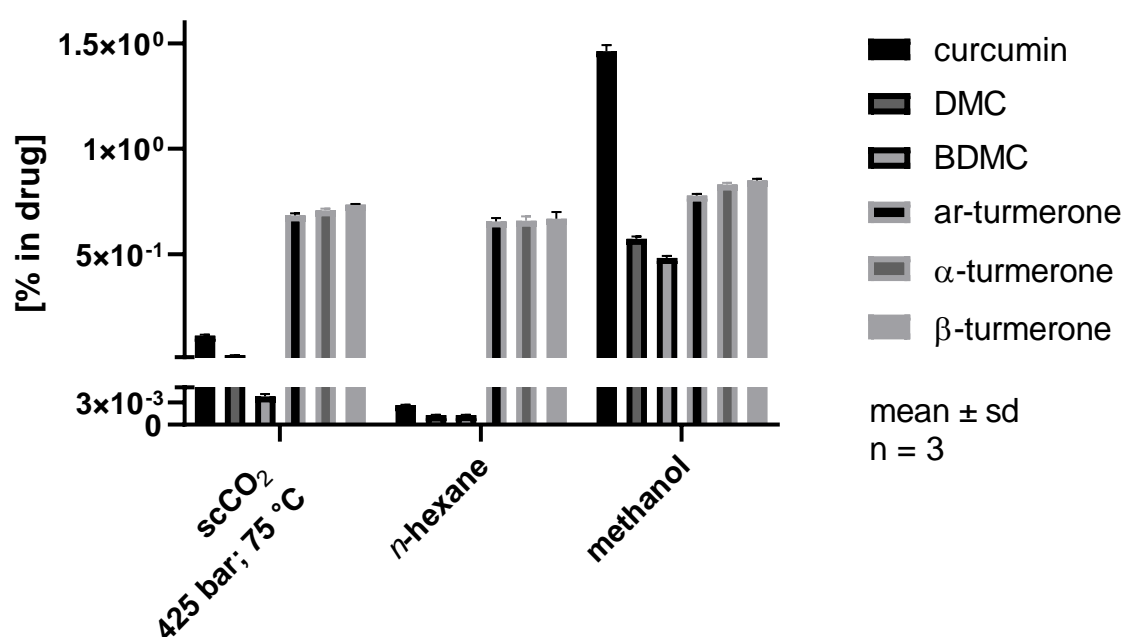


Figure 18 Comparison of a scCO₂ extract characterized by maximum curcumin and ar-turmerone yields with *n*-hexane and methanol extracts [1].

3.2.4. WATER CONTENT IN EXTRACTS

It is known from the literature that residual water in the drug is co-extracted during the scCO₂ extraction process, especially at higher temperatures [1,91]. To this end, the water content in the scCO₂ extracts, that were withdrawn directly from the separator according to Table 6, was determined (Figure 19) [1]. As expected, the water content for the three scCO₂ extracts 42535, 42555 and 42575 increases as temperature increases, from approximately 30% for 42535 to 56% for 42575 [1]. The high amount of co-extracted water again underlines the role of scCO₂ as a quadrupolar solvent [1]. In contrast, the conventional solvent extracts, as well as the scCO₂ extract, that was taken from the plant as a methanolic solution with subsequent removal of the solvent, were considered to be water-free due to the solvent removal during production [1].

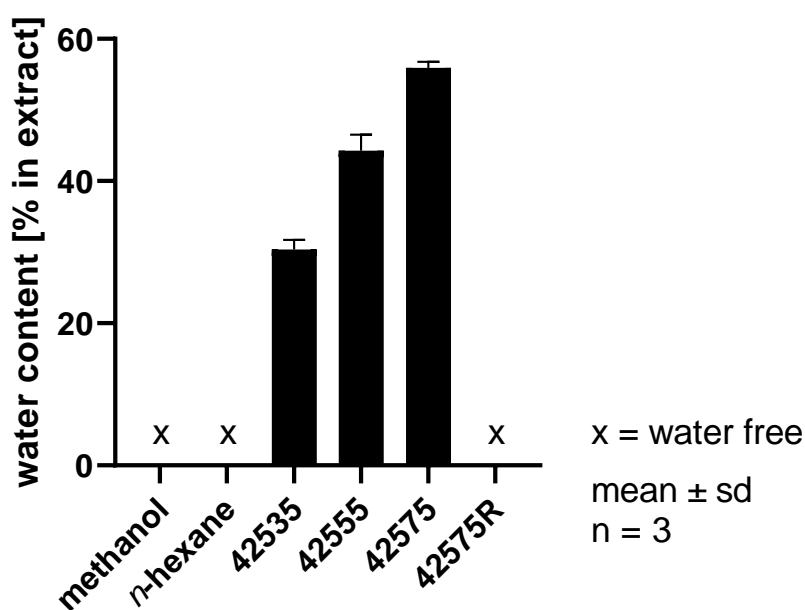


Figure 19 Water content in conventional solvent extracts with the solvents methanol and n-hexane and in scCO₂ extracts produced at 425 bar and 35 °C (42535), 55 °C (42555), 75 °C (42575), and 75 °C dissolved in methanol with subsequent removal of solvent (42575R); determined using Karl Fischer semi-micro water determination [1].

3.3. STABILITY STUDY OF EXTRACTS

The hydrolytic degradation of curcumin has been described to follow second order kinetics and to be highly dependent on the pH value of the aqueous phase [1,23]. Its antioxidant activity has been explained as a degradation reaction driven by its phenolic groups [1,253]. In order to evaluate whether the different solvents and extraction conditions during scCO₂ extraction affect the compound stability, samples were stored at 22 and 40 °C in the dark [1]. Remarkably, all extracts separated into at least two phases after storage of only 28 days [1]. The *n*-hexane extract and the scCO₂ extracts separated into a clear oily phase on top of a cloudy semi-solid phase [1]. In addition, the scCO₂ extracts that were directly recovered from the separator (42535, 42555, and 42575) developed a third phase consisting of small water drops at the bottom of the storage containers [1]. The methanol extracts showed separation into a clear, fluid oily phase at the bottom of the containers layered by a second phase which became harder and coarser with time [1]. In the literature, the growth of curcumin crystals in aqueous solutions has already been described when the solubility limit is exceeded [1,254]. Likewise, methanol extracts showed the formation of coarse crystals [1]. All other extracts remained either liquid or semi-solid with visibly small crystals only [1]. Thus, all extracts were thoroughly homogenized prior to sample analysis [1]. Figure 20 to Figure 25 show the concentration profiles of the main compounds during six months of storage [1].

Both the methanol extract (Figure 20, methanol) and the *n*-hexane extract (Figure 21, *n*-hexane) revealed almost no change in the concentration of the marker substances throughout storage [1]. Figure 22 to Figure 24 show the contents of individual constituents of the scCO₂ extracts that were produced under maximum pressure (425 bar) and at different temperatures (35 °C, 42535; 55 °C, 42555; 75 °C, 42575) [1]. All these extracts were directly recovered from the separator without the addition of any further solvents [1]. The extract produced at 35 °C did not show significant degradation of its constituents over the period considered, however degradation tendencies are evident in the extracts which were prepared at higher temperatures [1]. For the extract prepared at 55 °C, there were slight degradation tendencies of approximately 10% for α - and β - turmerone and 5% for the curcuminoids and ar-turmerone which were observed after 168 days [1]. The extract produced at 75 °C showed statistically significant decreases of about 30% in content for all three

turmerones after 168 days and of about 30% for the curcuminoids after 168 days, although that was not statistically significant [1]. However, no degradation products were detected using HPLC-DAD [1]. On the contrary, an extract that was also prepared at 425 bar and 75 °C, but dissolved in methanol for the removal from the separator, showed no degradation during storage at all (Figure 25, 42575R) [1].

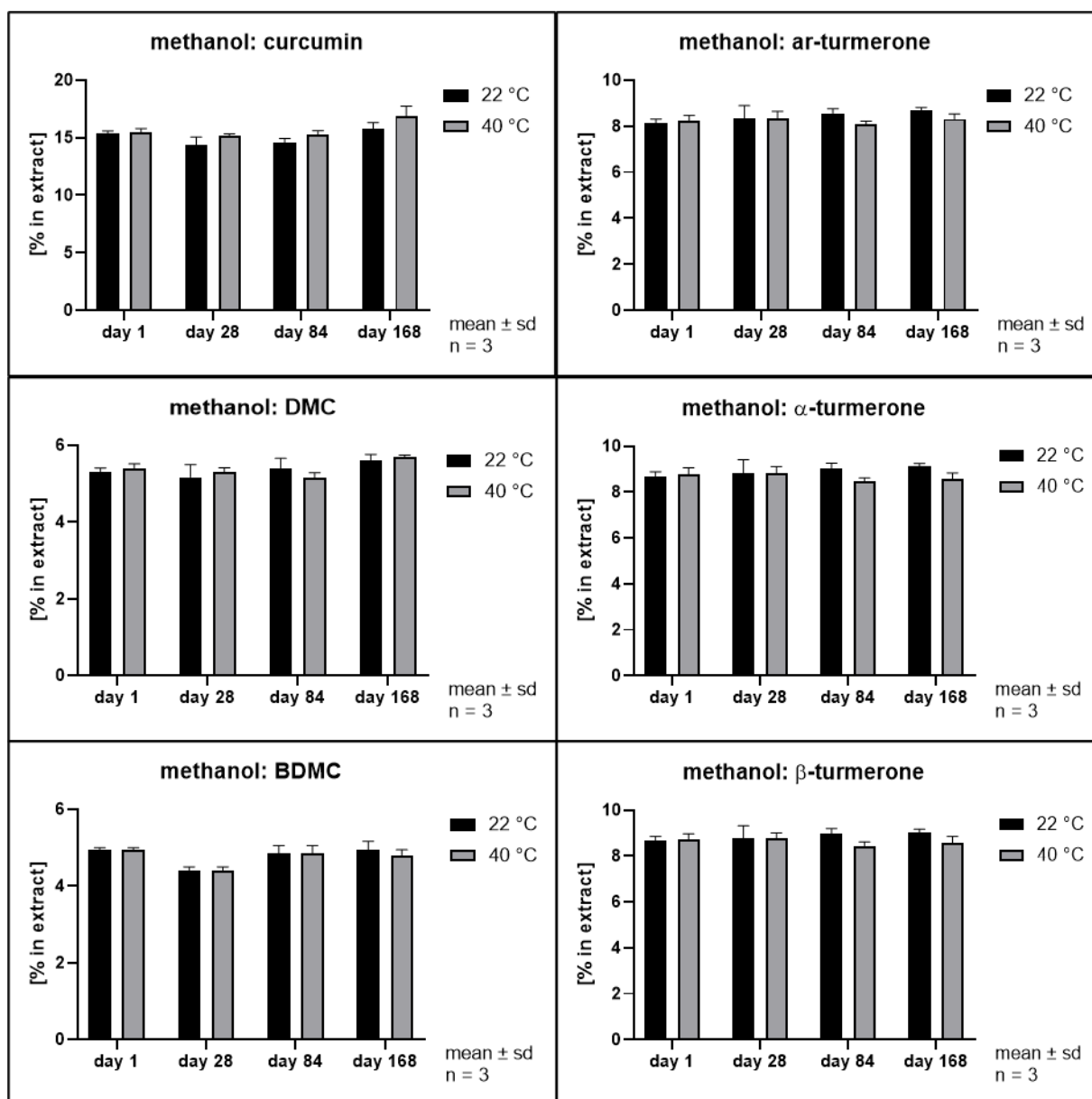


Figure 20 Contents of individual curcuminoids and turmerones in **methanolic solvent extracts** throughout storage [1].

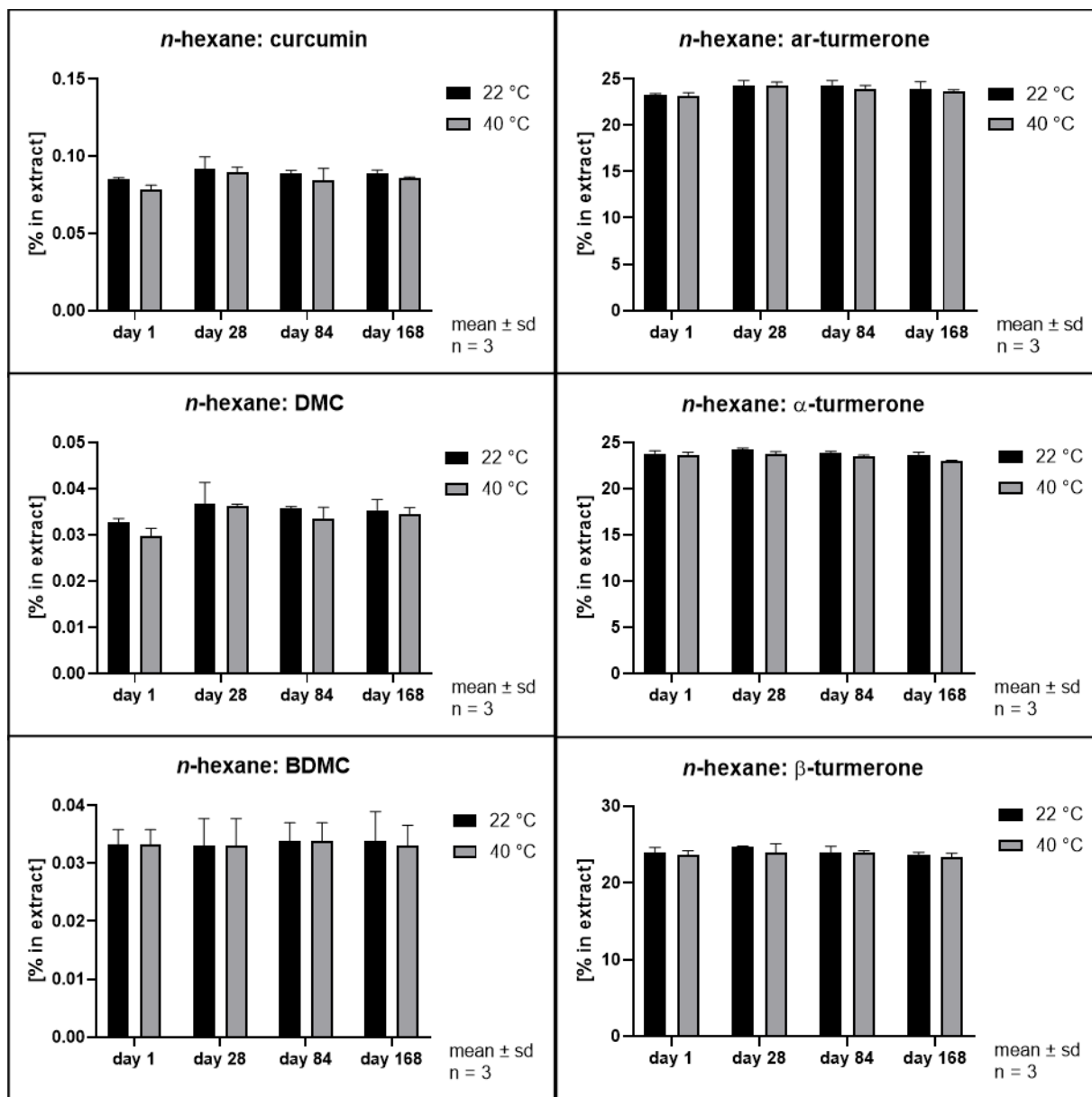


Figure 21 Contents of individual curcuminoids and turmerones in *n*-hexane solvent extracts throughout storage [1].

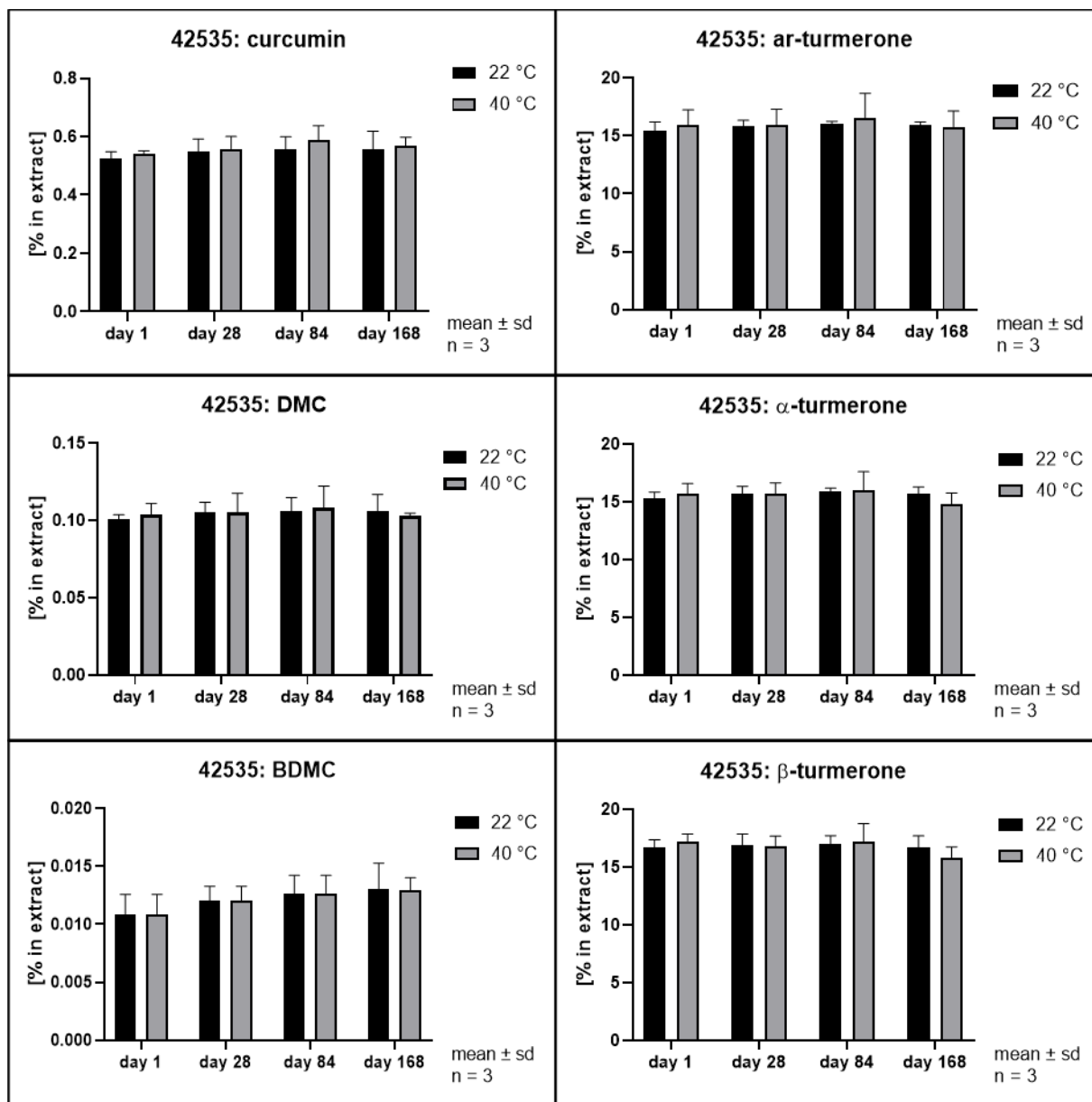


Figure 22 Contents of individual curcuminoids and turmerones in *scCO*₂ extracts throughout storage, extraction at 425 bar and 35 °C [1].

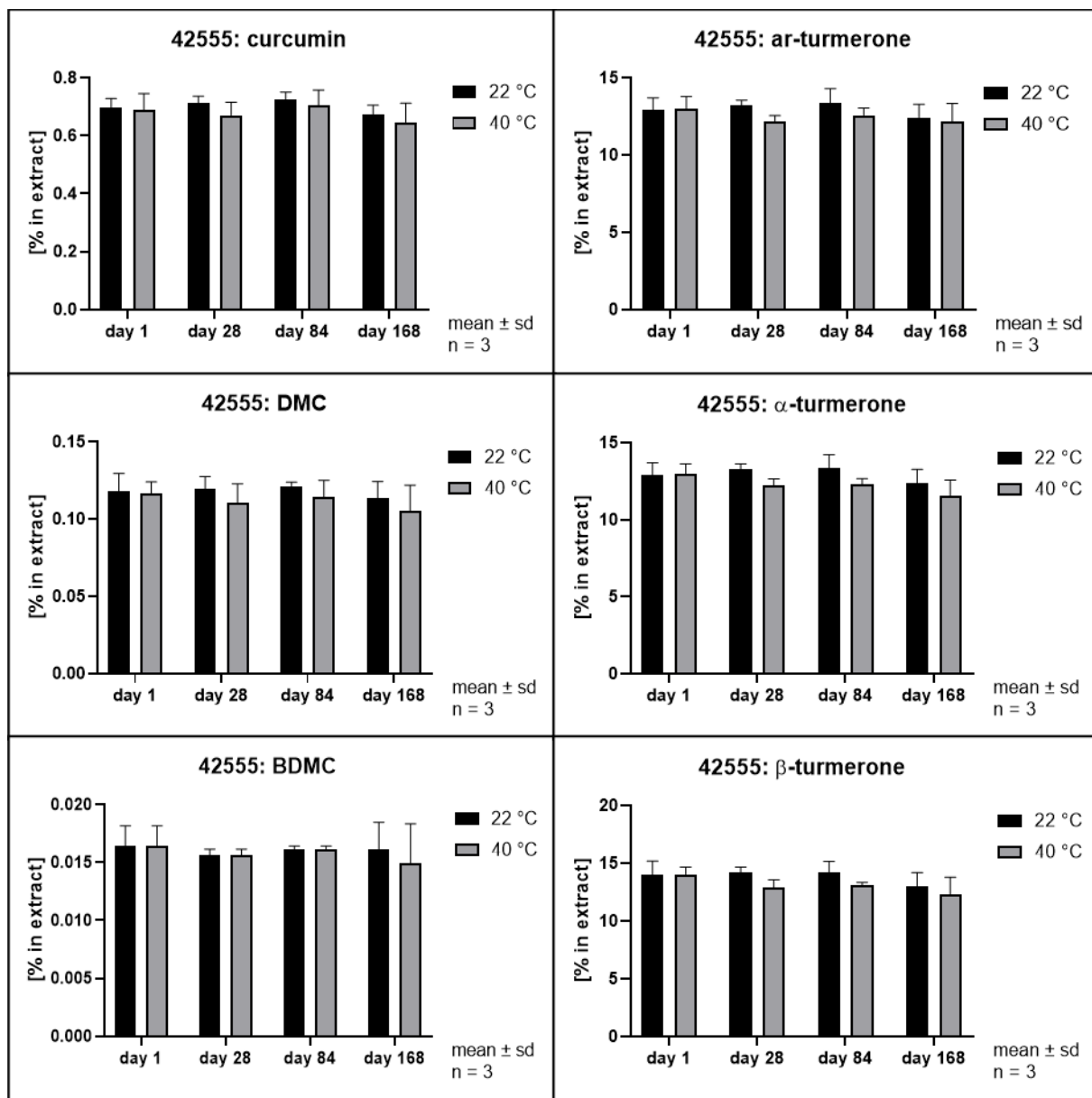


Figure 23 Contents of individual curcuminoids and turmerones in *scCO₂* extracts throughout storage, extraction at 425 bar and 55 °C [1].

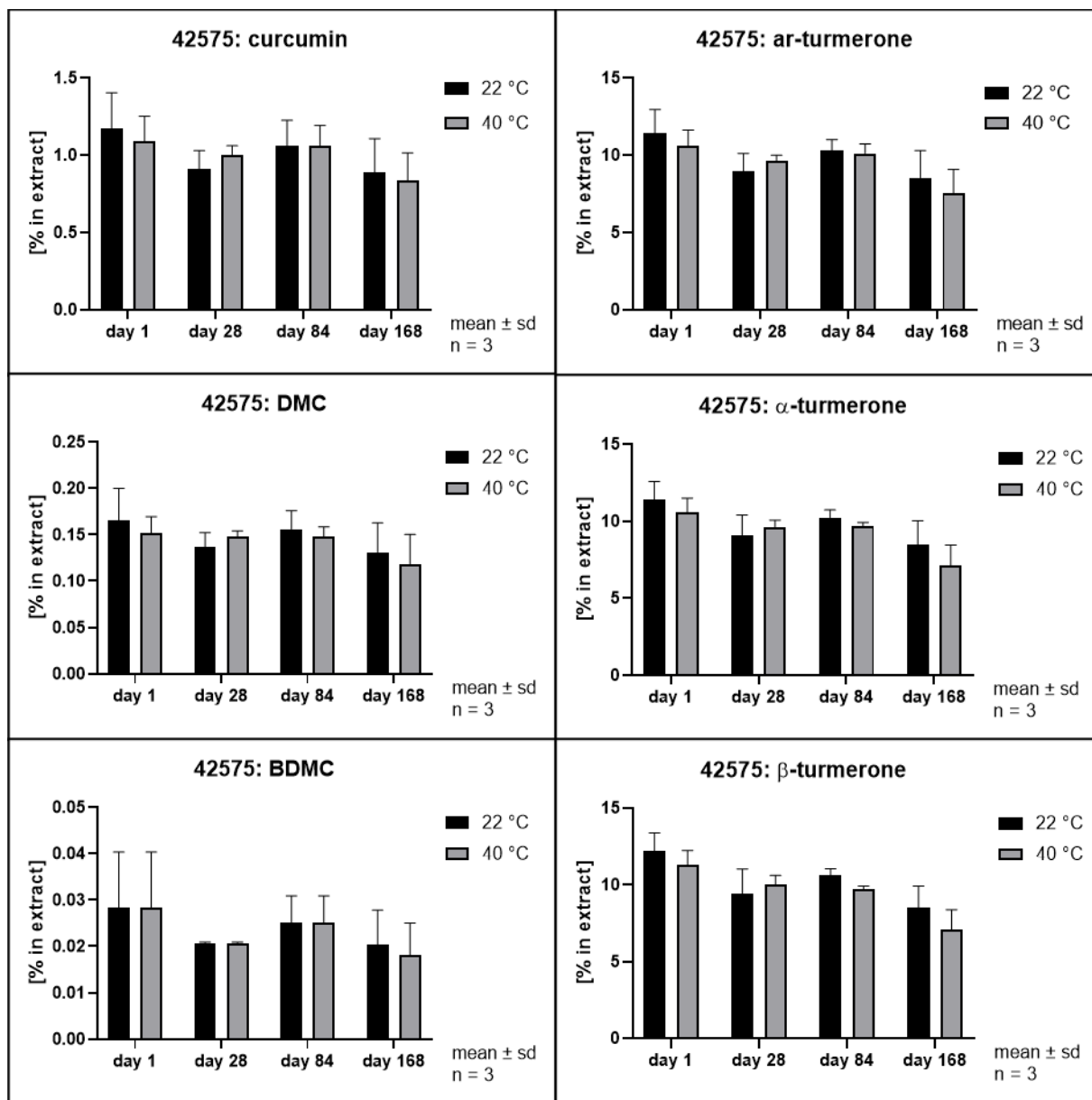


Figure 24 Contents of individual curcuminoids and turmerones in *scCO*₂ extracts throughout storage, extraction at 425 bar and 75 °C [1].

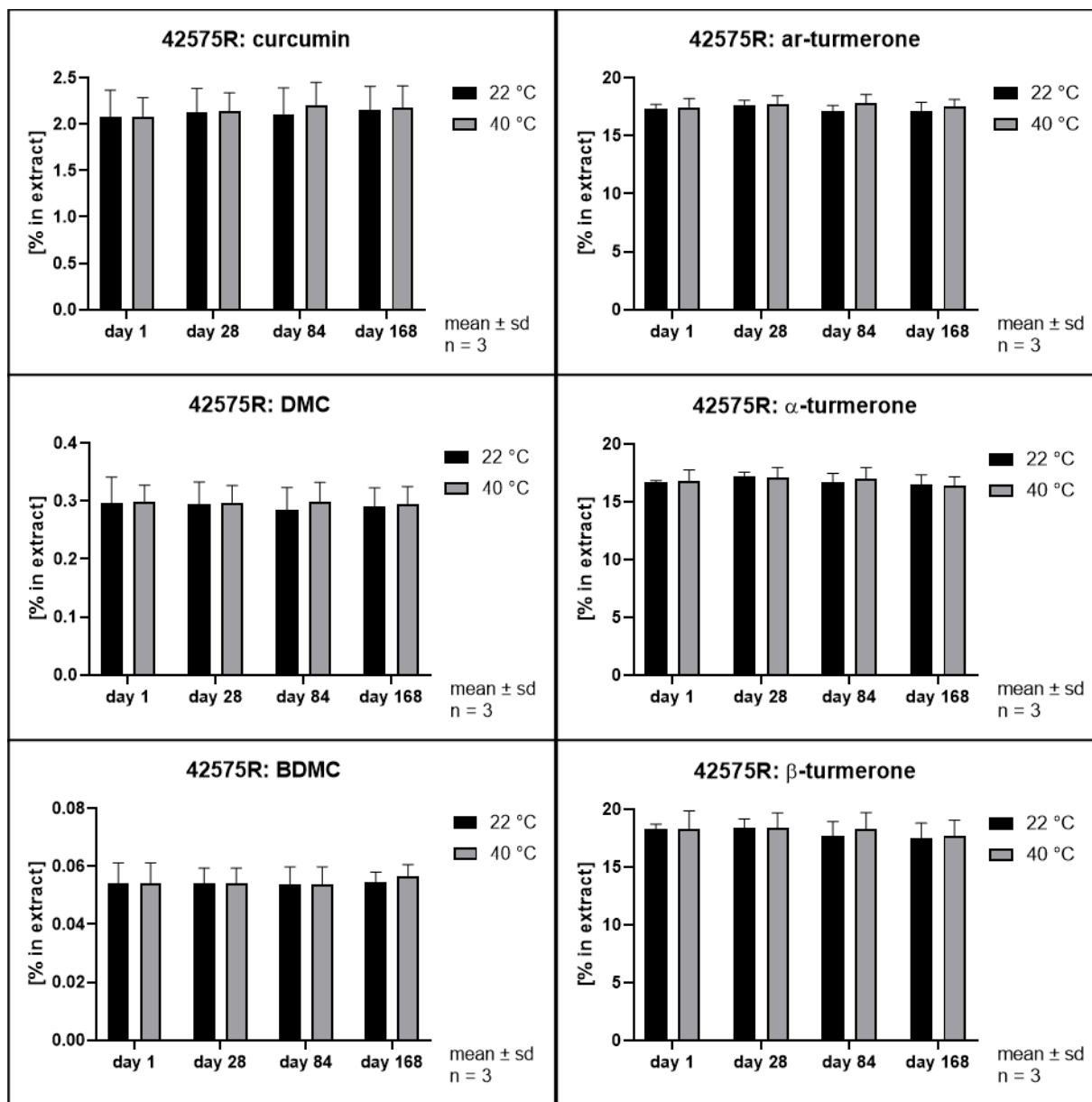


Figure 25 Contents of individual curcuminoids and turmerones in *scCO*₂ extracts throughout storage, extraction at 425 bar and 75 °C, extract recovery via methanolic solution [1].

Clearly, dissolving the extract in methanol and subsequent removal of the organic solvent improved the storage stability of the extract (42575 vs. 42575R) [1]. This follows an increase in the concentrations of the major components and a decrease in the water content (Figure 19) [1]. This can be explained by the simultaneous removal of water when methanol was removed, which in turn increased the content of the marker compounds in the remaining extract [1]. Obviously, a higher water content in the extracts is responsible for the faster degradation seen in extracts that have been prepared at higher temperatures [1], as displayed in Figure 26. Lower water content on the other hand seems not to affect storage stability accordingly.

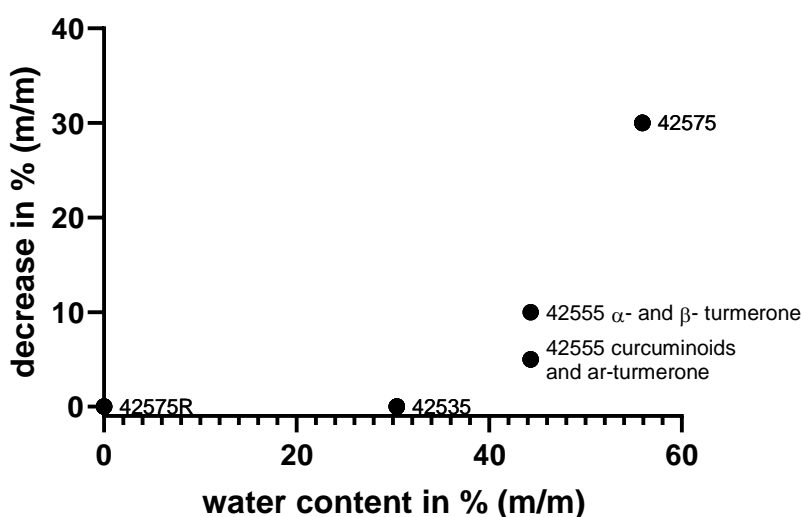


Figure 26 Decrease in concentration of marker substances after 168 days in relation to the initial water content of the scCO₂ extracts produced 425 bar and 35, 55, and 75 °C (42535, 42555, 42575) and recovered via methanolic solution (42575R).

Due to the presence of CO₂, the pH value of the aqueous phase of the extracts was found to be slightly acidic [1,91]. Thus, a very poor solubility of the curcuminoids in this water phase can be assumed [1,23]. It has been described that the hydrolytic degradation of curcumin follows a second order kinetics and that the half-life at a pH between 3 and 6 ranges from 146 to 175 days [1,23]. This is almost in line with the results demonstrated for the curcuminoids of extract 42575 (Figure 24) [1]. The poor water solubility of curcuminoids and the lower water content of extracts recovered at lower temperatures might be an explanation for the low degradation rates of the curcuminoids in extracts 42535 and 42555 [1]. The relatively slow acid-catalysed

hydrolytic degradation of curcumin is further delayed by its pronounced solubility in the lipid phase, by its crystallization during separation from scCO₂ following extraction and by recrystallization during storage [1,254,255]. This further explains the more pronounced degradation of curcumin in the scCO₂ extract with the highest water content (42575) [1]. Curcumin is known to be strongly susceptible to autoxidative degradation at neutral and basic pH [1,253,256,257] in an aqueous surrounding, whereas ar-turmerone has been described as degradable upon oxidative, photolytic, and thermal triggering [1,258]. This suggests that turmerone as well as curcuminoid degradation may be triggered by autooxidation in the presence of co-extracted water [1]. In contrast, specific degradation routes have not yet been described in the literature for the turmerones [1]. However, their highly lipophilic character alongside very poor solubility in water may be the reason for their very slow degradation, even in the extract characterized by the highest water content (42575) [1].

Interestingly, storage temperature (22 or 40 °C) only slightly and insignificantly affected the stability of the extracts, as can be deduced from Figure 20 to Figure 25 [1]. This was unexpected as according to the van't Hoff rule a significantly higher reaction rate should result at higher temperatures [1,259]. However, our results are in line with the behaviour of curcumin in acidic oil-in-water emulsions and solutions as published by Kharat et al. [1,254]. A possible explanation for this deviation from van't Hoff's rule might be the overlap of several effects including the very poor water solubility [260,261], changes in distribution equilibrium and recrystallization due to distinct polymorphism of curcumin [1,255]. This results in a very complex scenario which is typical of multicomponent mixtures, but prevents the identification of monocausal explanations [1].

3.4. DEVELOPMENT OF CAPSULE FORMULATIONS WITH scCO₂ CURCUMA EXTRACT

3.4.1. COMPATIBILITY OF COMPONENTS FOR CAPSULE FORMULATIONS

At first, compatibility of all components for capsule formulation had to be investigated. As compatibilities of hard fat, polyethylene glycol and mesoporous silica particles with hard gelatine capsule shells have already been confirmed [158,181,203,234], the behaviour after the addition of the scCO₂ extract had to be tested. The used scCO₂ extract was produced at optimum extraction conditions (425 bar/ 75 °C) and had a very high water content of 56% according to 3.2.4. Hard gelatine capsule shells soften very quickly in the presence of water or they already dissolve in slightly acidic water phases, especially at temperatures over 30 °C [262]. Therefore, the water content of the extract may cause incompatibilities when filled into capsules.

Hard fat has proven to be practically insoluble in water [162,163]. As a matrix-forming excipient, hard fat may allow emulsification of the water in the extract during mixing (according to 2.2.14.2) and rapid solidification after filling the melt into the capsules [263]. This could be enhanced by a comparably high hydroxyl value for Witepsol W45 (corresponding to high amounts of mono- and diesters) or the addition of a surfactant in case of Witepsol S58. PEG 4000 on the other hand is easily soluble in water [164]. The water, as well as the lipophilic parts of the extract, might be bound within the PEG 4000 matrix as a solid dispersion [264]. In contrast to the matrix forming out of melt, Aeroperl silica particles are able to entrap liquids and solids onto their porous surface by adsorption. The composition of substances loaded onto the silica surface determines the interactions of adsorption and their release [229]. Since silanol groups on the silica surface are likely to form H-bonds with water or other hydrophilic molecules [220], the binding of water in addition to lipophilic substances should be possible.

Preliminary studies showed that, independent from the matrix-forming excipient, all formulations using the raw scCO₂ extract softened the capsule shells and led to severe deformation even at extract concentrations below 20% at least after one day. Obviously, all formulations comprising the raw extract were not suitable to be filled into hard gelatine capsules.

The high amount of water in the raw scCO₂ extract was clearly not sufficiently bound within any of the matrix systems to avoid diffusion into the capsule shells. As an additional measure, the scCO₂ extract was dried before further processing until a mass reduction of about 55% was reached, which means that approximately 98 % of the 56% water content had been removed.

As a suitable method, freeze-drying was chosen.

Freeze drying according to 2.2.10 led to a 55.3% mass reduction of the raw extract. Compatibility tests using this dried extract showed no softening of capsule shells or deformation.

The possible migration of other extract components from the filling into the capsule shell was not expected for the scCO₂ extract, since this has been described mostly for hydrophilic, water-soluble substances [158].

3.4.2. LOADING AND CHARACTERISATION OF MATRIX SYSTEMS

Liquids in unsealed hard gelatine capsules tend to leak from the capsules by being drawn into the gap between both capsule shells by capillary forces. Therefore, hard capsules are frequently sealed when liquid fillings are used [172]. With the intention of eliminating the need for sealing, the capsule filling had to be designed in such a way as to ensure that the liquid extract inside was completely bound by a matrix substance.

A method for determination of the loading capacity was developed for characterisation of the loaded matrix systems for capsule filling (2.2.11). The same manufacturing process was used for all samples to minimise possible influences on the microstructure.

Table 13 Maximum loading capacity for freeze-dried scCO₂ extract (425 bar; 75 °C) in different matrix systems in % (m/m): hard fat Witepsol W45, hard fat Witepsol S58, PEG 4000, Aeroperl 300. Leakage on filter paper marked with arrows.


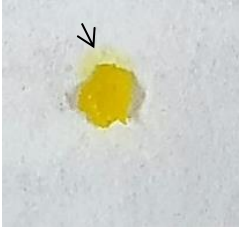

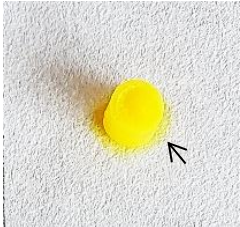







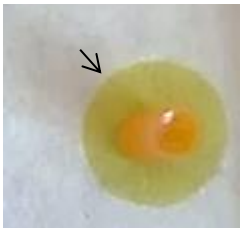


	Results according to Method 2.2.11.1		Results according to Method 2.2.11.2.	
	max. loading capacity	overloaded	max. loading capacity	overloaded
Witepsol S58	 19.4%	 24.9%	 19.4%	 24.9%
Witepsol W45	 24.9%	 28.8%	 24.9%	 28.8%
PEG 4000	 24.9%	 28.8%	 57.3%	 64.2%
Results according to Method 2.2.11.3				
	max. loading capacity		overloaded	
Aeroperl 300 Pharma	 64.2%		 71.7%	

Table 13 shows photographs of extract-exciipient mixtures at the maximum determined loading capacities as well as the corresponding approximately 5 % overloaded matrix system. The leaked liquid scCO₂ extract is displayed marked with arrows. Binding capacity was tested with two slightly different methods (2.2.11.1 and 2.2.11.2).

Table 14 Summary of determined loading capacity: stable (+), leakage (-), stable according to method 2.2.11.2 but not according to method 2.2.11.1 (+/-); To simplify the presentation, only the data surrounding the maximum loading capacities is shown. Melting points according to safety data sheets.

Matrix	Melting Point [°C] [ref.]	Extract Concentration [% (m/m)]								
		19.4	21.2	24.9	26.8	57.3	60.6	64.2	67.8	
Witepsol S58	31.5 – 33.5 [162]	+	-	-	-	-	-	-	-	-
Witepsol W45	33.5 – 35.5 [163]	+	+	+	-	-	-	-	-	-
PEG 4000	50 – 58 [164]	+	+	+	+/-	+/-	-	-	-	-
Aeroperl 300 Pharma	> 2000 [165]	+	+	+	+	+	+	+	+	-

Table 14 summarizes the loading capacities determined for the four matrix systems. To simplify the presentation, only the data surrounding the limits of loading capacity is displayed. Interestingly, the lipophilic hard fat matrices held the lowest extract content of approximately 20 to 25%, whereas the hydrophilic PEG 4000 carried over 57% of the lipophilic extract and mesoporous Aeroperl carried even more at over 64%.

Regarding the hard fat matrices, Witepsol S58 showed the lower maximum loading capacity (19.4%) when compared with Witepsol W45 (24.9%). The results of both methods coincide for the hard fat matrices. As the oil-binding capacity of hard fat is highly affected by the composition of the mixture, various effects could explain these results: (1) The higher melting point of Witepsol W45 compared to Witepsol S58, displayed in Table 14, indicates a higher solid fat content and therefore lower mobility of the molecules which results in higher oil-binding capacity [192]. (2) Since the liquid components of the bound extract are lipophilic molecules with turmerones as the main components, a high compatibility with the surface of the lipophilic nanoplatelets from the hard fat matrix can be assumed [194]. (3) Surface-active additives in Witepsol S58 may affect the nano- and microstructure and therefore the oil-binding capacity [193]. For a detailed clarification of the crucial effects on extract-binding in hard fat matrices, further experiments should be performed.

For the PEG matrix, maximum loading capacities of 24.9% (method 2.2.11.1) and 57.3% (method 2.2.11.2) were determined. Interestingly, only here did the determined maximum loading capacity differ, by factor 2, depending on the method used. The difference between these two methods not only originates from the differing contact area to the filter paper, but might also be affected by the pipetting process of the homogenised melt into the plastic ring and the slightly faster solidification due to higher contact with unheated surfaces in method 2.2.11.2. The pipetting may affect the mixing and emulsification into smaller droplets of extract in the PEG matrix system immediately before cooling. In addition, the initiation of crystallisation by cooling and shear stress due to the pipetting may result in a different crystal structure and therefore a higher extract loading capacity [130,210,211]. Further experiments such as differential scanning calorimetry or microscopic images may confirm this hypothesis.

In case of the scCO₂ extract, PEG was the only hydrophilic matrix system that carried the lipophilic liquid out of the melt and additionally has the highest melting point for the plain matrix. These could be the reasons why the discrepancy in the results of the two methods only occurs with this matrix system. With regard to capsule filling, method 2.2.11.2 appears to be closer to the processing conditions due to the pipetting step and the faster cooling. Since the incorporated scCO₂ extract was a complex multicomponent system, many incorporation mechanisms such as encapsulation or co-crystallization seemed possible, causing for example increasing hydrophobicity and decreasing crystallinity, due to extract components, that may also lead to increasing oil loading capacity [130].

The Aeroperl 300 matrix system shows the highest loading capacity of nearly 65%. It is noticeable that the overloaded matrix differs not only by leakage but also by a visibly clear decrease in flowability from the matrix at maximum loading capacity. The photograph shows the lumpy, sticky texture of the overloaded Aeroperl matrix in contrast to the powdery, freely flowing Aeroperl matrix at maximum loading. The maximal load for the scCO₂ turmeric extract of approximately 65% is in line with the oil loading capacities reported in the literature for propylene glycol dicaprylocaprate or oil from eucalyptus, peppermint, lemongrass and citronella [227,232–234]. However, when looking at the photographs, it seems unlikely that the extract is adsorbed exclusively in the pores. Rather, it seems plausible that the incorporation into the pores has already been exceeded and the extract was not only absorbed in the pores but

was also adsorbed to the outer surface of the particles. This explains changes in flowability. Supposedly, the crystallized components of the scCO₂ extract adsorbed onto the outer surface of the carriers or got dragged into the pores with the liquid extract.

A closer look at the melting points of the matrix substances displayed in Table 14 reveals that there seemed to be a relationship between extract loading capacity and melting point, at least for the matrix systems loaded by melting. Perhaps the solidification of the extract-loaded melt at room temperature happened faster for the PEG matrix from 60 °C, than for the hard fat matrices from 40 °C. The faster increase in viscosity might as well include the faster immobilisation of entrapped extract. Further investigations with different cooling rates could help clarify whether the loading capacity, in general, is affected by the cooling rate from melt-to-solid state.

The highest extract loading capacity for the mesoporous silica carriers is presumably a consequence of the combined mechanisms of hydrophilic adsorption by H bonds and capillary forces that dragged the liquid components into the pores of the particles.

3.4.3. MICROSCOPIC CHARACTERISATION OF MELT MATRIX SYSTEMS

Triacylglycerols (TAG) are known for forming anisotropic, birefringent crystals that can be seen using polarized light microscopy [180,184]. Since the influence of microstructure and crystal size on oil-binding capacity has already been confirmed for different TAGs [180,184–186], the influence of the scCO₂ extract on the microscopic structure was investigated. Moreover, the complex influence of scCO₂ extract on polyethylene glycol (PEG) was examined, since PEG is known for co-crystallization with different APIs [211,265] and encapsulation of liquid essential oil [130,212,215]. Also, curcuminoids have a strong tendency to form birefringent crystals [141].

Figure 27 displays polarization microscopic images of the pure matrix substances Witepsol S58 and W45, PEG 4000 and the pure scCO₂ extract. Figure 28 shows polarization microscopic images of all matrix formulations loaded via melt. Figure 28 displays the matrix systems loaded with extract at maximum loading capacity in the middle, on the left is the matrix system containing an extract concentration 5% below the determined maximum loading capacity and on the right is the matrix system containing an extract concentration 5% above the determined maximum loading capacity. For the matrix system, 5% above a maximum loading capacity leakage can be expected according to 3.4.2.

For the Witepsol S58, which is the hard fat with the additional surface-active ingredients, crystal textures were displayed in all three extract concentrations as well as in the pure substance. However, their accumulation and the contact between them seemed to decrease with increasing extract concentration. The size of the crystal textures at the extract concentration 5% below maximum loading capacity appeared to be around 250 µm and therefore smaller than for the other two concentrations where they were about 500 µm in size; for the pure matrix the crystal textures were below 50 µm. Additionally, small crystals were visible with a yellowish contrast to the matrix, originating from the extract component (shown in Figure 27) and whose concentration increases with increasing extract concentration. The appearance of the matrix of the Witepsol W45 differed a lot from the Witepsol S58 as there was no crystal texture visible for the extract holding matrices, but rather a filamentous structure in all concentrations. In the pure matrix of Witepsol W45, on the contrary, a distinct crystal texture was visible. In addition, even more small extract crystals were observed than for Witepsol S58.

As expected, the microscopic images of the PEG 4000 matrix and formulations differed considerably from those of the hard fat matrices. All images showed colourful crystal textures that touched each other, but their sizes seemed to decrease with increasing extract concentration. The pure PEG 4000 entirely consisted of large distinct crystals and for the lowest extract concentration, there were areas of large crystal textures and some areas with very small ones. The frequency of largely textured areas decreased with increasing extract concentration in favour of smaller crystal textures. Interestingly, no crystals were visible originating from the extract, although the extract concentrations here were significantly higher than in the hard fat formulations.

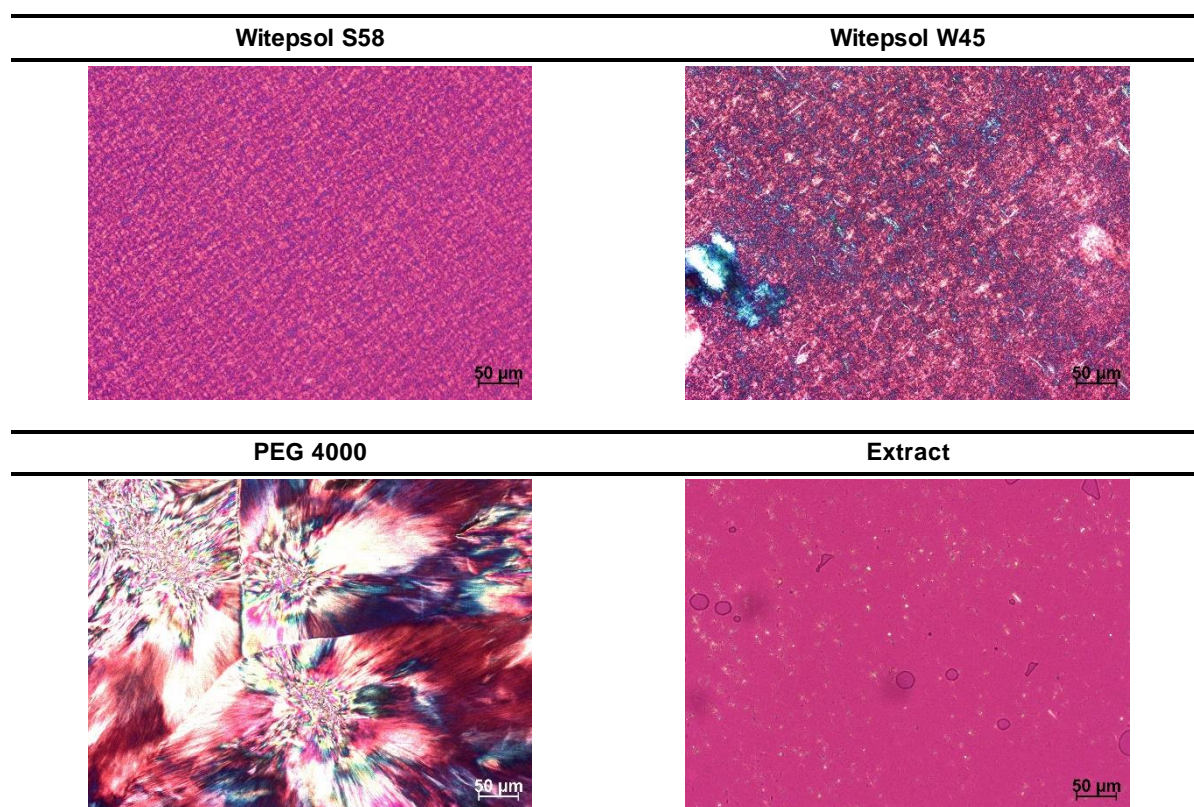


Figure 27 Microscopic images of pure substances of Witepsol S58, Witepsol W45, PEG 4000, and dried scCO₂ extract; images were taken via polarisation microscopy, magnification 20x.

None of the images shows a homogeneously dispersed extract and no signs of phase separation of liquid and solid constituents within the matrix, even when the maximum loading capacity was exceeded.

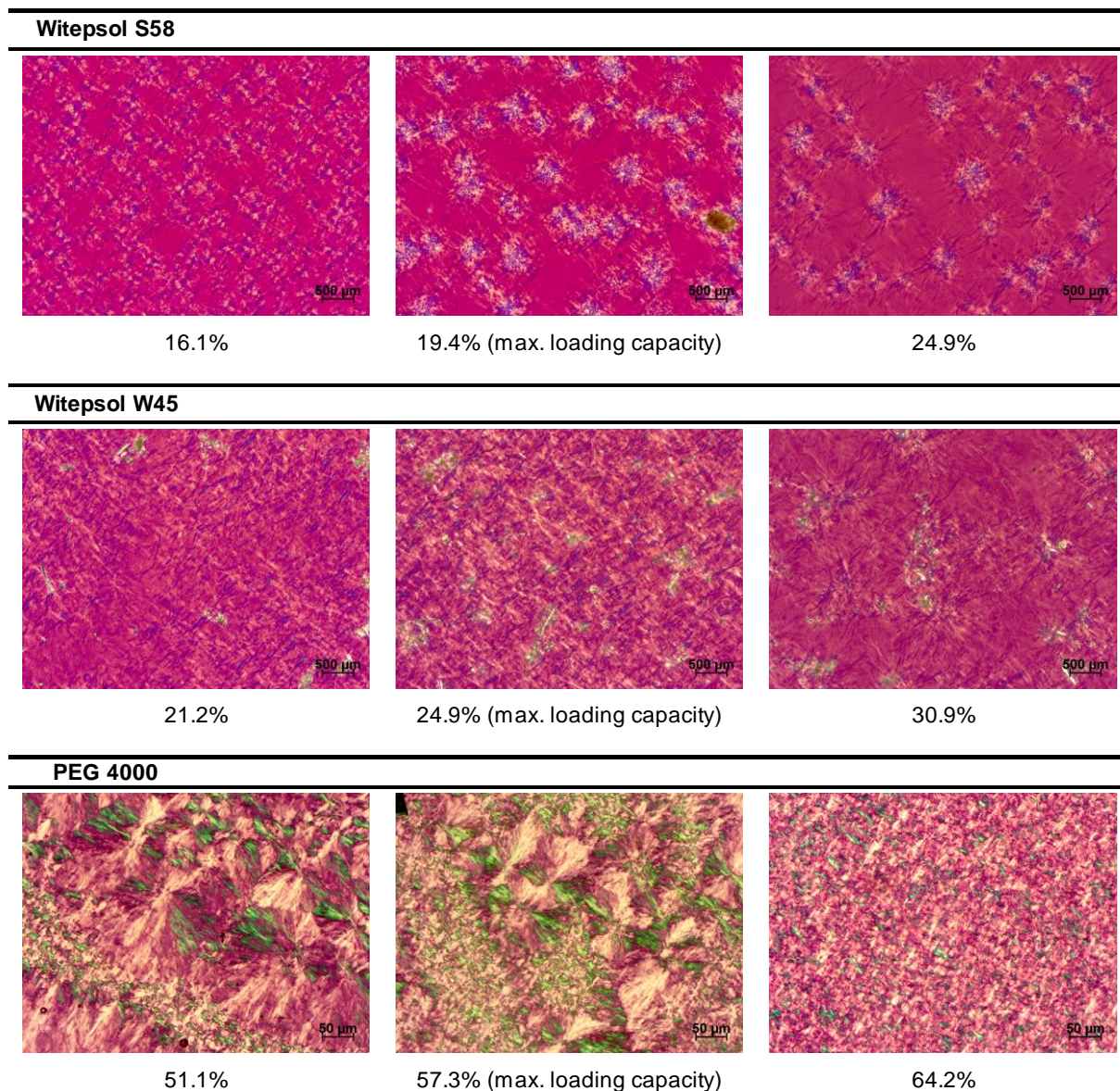


Figure 28 Microscopic images of Witepsol S58, Witepsol W45, and PEG 4000 with dried scCO₂ extract in different concentrations [% (m/m)], images were taken via polarisation microscopy, magnification 20x (PEG 4000) or 40x (hard fat).

Birefringence is an indication of ordered crystalline structures within a matrix. The fact that these decrease with increasing extract concentration indicates that the extract disturbs crystallization or even leads to smaller, less visible crystals.

The bigger size of microstructural elements for the Witepsol S58 than for Witepsol W45 goes in line with its lower extract loading capacity. As already mentioned in 3.4.2, bigger crystal sizes lead to the exclusion of liquid components and therefore lower oil-binding capacity [180,184,185]. Crystal size can be affected by the production process as well as the composition of the formulation. As the processing conditions, especially the cooling process, were almost the same, differences in the hard fat matrix substances may have been responsible for the different appearances.

The surface-active additives in Witepsol S58 are polyoxyethylene (25) cetyl stearyl ether and stabilised glyceryl ricinoleat [162]. They raise the hydroxyl value of the hard fat, shown in Table 4, and thus increase solubility of hydrophilic or amphiphilic substances. It seems possible that the combination of additional surfactants and the lower melting point (Table 14) caused the lower extract loading capacity for Witepsol S58 compared with Witepsol W45, but the limited scope of matrix variation in this study can only allow limited assumptions.

3.4.4. UNIFORMITY OF DOSAGE UNITS ACCORDING TO PH. EUR. 2.9.40

For the evaluation of the capsule production method for the developed capsule formulations, uniformity of dosage units was tested according to Ph. Eur. 2.9.40 (2.2.16) [243]. Three batches of each formulation were prepared according to 2.2.14 with scCO₂ extract concentrations shown in Table 15. The tested extract concentrations were chosen exceptionally close to the maximum loading capacity. Negative deviations in terms of uniformity are not to be expected for the formulations when concentrations are changed below the maximum loading capacity.

Table 15 Extract and component concentrations of capsule formulations tested in MV and CU.

Matrix	Extract Concentration [%]	Extract Concentration [mg/capsule]	Curcuminoids [mg/capsule]	Turmerones [mg/capsule]
Witepsol S58	21.2	95	2.44	57.30
Witepsol W45	16.1	71	1.83	42.94
PEG 4000	21.2	109	2.82	66.40
Aeroperl 300 Pharma	57.3	127	3.25	76.58

3.4.4.1. UNIFORMITY OF DOSAGE UNITS: MASS VARIATION

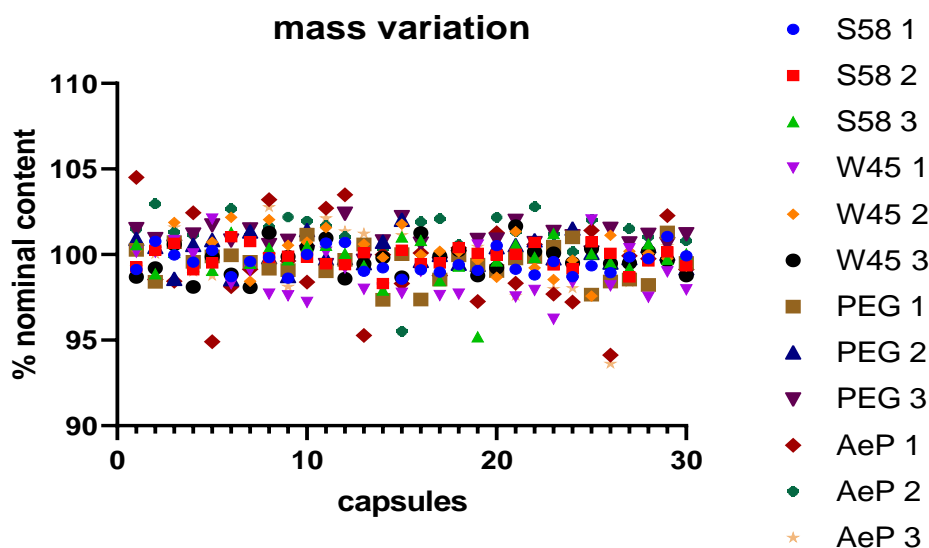


Figure 29 Mass Variation test according to Ph. Eur. 2.9.40 for three batches of each formulation: nominal capsule content refers to extract concentration shown in Table 15.

Figure 29 shows the nominal extract contents calculated from the masses of the capsule fillings. All batches analysed showed nominal contents of 93.6 to 104.5%. Remarkably, the formulations based on mesoporous silica particles showed the largest variation within one batch compared to the other matrix systems. All capsules passed the criteria of an acceptance value $< L1$ and deviation $< L2$. Strictly defined, only the capsules filled with loaded mesoporous silica carriers should be assessed according to MV, because they are the only ones that carry enough extract ($\geq 25\%$, ≥ 25 mg/capsule).

3.4.4.2. UNIFORMITY OF DOSAGE UNITS: CONTENT UNIFORMITY

Figure 30 displays the nominal curcuminoid contents and Figure 31 shows the nominal turmerone content of 10 capsules analysed from each batch. All batches showed nominal contents between 85.4 and 105.5% for the curcuminoids and between 86.5 and 110.5% for the turmerones. All tested batches passed the criteria of an acceptance value $< L1$ and deviation $< L2$ for the curcuminoids and turmerones, although for both groups two batches of the formulations based on Witepsol S58 had individual capsules that differed in content to such an extent that they almost failed the criterion for deviation $< L2$. This indicates that homogenization in the manufacturing of the capsule formulations based on Witepsol S58 could potentially be optimized.

content uniformity curcuminoids

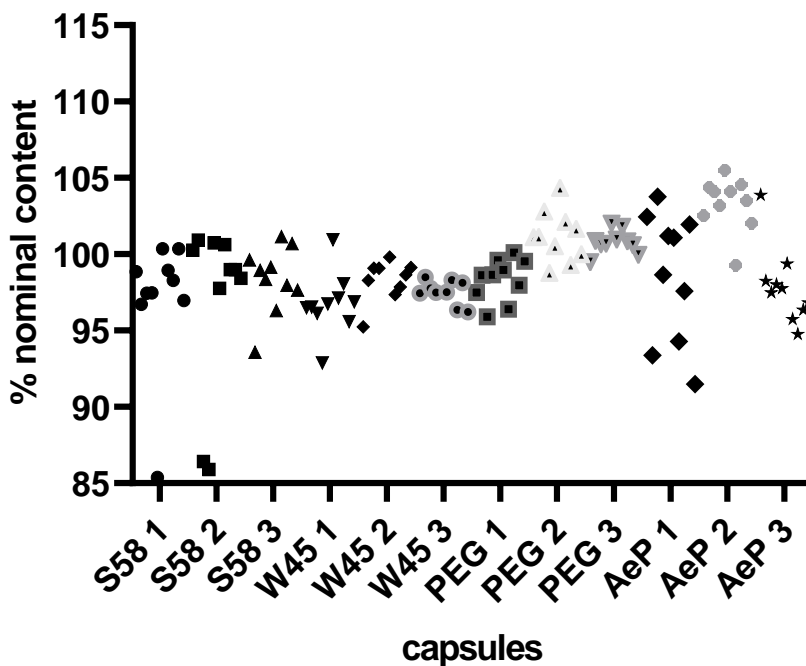


Figure 30 Content Uniformity test according to 2.9.40 for three batches of each formulation: nominal contents of the sum of curcuminoids (curcumin, demethoxycurcumin, bisdemethoxycurcumin) capsules, all contents refer to target contents shown in Table 15.

content uniformity turmerones

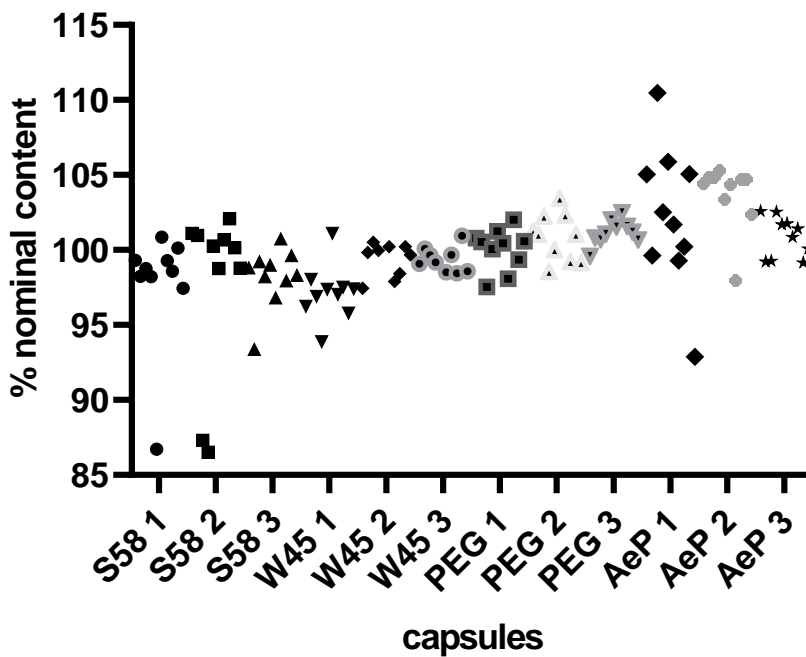


Figure 31 Content Uniformity test according to 2.9.40 for three batches of each formulation: nominal contents of the sum of turmerones (ar-turmerone, α -turmerone, β -turmerone) capsules, all contents refer to target contents shown in Table 15.

3.5. STABILITY STUDY OF CAPSULE FORMULATIONS WITH sCCO₂ EXTRACT

Physical and chemical stability of the capsule formulations was tested over 3 months of storage. The extract for all capsules was pooled and homogenised after freeze drying, to equalize the initial conditions for all formulations. Although storage temperatures of hard gelatine capsules should not exceed 30 °C according to Ph. Eur. [242], capsules were stored in a temperature cycle with a maximum temperature of 40 °C and a minimum of -5 °C, repeating every 24 h, in addition to storage at 22 °C (see chapter 2.2.15). To prevent the capsule shells from softening or embrittlement due to fluctuations in humidity, relative humidity was set at 43% r.h., which is within the recommended 35- 65% r.h. [266]. Chemical stability of only the developed capsule formulation was tested during storage at room temperature (22 °C) by HPLC-DAD measurements.

Beside the risk of softening or embrittlement of the capsule shells due to moisture transfer or interaction with the filling material, the possibility of up to 0.4% moisture sorption is described in the literature [200,233,267,268]. Although or because the addition of the sCCO₂ extract may affect the moisture sorption of the components of the formulations, the influence of moisture on the mass of the dosage forms was expected to be low to neglectable.

Table 16 summarizes the physical stability of the four tested capsule formulations when stored isothermally at 22 °C or in a temperature cycle test. Evidently, all tested formulations were physically stable for 84 days when stored at 22 °C, which means no leakage, softening, embrittlement, or other visible changes at all. Storage in the temperature cycle test (-5/40 °C,) revealed that only the PEG 4000 and Aeroperl 300 matrix formulations were physically stable for 84 days. Both hard fat formulations, with Witepsol W45 and Witepsol S58, were physically unstable and showed leakage already after the first day, detected as stains on the underlying filter paper. However, in addition to this, no further physical changes throughout storage were detected in any of the capsule formulations. Even after opening of the capsules, no expulsion of extract or oil migration was visible.

Table 16 physical stability of capsule formulations over storage upon 3 months: stable (+), leakage (-); all capsules contain scCO₂ extract produced at 425 bar and 75 °C in different concentrations: 21.2% in Witepsol W45, 16.1% in Witepsol S58, 21.2% in PEG 4000 and 57.3% in Aeroperl 300 Pharma.

Matrix	Storage Days in Temperature Cycle (-5 to 40 °C)				
	1	7	14	28	84
Witepsol S58	-	-	-	-	-
Witepsol W45	-	-	-	-	-
PEG 4000	+	+	+	+	+
Aeroperl 300 Pharma	+	+	+	+	+

Matrix	Storage Days at 22 °C				
	1	7	14	28	84
Witepsol S58	+	+	+	+	+
Witepsol W45	+	+	+	+	+
PEG 4000	+	+	+	+	+
Aeroperl 300 Pharma	+	+	+	+	+

Since 40 °C exceeds the melting temperature of both hard fat matrices, shown in Table 14, the filling melted during storage, seeped into the gap between both capsule shells and leaked out of the capsule. For PEG 4000 and Aeroperl 300, that does not melt at all, melting points were not exceeded during storage.

As expected, no relevant changes in capsule mass were observed for all capsule formulations stored at room temperature as shown in Figure 32.

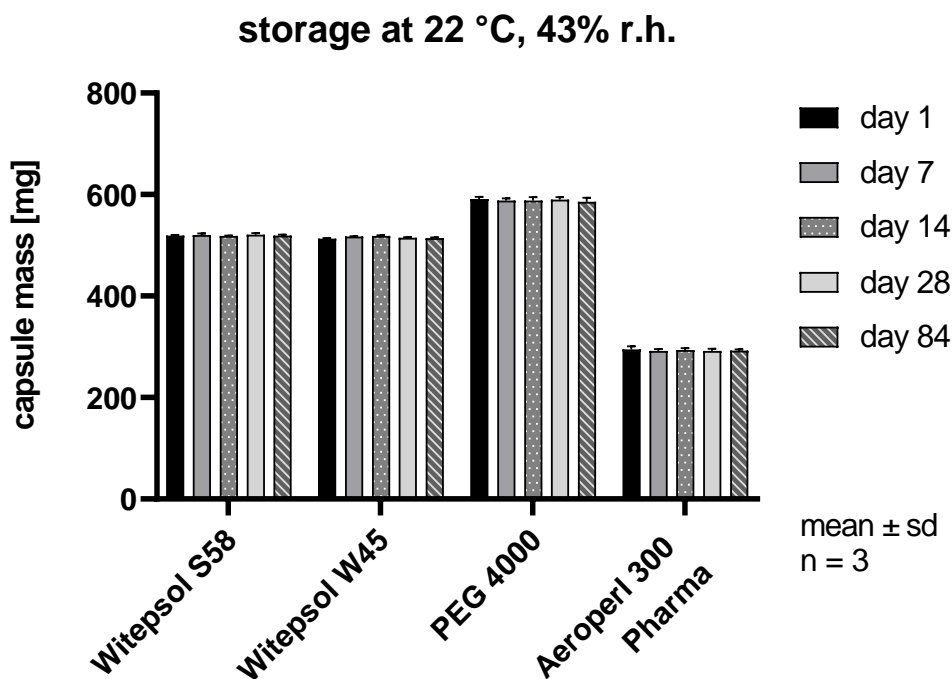


Figure 32 capsule masses throughout 84 days of storage at 22 °C and 43% r.h.

The concentration profiles of the marker substances - curcumin, demethoxycurcumin (DMC), bisdemethoxycurcumin (BDMC), ar-turmerone, α -turmerone, β -turmerone - during three months of storage at 22 °C are displayed in Figure 33 to Figure 36.

The capsule formulations based on hard fat, respectively Witepsol S58 (Figure 33, Witepsol S58) and Witepsol W45 (Figure 34, Witepsol W45) revealed almost no changes in the concentrations of the marker substances throughout storage with a maximum decrease of the β -turmerone concentration of 5-6%, while the concentrations of all other regarded components showed decreases below 3%. Figure 35 shows the contents of individual constituents of the PEG 4000-based capsule formulation. Statistically significant decreases in content were observed for all marker substances except for ar-turmerone. All three curcuminoids and β -turmerone revealed a decrease in content of approximately 10% whereas α -turmerone showed a decrease of only 5% after 84 days. For ar-turmerone no decrease in content was shown. Figure 36 shows the content of individual constituents of the formulation based on mesoporous silica. Here too, statistically significant decreases in content were observed. Curcumin, DMC, and β -turmerone showed decreases of 7 to 8% and the

content of α -turmerone decreased by 5%. BDMC and ar-turmerone content decreased by 3% after 84 days, however this was not statistically significant.

As per the stability study of the plain extracts, no degradation products were detected by HPLC-DAD.

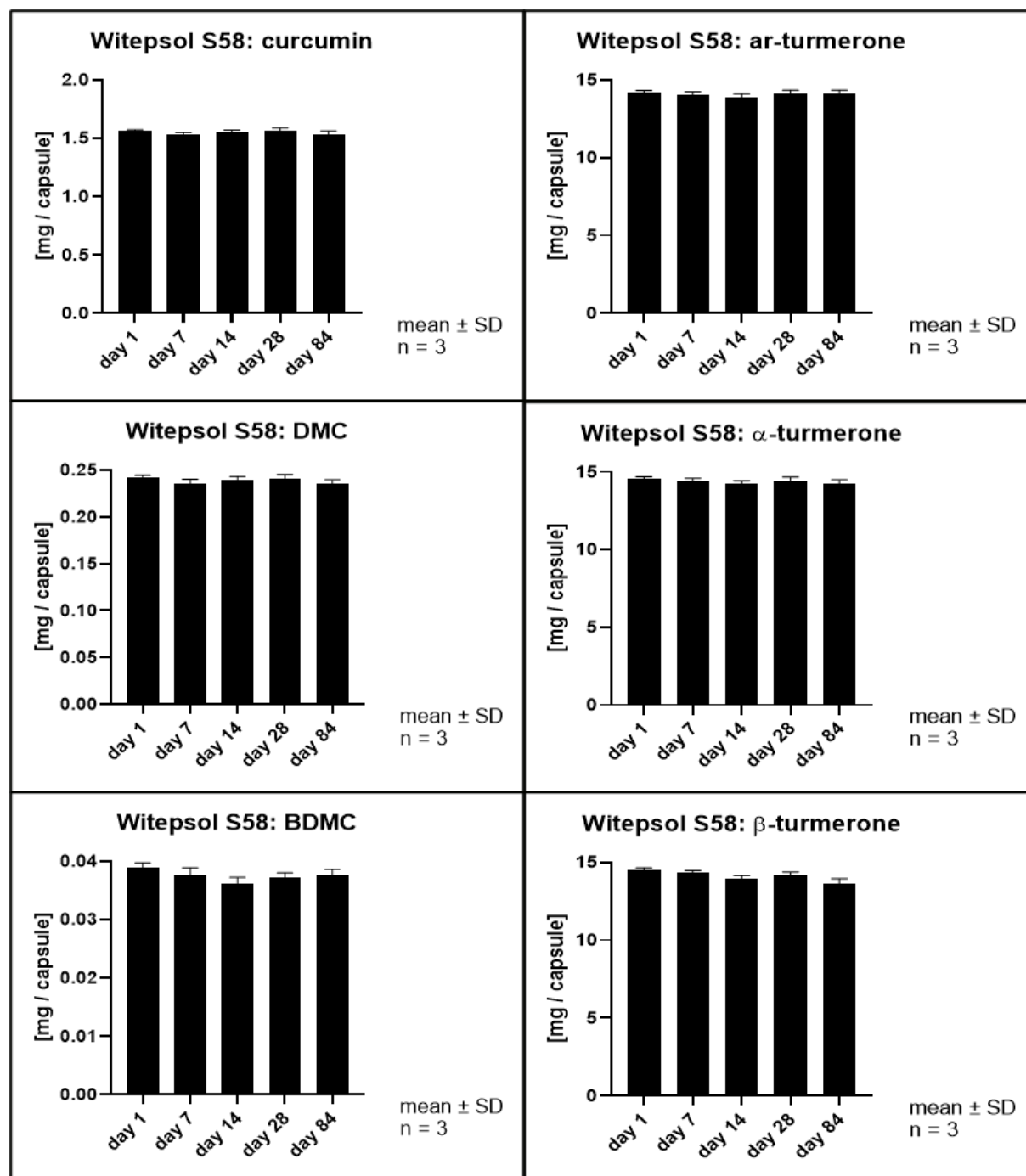


Figure 33 Contents of individual curcuminoids and turmerones in **hard gelatine capsules with 16.1% scCO₂ extract in hard fat Witepsol S58** throughout storage, scCO₂ extract: extracted at 425 bar and 75 °C, freeze-dried. Statistical differences were analysed with a two-way ANOVA (analysis of variance) followed by Tukey's multiple comparison test, statistically significant differences shown with asterisks (*), **** denoting $p \leq 0.0001$, *** $p \leq 0.001$, ** $p \leq 0.01$, * $p \leq 0.1$.

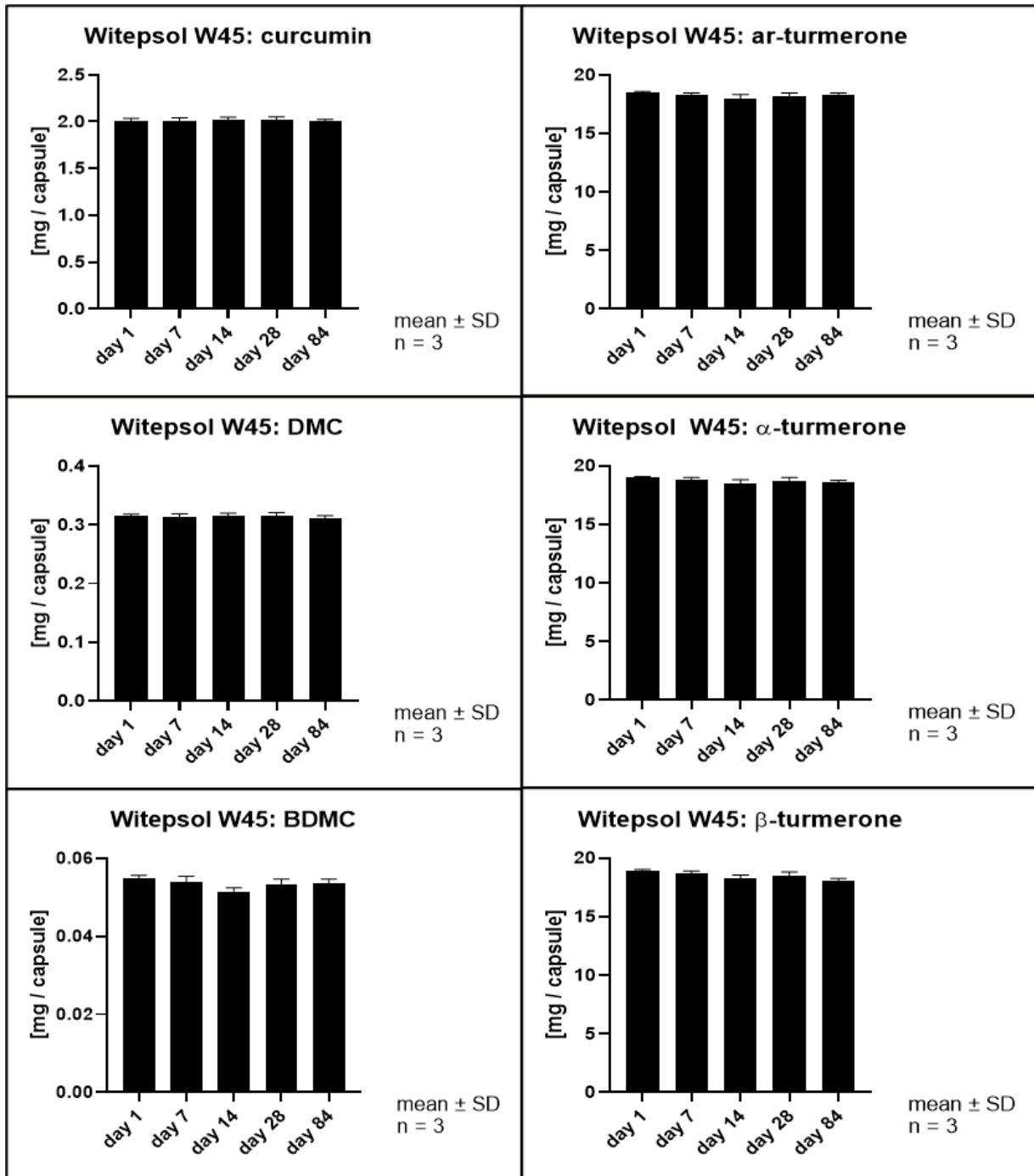


Figure 34 Contents of individual curcuminoids and turmerones in **hard gelatine capsules with 21.2% scCO₂ extract in hard fat Witepsol W45** throughout storage, scCO₂ extract: extracted at 425 bar and 75 °C, freeze-dried. Statistical differences were analysed with a two-way ANOVA (analysis of variance) followed by Tukey's multiple comparison test, statistically significant differences shown with asterisks (*), **** denoting $p \leq 0.0001$, *** $p \leq 0.001$, ** $p \leq 0.01$, * $p \leq 0.1$.

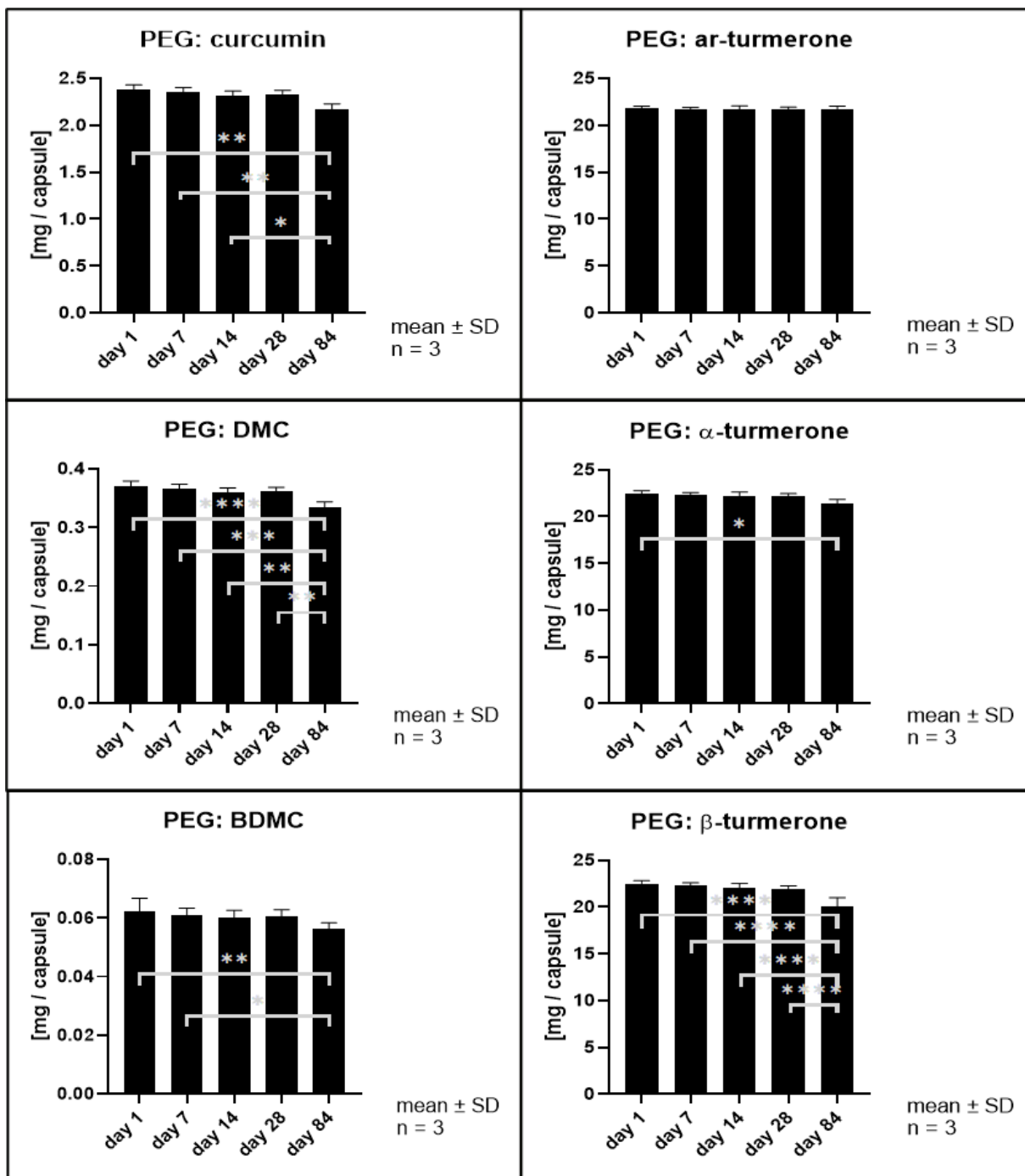


Figure 35 Contents of individual curcuminoids and turmerones in **hard gelatine capsules with 21.2% scCO₂ extract in PEG 4000** throughout storage, scCO₂ extract: extracted at 425 bar and 75 °C, freeze-dried. Statistical differences were analysed with a two-way ANOVA (analysis of variance) followed by Tukey's multiple comparison test, statistically significant differences shown with asterisks (*), **** denoting $p \leq 0.0001$, *** $p \leq 0.001$, ** $p \leq 0.01$, * $p \leq 0.1$.

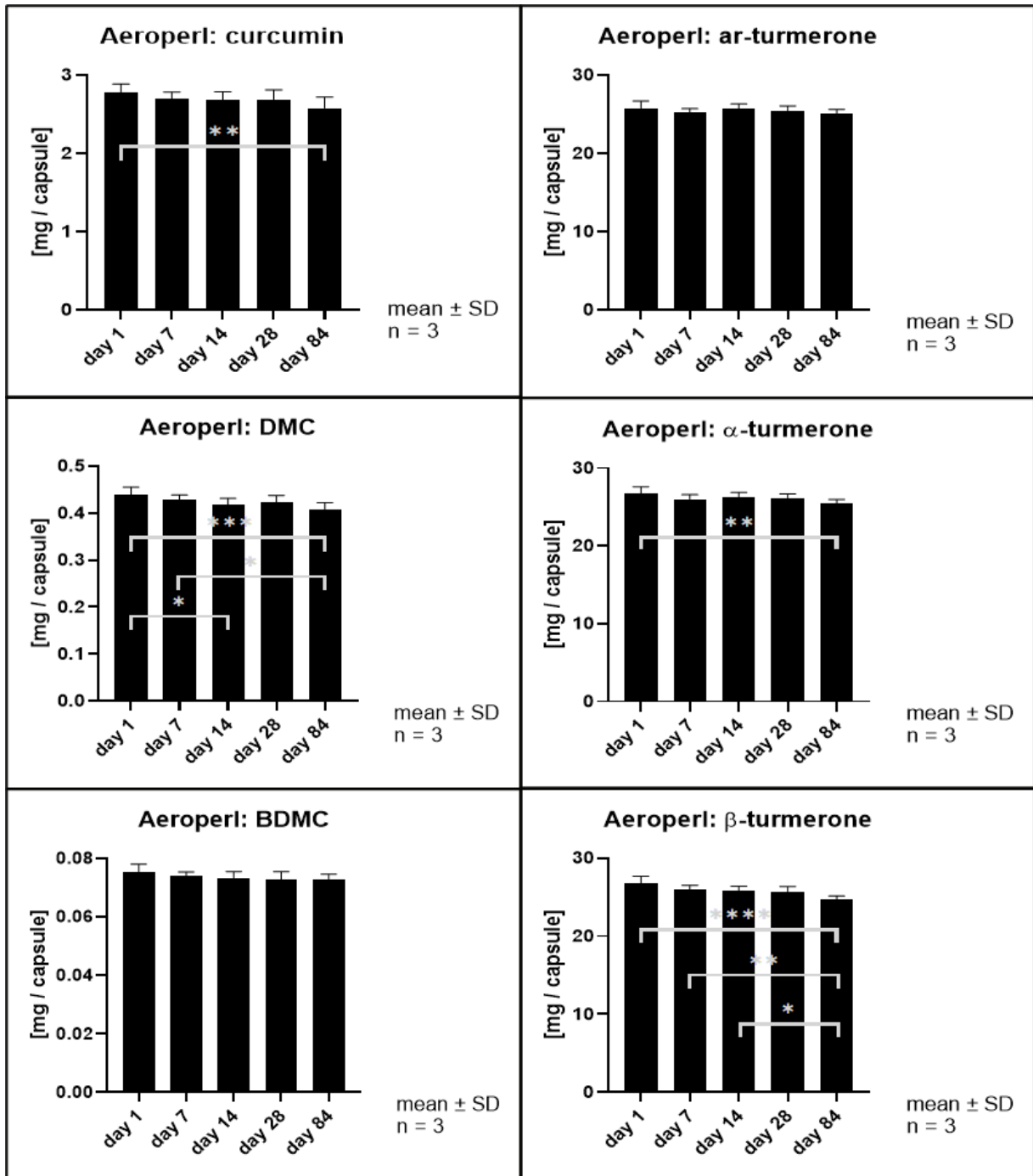


Figure 36 Contents of individual curcuminoids and turmerones in **hard gelatine capsules with 57.3% scCO₂ extract in Aeroperl300 Pharma** throughout storage, scCO₂ extract: extracted at 425 bar and 75 °C, freeze-dried. Statistical differences were analysed with a two-way ANOVA (analysis of variance) followed by Tukey's multiple comparison test, statistically significant differences shown with asterisks (*), **** denoting $p \leq 0.0001$, *** $p \leq 0.001$, ** $p \leq 0.01$, * $p \leq 0.1$.

In the literature, competitive adsorption phenomena are described for moisture and API adsorbed onto mesoporous silica particle surfaces [140,220,269,270]. The water is described as loosening the adsorption of the API and consequently changes its properties. Since no expulsion of extract has been observed, the extract seems more likely to have covered the hydrophilic surface of the mesoporous silica particle and therefore caused a reduction of hygroscopicity and contact surface for water [233,270]. In cases of hard fat or PEG structural changes in order to reduce its internal energy possibly lead to changes in oil loading capacity [186,193,212]. The fact that no expulsion was observed after 3 months of storage indicates no relevant structural changes affecting extract loading capacity.

The hard fat formulations appeared to be chemically relatively stable, whilst the PEG 4000 and Aeroperl 300 formulations showed significant decreases in content. This indicates that the surrounding air (oxygen, relative humidity) as well as the dried extract alone cannot have caused substance loss or degradation. The influence of the matrix substances must have led to a decrease in content. High temperatures during capsule production (60°C for PEG 4000) may not have affected the stability of the extract, as the production temperature of the scCO₂ extract was already 75 °C - much higher than the highest melting temperature and applied for over 1 h during extraction, much longer than during capsule preparation. However, the combination of the increased temperature during capsule preparation and the matrix substance could have led to increased reaction probability, especially in the formulation with the PEG 4000 matrix since PEG tends to thermally induced autoxidation [204,205,271,272].

The results for the hard fat matrices are consistent with the stability study of the plain extract, regarding the water-free extract 42575R in chapter 3.3, that is most closely corresponding to the freeze-dried extract 42575 used for the capsule formulations. Considering the fact that lipophilic substances, such as hard fat, are used to prevent flavour agents from oxidation or damage due to hydrophilic reactions [179,273], chemical stability of the six marker substances was expected for the plain hard fat formulation with Witepsol W45. The addition of surface-active substances in the case of Witepsol S58 seems not to have relevantly affected storage stability of the compounds when directly comparing Witepsol S58 and Witepsol W45. It is possible that the incorporation of the extract into the lipophilic hard fat matrix prevents contact

of the extract with oxygen and water from the environment, thus avoiding instability reactions.

In contrast to the capsule formulations based on the lipophilic hard fat matrices, the PEG 4000 and Aeroperl 300 Pharma matrix formulations showed a significant decrease in content as shown in the figures Figure 35 and Figure 36 and in Table 17 in comparison with the decrease of the raw, undried extract 42575. The degradation for PEG and Aeroperl formulations seems comparable to the degradation of the plain extract 42575 after 84 days. With 5-10% for the curcuminoids and approximately 10% for the turmerones, the raw extract 42575 showed the highest decrease. The only exceptions were the DMC content, which showed the lowest decrease for the raw extract and the highest for the PEG 4000 formulation, and the curcumin content, which revealed proportional decrease for both plain extract and PEG 4000 formulation.

The storage properties of the matrix substances used differ considerably in regard to the possible protective properties and high storage stability for hard fats with a high amount of triglycerides [179,273], the possible catalytic properties for mesoporous silica particles driven by the high surface area, the molecular mobility and proton transfer via H-bonds [220,274,275], and the autoxidative potential for PEG during storage, depending on storage temperature and molecular weight [204,205,271,272].

Different degradation mechanisms have been described for curcuminoids and essential oils in the literature [23,253,276–279]. For curcuminoids hydrolytic degradation as well as radical-driven reactions, or Michael reaction mechanisms are postulated [23,253,279]. They are either driven by the phenolic groups or the first carbon atom after the aromatic ring on the ferulic acid subunits and they depend on the surrounding solvent. The degradation or rearrangement of terpenoids in essential oils is, among other mechanisms, characterized as oxidation or polymerization of conjugated double bonds initiated by allyl groups [276–278]. In all reactions water, temperature, surrounding oxygen, pH value of the environment and interactions with other components possibly contribute.

Remarkably, the degradation pattern of individual compounds differed when comparing the capsule formulations with the plain extract. Especially ar-turmerone showed little-to-no decrease in concentration in the capsule formulations, whereas the concentration of ar-turmerone decreased like the α - and β -turmerone concentrations in the plain extract 42575. The plain extract 42555 (Figure 26) on the other hand

showed a decrease of turmerones similar to the capsule formulations after 168 days of storage. Ray et al. and Singh et al. described α - and β -turmerone to be less stable than ar-turmerone [277,278]. They postulated that the conjugated double bonds induced instability and therefore tend to oxidation or remodelling to the more stable ar-turmerone. It can be supposed that the degradation reactions of the turmerones in the plain extract with very high water content are faster than in the capsule formulations or in the plain extract with lower water content.

Table 17 Decrease in concentration after storage of 84 days at room temperature in % (m/m). The amount of decrease was calculated referred to the mean concentration after 1 day of storage at room temperature. Only the formulations and extract with a relevant decrease in concentration after 84 days are displayed.

Matrix	Decrease in Concentration after Storage of 84 Days at 22 °C in % (m/m)					
	curcumin	DMC	BDMC	ar-turmerone	α -turmerone	β -turmerone
PEG 4000	9	10	10	0	5	10
Aeroperl 300 Pharma	7	7	3	3	5	8
pure scCO ₂ 42575	9	5	11	10	10	12

The initial water content of the capsule formulations was deliberately kept low (3.4.1). During storage, no increase in capsule mass was detected for any of the formulations (Figure 32). The decrease in content of the components nevertheless indicates chemical degradation reactions. A decrease in content of the individual components was already observed to be related to the water content of the plain extract in 3.3. It seems possible that the surrounding humidity, due to the storage conditions combined with the hydrophilic properties of the PEG 4000 and Aeroperl 300 Pharma matrices, caused the decrease in the concentrations of the individual components that was observed for the capsule formulations. Both matrices form H-bonds and build an acidic solution when suspended/dissolved in water (Table 4). This may catalyse degradation reactions even when only limited amounts of water are available.

Stein et al. describe the oxidative degradation of PEG as depending on its molecular weight; higher molecular weight thereby leads to a higher oxidative degradation rate [204,205]. The autoxidation is further described as a temperature dependent reaction that increases with ageing of the PEG and which can be prevented by the addition of antioxidants or the absence of oxygen [204,205,271,272,280]. The decrease in melting

point is related to the molecular weight of the PEG. Staub detected no active oxygen for PEG 4000 stored at 25 and 40 °C for 14 days whereas PEG 400 showed active oxygen from the very first day [281]. It is explained by differences in the state of aggregation (PEG 400 is liquid, PEG 4000 is solid at room temperature) that cause differences in mobility and contact to oxygen. Since the PEG 4000 formulations were stored in solid state, no rapid oxidation reactions were expected, but the decrease in compound concentration in Figure 35 and Table 17 show that unlike the hard fat formulations, some reactions or rearrangements did happen, probably supported by the PEG 4000 matrix.

O'Reilly Beringhs discovered that API loaded mesoporous silica particles can catalyse degradation reactions such as hydrolysis of quercetin, even in the solid state, according to the specific pH value of the silica particles [275]. The hydrophilicity of the silica particle that can cause competitive H-bonding between water and an API has been described in the literature [140,220,269,274,275]. It has been found to increase molecular mobility and catalyse oxidation reactions in the presence of water. Although oil loading has been found to decrease hydrophilicity of the particles' surface [233,270], interactions between the silanol groups and the extract compounds cannot be excluded and therefore might influence the compounds' stability.

In addition to all possible degradation mechanisms of the single components, different mixed effects influenced by hydrophilicity, surrounding moisture and molecular state of the reactants have to be considered.

Unfortunately, the most stable capsule formulations were obtained using hard fat that, on the contrary, showed the lowest extract loading capacity.

4. SUMMARY AND CONCLUSION

ScCO₂ appears to be an ideal alternative for the extraction of essential oils from turmeric as illustrated for the turmerones [1]. Even at relatively low temperatures, the absolute amount of extracted turmerones in scCO₂ extracts reaches its maximum [1]. The absolute amount of extracted turmerones is comparable to methanol and *n*-hexane extracts. The recovery rates of the curcuminoids, which are much more polar than the turmerones, can be enhanced by selecting optimal extraction conditions [1]. Although their concentration remained about 15 times below that of a comparable methanol extract [1], they significantly exceeded the curcuminoid concentration of a comparable *n*-hexane extract by 500 times. Consequently, scCO₂ extraction of turmeric is not directly comparable to conventional solvent extraction, neither with methanol as a polar solvent nor with *n*-hexane as a non-polar solvent, with regard to the compound profiles of the corresponding extracts [1].

Storage trials of the methanol, *n*-hexane and scCO₂ extracts revealed the superior stability of all extracts compared with the scCO₂ extract produced at 75 °C and 425 bar and directly recovered from the extraction unit [1]. Obviously, the co-extracted water negatively affects the extract stability [1]. As the co-extracted amount of water increases with increasing extraction temperature and pressure, optimum scCO₂ extraction conditions occur at the expense of storage stability which is reduced [1]. As a consequence, the removal of moisture must be considered before storing the scCO₂ extracts [1]. It is worthwhile mentioning that pre-drying of the powdered turmeric is not recommended, as it would affect the outcome of the scCO₂ extraction process [1].

The removal of water from the scCO₂ extract produced at 75 °C and 425 bar, e.g. by freeze drying is a mandatory step before using it for hard gelatine capsule formulations since none of the tested matrix systems (hard fat, PEG, mesoporous silica) was able to bind the intrinsic water sufficiently. Embedding of the freeze-dried extract in hard fat (Witepsol W45 and Witepsol S58), PEG 4000, and mesoporous silica particle (Aeroperl 300 Pharma) is possible with different maximum extract loading capacities for the matrices: 64.2% in Aeroperl 300 Pharma, 57.3% in PEG 4000, 24.9% in Witepsol W45 and 19.4% in Witepsol S58. Adsorption and embedding into the porous surface structure of the silica clearly revealed the highest drug-to-excipient ratio.

During 84 days of storage, none of the developed capsule formulations appeared to be superior to the others regarding physical and chemical stability. Loaded with freeze-

dried scCO₂ extract, hard fat, Macrogol and mesoporous silica formed physically stable capsule formulations at 22 °C and 43% r.h. During temperature-cycling in the range from -5 to 40 °C, only Macrogol and mesoporous silica-based formulations still showed physical stability. Based on six marker substances, both hard fat-based capsule formulations showed higher chemical stability compared with Macrogol and mesoporous silica-based formulations. Interestingly, the latter two hydrophilic matrices showed reduced chemical stability of the incorporated scCO₂ extract, although the water had been removed from the extract beforehand.

Based on the results from storage trials, it can be presumed that hydrophilic interactions cause instabilities in the marker substances in scCO₂ extract. This affects the pure scCO₂ extract, as well as the developed capsule formulations. Possible improvement of stability of the capsule formulations depends on the actual type of interaction. In case of oxidative degradation reactions, the addition of antioxidant additives may improve storage stability, e.g., butylated hydroxyanisole (BHA) or butylated hydroxytoluene (BHT) can be suggested. Hydrolytic degradation can be prevented with a shift to more acidic pH values, which slow down hydrolytic degradation, or with strict separation from water, respectively hydrophilic compounds, that may catalyse hydrolytic degradation. However, complete removal of water is not recommended since the hard gelatine capsule shells still need the equilibrium of water in content, shell and surroundings for stability. Apart from the focus on hydrophilic interactions, the hard fat-based formulations could be improved (enhancing the extract loading capacity) by changing the composition of the hard fat in terms of its crystallization properties. Release study would have been the next step of capsule development.

Furthermore, it would be interesting to investigate the limitations of scCO₂ extraction by extending the range of extraction conditions toward higher pressure and temperature settings. A more detailed investigation of the extraction process, such as the extraction of water from the drug material, or the influence of particle size of the drug material in the extractor, could have followed the described extraction experiments.

5. INDICES

5.1. LIST OF FIGURES

Figure 1 Schematic painting of <i>Curcuma longa</i> L. [3].	1
Figure 2 Molecular formula of the three main curcuminoids from <i>Curcuma longa</i> L.: curcumin, demethoxycurcumin (DMC), and bisdemethoxycurcumin (BDMC); drawn with ADC/ChemSketch.	3
Figure 3 Molecular formula of the three main turmerones from <i>Curcuma longa</i> L.: ar-turmerone, α -turmerone, and β -turmerone; drawn with ADC/ChemSketch.	5
Figure 4 Phase diagram of CO ₂ , data reference [77].	8
Figure 5 T,S-diagram of CO ₂ with isotherms (T) in °C, isentropes (S) in KJ/kg*K, isobars (p) in bar, isenthalps (H) in kcal/kg, constant density (D) curves in kg/L, and aggregate states, data reference [83].	9
Figure 6 Surface active additives contained in Witepsol S58; drawn with ADC/ChemSketch.	19
Figure 7 SEM images of Aeroperl 300 Pharma at 500 \times magnification (left) and 5000 \times magnification (right), published by Söpper [227].	22
Figure 8 Simplified schematic depiction of the scCO ₂ pilot plant unit [1].	32
Figure 9 T,S-diagram of CO ₂ with isotherms in °C, isentropes in KJ/kg*K, isobars in bar, isenthalps in kcal/kg, and aggregate states, data reference [83]. The red isobar marks the separation pressure during the scCO ₂ extractions. The points A to D mark the most extreme extraction conditions: A 425 bar and 75 °C, B 150 bar and 75 °C with isenthalpic pressure relief to separation (purple), C 425 bar and 35 °C, D 75 bar and 35 °C framing the whole range of pressure and temperature conditions investigated (displayed in yellow). Point E (75 bar and 75 °C) marks a combination of extraction conditions that cannot be realized with the current pilot plant.	33
Figure 10 Extraction method for scCO ₂ extract from hard fat matrix. The steps 1 to 6 were repeated 3 times with the same sample. Supernatants were united and filled up to 10 mL with methanol.	44
Figure 11 Total ion current (TIC) and UV chromatogram of methanol and n-hexane extracts; 1: bisdemethoxycurcumin (BDMC); 2: demethoxycurcumin (DMC); 3: curcumin; 4: ar-turmerone; 5: α -turmerone; 6: β -turmerone [1].	50
Figure 12 Total ion current (TIC) of n-hexane soluble fraction of methanol extract: 1: α -curcumene; 2: α -zingiberene; 3: β -bisabolene; 4: β -sesquiphellandrene; 5: ar-turmerone; 6: α -turmerone; 7: β -turmerone.	52
Figure 13 Comparison of curcuminoid content (curcumin, demethoxycurcumin DMC, bisdemethoxycurcumin BDMC) in: scCO ₂ extract after direct recovery from the separator; extract resulting from the re-extraction of the remaining drug material from scCO ₂ extraction; sum of extracted content in total form scCO ₂ extraction and re-extraction; methanolic solvent extraction; all data related to drug before extraction.	55

Figure 14 Comparison of turmerone content (ar-turmerone, α -turmerone, β -turmerone) in: scCO ₂ extract after direct recovery from the separator; extract resulting from the re-extraction of the remaining drug material from scCO ₂ extraction; sum of extracted content in total form scCO ₂ extraction and re-extraction; methanolic solvent extraction; all data related to drug before extraction.....	56
Figure 15 Response contour plot illustrating the extract yields depending on pressure and temperature; the area marked in grey represents combinations of pressure and temperature settings, which were not investigated; recovery rate related to the drug material in % (m/m) [1]......	57
Figure 16 Response contour plots illustrating the recovery rates of all target compounds (curcumin, demethoxycurcumin (DMC), bisdemethoxycurcumin (BDMC), ar-turmerone, α -turmerone, β -turmerone) depending on pressure and temperature; the areas marked in grey represent combinations of pressure and temperature settings, which were not investigated; recovery rates are related to the drug material in % (m/m) [1].	58
Figure 17 Prediction profiler diagrams with confidence intervals of significance level 0.05 show the separate influence of pressure and temperature on the recovery of all target compounds ((curcumin I, demethoxycurcumin II (DMC), bisdemethoxycurcumin III (BDMC), ar-turmerone IV, α -turmerone V, β -turmerone VI). The optimum extraction conditions for maximal compound recovery are marked with the red dotted lines: 425 bar and 75 °C [1].	59
Figure 18 Comparison of a scCO ₂ extract characterized by maximum curcumin and ar-turmerone yields with n-hexane and methanol extracts [1].	61
Figure 19 Water content in conventional solvent extracts with the solvents methanol and n-hexane and in scCO ₂ extracts produced at 425 bar and 35 °C (42535), 55 °C (42555), 75 °C (42575), and 75 °C dissolved in methanol with subsequent removal of solvent (42575R); determined using Karl Fischer semi-micro water determination [1].	62
Figure 20 Contents of individual curcuminoids and turmerones in methanolic solvent extracts throughout storage [1].	64
Figure 21 Contents of individual curcuminoids and turmerones in n-hexane solvent extracts throughout storage [1].	65
Figure 22 Contents of individual curcuminoids and turmerones in scCO₂ extracts throughout storage, extraction at 425 bar and 35 °C [1].	66
Figure 23 Contents of individual curcuminoids and turmerones in scCO₂ extracts throughout storage, extraction at 425 bar and 55 °C [1].	67
Figure 24 Contents of individual curcuminoids and turmerones in scCO₂ extracts throughout storage, extraction at 425 bar and 75 °C [1].	68
Figure 25 Contents of individual curcuminoids and turmerones in scCO₂ extracts throughout storage, extraction at 425 bar and 75 °C, extract recovery via methanolic solution [1]......	69

Figure 26 Decrease in concentration of marker substances after 168 days in relation to the initial water content of the scCO ₂ extracts produced 425 bar and 35, 55, and 75 °C (42535, 42555, 42575) and recovered via methanolic solution (42575R).	70
Figure 27 Microscopic images of pure substances of Witepsol S58, Witepsol W45, PEG 4000, and dried scCO ₂ extract; images were taken via polarisation microscopy, magnification 20x.	79
Figure 28 Microscopic images of Witepsol S58, Witepsol W45, and PEG 4000 with dried scCO ₂ extract in different concentrations [% (m/m)], images were taken via polarisation microscopy, magnification 20x (PEG 4000) or 40x (hard fat).	80
Figure 29 Mass Variation test according to Ph. Eur. 2.9.40 for three batches of each formulation: nominal capsule content refers to extract concentration shown in Table 15.	83
Figure 30 Content Uniformity test according to 2.9.40 for three batches of each formulation: nominal contents of the sum of curcuminoids (curcumin, demethoxycurcumin, bisdemethoxycurcumin) capsules, all contents refer to target contents shown in Table 15.	84
Figure 31 Content Uniformity test according to 2.9.40 for three batches of each formulation: nominal contents of the sum of turmerones (α-turmerone, β-turmerone) capsules, all contents refer to target contents shown in Table 15.	84
Figure 32 capsule masses throughout 84 days of storage at 22 °C and 43% r.h.	87
Figure 33 Contents of individual curcuminoids and turmerones in hard gelatine capsules with 16.1% scCO₂ extract in hard fat Witepsol S58 throughout storage, scCO ₂ extract: extracted at 425 bar and 75 °C, freeze-dried. Statistical differences were analysed with a two-way ANOVA (analysis of variance) followed by Tukey's multiple comparison test, statistically significant differences shown with asterisks (*), **** denoting p ≤ 0.0001, *** p ≤ 0.001, ** p ≤ 0.01, * p ≤ 0.1.	88
Figure 34 Contents of individual curcuminoids and turmerones in hard gelatine capsules with 21.2% scCO₂ extract in hard fat Witepsol W45 throughout storage, scCO ₂ extract: extracted at 425 bar and 75 °C, freeze-dried. Statistical differences were analysed with a two-way ANOVA (analysis of variance) followed by Tukey's multiple comparison test, statistically significant differences shown with asterisks (*), **** denoting p ≤ 0.0001, *** p ≤ 0.001, ** p ≤ 0.01, * p ≤ 0.1.	89
Figure 35 Contents of individual curcuminoids and turmerones in hard gelatine capsules with 21.2% scCO₂ extract in PEG 4000 throughout storage, scCO ₂ extract: extracted at 425 bar and 75 °C, freeze-dried. Statistical differences were analysed with a two-way ANOVA (analysis of variance) followed by Tukey's multiple comparison test, statistically significant differences shown with asterisks (*), **** denoting p ≤ 0.0001, *** p ≤ 0.001, ** p ≤ 0.01, * p ≤ 0.1.	90

Figure 36 Contents of individual curcuminoids and turmerones in **hard gelatine capsules with 57.3% scCO₂ extract in Aeroperl 300 Pharma** throughout storage, scCO₂ extract: extracted at 425 bar and 75 °C, freeze-dried. Statistical differences were analysed with a two-way ANOVA (analysis of variance) followed by Tukey`s multiple comparison test, statistically significant differences shown with asterisks (*), **** denoting $p \leq 0.0001$, *** $p \leq 0.001$, ** $p \leq 0.01$, * $p \leq 0.1$91

5.2. LIST OF TABLES

Table 1 Critical pressure and temperature for different substances for supercritical fluid extraction, data references [75–77].	7
Table 2 properties of gas, supercritical fluid, and liquid of CO ₂ , data reference [75,80].	8
Table 3 Examples of application of scCO ₂ in research and industries.	12
Table 4 Overview of capsule filling matrices: hard fat (Witepsol S58, Witepsol W45), polyethylene glycol (PEG 4000), and mesoporous silica particle (Aeroperl 300 Pharma).	14
Table 5 Experimental conditions according to a full factorial design in the correct experimental order [1].	34
Table 6 Characteristics of the extracts monitored in the stability study [1].	35
Table 7 Freeze drying method for scCO ₂ extracts.	40
Table 8 Extract concentration in capsule formulation calculated as raw extract and correspondingly calculated as dried extract, which is equivalent to 45% of the undried mass. Only the most interesting concentrations are displayed...	41
Table 9 Concentration of extract loading in capsule formulations analysed in stability study. For the exact compositions of the tested capsule formulations refer to the appendix Table 19.	47
Table 10 Course of Temperature during storage in the temperature cycling test (TC).	47
Table 11 Retention times (R _t), UV- and mass spectrometric data of active substances of turmeric. Only the most intense m/z ratios of fragment ions are displayed. (P precursor ion) [1].	51
Table 12 Retention times (R _t), UV- and mass spectrometric data of active substances of n-hexane soluble fraction of methanolic extract from turmeric. Only the most intense m/z ratios of fragments are displayed in their relative intensity to the base peak (% bp).....	53
Table 13 Maximum loading capacity for freeze-dried scCO ₂ extract (425 bar; 75 °C) in different matrix systems in % (m/m): hard fat Witepsol W45, hard fat Witepsol S58, PEG 4000, Aeroperl 300. Leakage on filter paper marked with arrows.....	74

Table 14 Summary of determined loading capacity: stable (+), leakage (-), stable according to method 2.2.11.2 but not according to method 2.2.11.1 (+/-); To simplify the presentation, only the data surrounding the maximum loading capacities is shown. Melting points according to safety data sheets.	75
Table 15 Extract and component concentrations of capsule formulations tested in MV and CU.....	82
Table 16 physical stability of capsule formulations over storage upon 3 months: stable (+), leakage (-); all capsules contain scCO ₂ extract produced at 425 bar and 75 °C in different concentrations: 21.2% in Witepsol W45, 16.1% in Witepsol S58, 21.2% in PEG 4000 and 57.3% in Aeroperl 300 Pharma.....	86
Table 17 Decrease in concentration after storage of 84 days at room temperature in % (m/m). The amount of decrease was calculated referred to the mean concentration after 1 day of storage at room temperature. Only the formulations and extract with a relevant decrease in concentration after 84 days are displayed.	94
Table 18 Results of all experiments of the experimental design according to 2.2.4.	124
Table 19 Composition of capsule formulations for stability study according to 2.2.15.	125

5.3. LIST OF EQUATIONS

Equation 1 Simplified reaction principle of Karl Fischer's titration of water with iodine (I ₂) and sulfur dioxide (SO ₂) [1].	39
Equation 2 Calculation of the A value [%]; C _{actual} = actual concentration [%]; C _{target} = target concentration [%].	48
Equation 3 Individual determination of contents of each capsule; x = content of capsule [%]; w = weight of capsule [mg]; \bar{w} = mean weight of capsule filling [mg].	48
Equation 4 Calculation of Acceptance Value (AV) according to general formula (Ph. Eur. 2.9.40); M = reference value; \bar{X} = mean of individual contents (x ₁ ;... x _i)[%]; k = acceptability constant (for 10 capsules k = 2.4, for 30 capsules k = 2.0); s = sample standard deviation.....	49

5.4. REFERENCES

1. Widmann, A.-K.; Wahl, M.A.; Kammerer, D.R.; Daniels, R. Supercritical Fluid Extraction with CO₂ of Curcuma Longa L. in Comparison to Conventional Solvent Extraction. *Pharmaceutics* **2022**, *14*, 1943, doi:10.3390/pharmaceutics14091943.
2. Eigner, D.; Scholz, D. Ferula Asa-Foetida and Curcuma Longa in Traditional Medical Treatment. *J. Ethnopharmacol.* **1999**, *67*, 1–6, doi:10.1016/S0378-8741(98)00234-7.
3. Chaumeton, F.P.; Poiret, J.L.M.; de Chamberet, J.-B.J.T.; Lubrecht, H.; Panckoucke, E.; Turpin, P.J.F. *Flore Médicale*; Tome Trois.; Imprimerie de C.L.F. Panckoucke: Paris;
4. Leong-Skornickova, J.; Šída, O.; Wijesundara, S.; Marhold, K. On the Identity of Turmeric: The Typification of Curcuma Longa L. (Zingiberaceae). *Bot. J. Linn. Soc.* **2008**, *157*, 37–46, doi:10.1111/J.1095-8339.2008.00788.X.
5. Prabhakaran Nair, K.P. *The Agronomy and Economy of Turmeric and Ginger - the Invaluable Medicinal Spice Crops*; 2013; ISBN 978-0-12-394801-4.
6. Kumar, N.; Sakhya, S.K. Ethnopharmacological Properties of Curcuma Longa: A Review. *Int. J. Pharm. Sci. Res.* **2013**, *4*, 103–112, doi:10.13040/IJPSR.0975-8232.4(1).03-12.
7. Ammon, H.P.T.; Wahl, M.A. Pharmacology of Curcuma Longa. *Planta Med.* **1991**, *57*, 1–7, doi:10.1055/S-2006-960004.
8. IUCN Nepal *National Register of Medicinal Plants*; IUCN Nepal: Kathmandu, 2000; ISBN 92-9144-048-5.
9. K. M. Nadkarni; A. K. Nadkarni *Dr. K. M. Nadkarni's Indian Materia Medica*; 3rd ed.; Taj Press: Delhi, 1908; Vol. 2; ISBN 81-7154-143-7.
10. Van Galen, E.; Kroes, B.; Llorente; Garcia, G.; Ensink, E. Assessment Report on Curcuma Longa L. (C. Domestica Valetton), Rhizoma. *Eur. Med. Agency* **2018**, 1–34.
11. Bruchhausen, F. von; Dannhardt, G.; Ebel, S.; Frahm, A. W.; Hackenthal, E.; Hansel, R.; Holzgrabe, U.; Keller, K.; Nürnberg, E.; Rimpler, H.; et al. *Hagers Handbuch Der Pharmazeutischen Praxis*; Springer Berlin: Heidelberg, 1998;
12. Xia, X.; Cheng, G.; Pan, Y.; Xia, Z.H.; Kong, L.D. Behavioral, Neurochemical and Neuroendocrine Effects of the Ethanol Extract from Curcuma Longa L. in the Mouse Forced Swimming Test. *J. Ethnopharmacol.* **2007**, *110*, 356–363, doi:10.1016/j.jep.2006.09.042.
13. Khattak, S.; Saeed-ur-Rehman; Shah, H.U.; Ahmad, W.; Ahmad, M. Biological Effects of Indigenous Medicinal Plants Curcuma Longa and Alpinia Galanga. *Fitoterapia* **2005**, *76*, 254–257, doi:10.1016/j.fitote.2004.12.012.
14. Ramírez-Tortosa, M.C.; Mesa, M.D.; Aguilera, M.C.; Quiles, J.L.; Baró, L.; Ramirez-Tortosa, C.L.; Martinez-Victoria, E.; Gil, A. Oral Administration of a Turmeric Extract Inhibits LDL Oxidation and Has Hypocholesterolemic Effects in Rabbits with Experimental Atherosclerosis. *Atherosclerosis* **1999**, *147*, 371–378, doi:10.1016/S0021-9150(99)00207-5.
15. Mohanty, I.; Arya, D.S.; Gupta, S.K. Effect of Curcuma Longa and Ocimum

- Sanctum on Myocardial Apoptosis in Experimentally Induced Myocardial Ischemic-Reperfusion Injury. *BMC Complement. Altern. Med.* **2006**, 6, 1–12, doi:10.1186/1472-6882-6-3.
16. Soni, K.B.; Rajan, A.; Kuttan, R. Reversal of Aflatoxin Induced Liver Damage Curcumin. *Cancer Lett.* **1992**, 66, 115–121, doi:10.1016/0304-3835(92)90223-i.
 17. Kuroda, M.; Mimaki, Y.; Nishiyama, T.; Mae, T.; Kishida, H.; Tsukagawa, M.; Takahashi, K.; Kawada, T.; Nakagawa, K.; Kitahara, M. Hypoglycemic Effects of Turmeric (*Curcuma Longa* L. Rhizomes) on Genetically Diabetic KK-Ay Mice. *Biol. Pharm. Bull.* **2005**, 28, 937–939, doi:10.1248/BPB.28.937.
 18. Nishiyama, T.; Mae, T.; Kishida, H.; Tsukagawa, M.; Mimaki, Y.; Kuroda, M.; Sashida, Y.; Takahashi, K.; Kawada, T.; Nakagawa, K.; et al. Curcuminoids and Sesquiterpenoids in Turmeric (*Curcuma Longa* L.) Suppress an Increase in Blood Glucose Level in Type 2 Diabetic KK-Ay Mice. *J. Agric. Food Chem.* **2005**, 53, 959–963, doi:10.1021/JF0483873/ASSET/IMAGES/LARGE/JF0483873F00003.JPEG.
 19. Li, S.; Yuan, W.; Deng Ping Wang, G.; Yang, P.; Aggarwal, B.B. Chemical Composition and Product Quality Control of Turmeric (*Curcuma Longa* L.). *Pharm. Crop.* **2011**, 2, 28–54, doi:10.2174/2210290601102010028.
 20. Chattopadhyay, I.; Biswas, K.; Bandyopadhyay, U.; Banerjee, R.K. Turmeric and Curcumin : Biological Act and Medicinal Applications. *Curr. Sci.* **2004**, 87, 44–53.
 21. Zielińska, A.; Alves, H.; Marques, V.; Durazzo, A.; Lucarini, M.; Alves, T.F.; Morsink, M.; Willemen, N.; Eder, P.; Chaud, M. V.; et al. Properties, Extraction Methods, and Delivery Systems for Curcumin as a Natural Source of Beneficial Health Effects. *Med. 2020, Vol. 56, Page 336* **2020**, 56, 336, doi:10.3390/MEDICINA56070336.
 22. Nisar, T.; Iqbal, M.; Raza, A.; Safdar, M.; Iftikhar, F.; Waheed, M. Turmeric: A Promising Spice for Phytochemical and Antimicrobial Activities. *J. Agric. Environ. Sci* **2015**, 15, 1278–1288, doi:10.5829/idosi.ajeaes.2015.15.7.9528.
 23. Tønnesen, H.H.; Karlsen, J. Studies on Curcumin and Curcuminoids VI. Kinetics of Curcumin Degradation in Aqueous Solution. *Zeitschrift für Leb. -Untersuchung und -forsch.* **1985**, 108, 402–404, doi:10.1007/BF01027775.
 24. Araújo, C.A.C.; Leon, L.L. Biological Activities of *Curcuma Longa* L. *Mem. Inst. Oswaldo Cruz* **2001**, 96, 723–728, doi:10.1590/S0074-02762001000500026.
 25. Maiti, K.; Mukherjee, K.; Gantait, A.; Saha, B.P.; Mukherjee, P.K. Curcumin-Phospholipid Complex: Preparation, Therapeutic Evaluation and Pharmacokinetic Study in Rats. *Int. J. Pharm.* **2007**, 330, 155–163, doi:10.1016/j.ijpharm.2006.09.025.
 26. Souza, C.R.A.; Osme, S.F.; Glória, M.B.A. Stability of Curcuminoid Pigments in Model Systems. *J. Food Process. Preserv.* **1997**, 21, 353–363, doi:10.1111/J.1745-4549.1997.TB00789.X.
 27. Hjorth Tennesen, H.I.; Karlsen, J.; Beijersbergen van Henegouwen, G. Studies on Curcumin and Curcuminoids: VIII. Photochemical Stability of Curcumin. *Zeitschrift für Naturforsch. - Sect. C J. Biosci.* **1986**, 183, 116–122, doi:10.1007/BF01041928.

28. Anand, P.; Kunnumakkara, A.B.; Newman, R.A.; Aggarwal, B.B. Bioavailability of Curcumin: Problems and Promises. *Mol. Pharm.* **2007**, *4*, 807–818, doi:10.1021/MP700113R/ASSET/IMAGES/MEDIUM/MP-2007-00113R_0003.GIF.
29. Lee, K.Y.; Gul, K.; Kim, A.N.; Rahman, M.S.; Lee, M.H.; Kim, J.I.; Kwak, D.; Shin, E.C.; Kim, H.J.; Kerr, W.L.; et al. Impact of Supercritical Carbon Dioxide Turmeric Extract on the Oxidative Stability of Perilla Oil. *Int. J. Food Sci. Technol.* **2020**, *55*, 183–191, doi:10.1111/IJFS.14261.
30. Chainani-Wu, N. Safety and Anti-Inflammatory Activity of Curcumin : *J. Altern. Complement. Med.* **2003**, *9*, 161–168, doi:10.1089/107555303321223035.
31. Chen, J.-J.; Tsai, C.-S.; Hwang, T.-L.; Shieh, P.-C.; Chen, J.-F.; Sung, P.-J. Sesquiterpenes from the Rhizome of *Curcuma Longa* with Inhibitory Activity on Superoxide Generation and Elastase Release by Neutrophils. *Food Chem.* **2010**, *119*, 974–980, doi:10.1016/j.foodchem.2009.07.060.
32. Sikora, E.; Bielak-Zmijewska, A.; Piwocka, K.; Skierski, J.; Radziszewska, E. Inhibition of Proliferation and Apoptosis of Human and Rat T Lymphocytes by Curcumin, a Curry Pigment. *Biochem. Pharmacol.* **1997**, *54*, 899–907, doi:10.1016/S0006-2952(97)00251-7.
33. Song, E.; Cho, H.; Kim, J.; Kim, N.; An, N.; Kim, J.; Lee, S.; Kim, Y. Diarylheptanoids with Free Radical Scavenging and Hepatoprotective Activity in Vitro from *Curcuma Longa*. *Planta Med.* **2001**, *67*, 876–877, doi:10.1055/s-2001-18860.
34. Donatus, I.A.; Vermeulen, S.; Vermeulen, N.P.E. Cytotoxic and Cytoprotective Curcumin Activities of Curcumin - Effects on Paracetamol-Induced Cytotoxicity, Lipid Peroxidation and Glutathione Depletion in Rat Hepatocytes. *Biochem. Pharmacol.* **1990**, *39*, 1869–1875, doi:10.1016/0006-2952(90)90603-I.
35. Rajakrishnan, V.; Menon, V.P.; Rajashekar, K.N. Protective Role of Curcumin in Ethanol Toxicity. *Phyther. Res.* **1998**, *12*, 55–56, doi:10.1002/(SICI)1099-1573(19980201)12:1<55::AID-PTR173>3.0.CO;2-0.
36. Sandur, S.K.; Pandey, M.K.; Sung, B.; Ahn, K.S.; Murakami, A.; Sethi, G.; Limtrakul, P.; Badmaev, V.; B. Aggarwal, B. Curcumin, Demethoxycurcumin, Bisdemethoxycurcumin, Tetrahydrocurcumin and Turmerones Differentially Regulate Anti-Inflammatory and Anti-Proliferative Responses through a ROS-Independent Mechanism. *Carcinogenesis* **2007**, *28*, 1765–1773, doi:10.1093/carcin/bgm123.
37. Jiang, C.-M.; Yang-Yen, H.-F.; Jong-Young Yen, J.; Lin, J.-K. Curcumin Induces Apoptosis in Immortalized NIH 3T3 and Malignant Cancer Cell Lines. *Nutr. Cancer* **1996**, *26*, 111–120, doi:10.1080/01635589609514468.
38. Shao, Z.M.; Shen, Z.Z.; Liu, C.H.; Sartippour, M.R.; Go, V.L.; Heber, D.; Nguyen, M. Curcumin Exerts Multiple Suppressive Effects on Human Breast Carcinoma Cells. *Int. J. cancer* **2002**, *98*, 234–240, doi:10.1002/IJC.10183.
39. Dorai, T.; Gehani, N.; Katz, A. Therapeutic Potential of Curcumin in Human Prostate Cancer-I. Curcumin Induces Apoptosis in Both Androgen-Dependent and Androgen-Independent Prostate Cancer Cells. *Prostate Cancer Prostatic Dis.* **2000**, *3*, 84–93, doi:10.1038/SJ.PCAN.4500399.
40. Chen, Y.S.; Ho, C.C.; Cheng, K.C.; Tyan, Y.S.; Hung, C.F.; Tan, T.W.; Chung,

- J.G. Curcumin Inhibited the Arylamines N-Acetyltransferase Activity, Gene Expression and DNA Adduct Formation in Human Lung Cancer Cells (A549). *Toxicol. Vitro.* **2003**, *17*, 323–333, doi:10.1016/S0887-2333(03)00020-1.
41. Oda, Y. Inhibitory Effect of Curcumin on SOS Functions Induced by UV Irradiation. *Mutat. Res. Lett.* **1995**, *348*, 67–73, doi:10.1016/0165-7992(95)00048-8.
 42. Zorofchian Moghadamtousi, S.; Abdul Kadir, H.; Hassandarvish, P.; Tajik, H.; Abubakar, S.; Zandi, K. A Review on Antibacterial, Antiviral, and Antifungal Activity of Curcumin. *Biomed Res. Int.* **2014**, *2014*, 1–12, doi:10.1155/2014/186864.
 43. Hu, Y.; Zhang, J.; Kong, W.; Zhao, G.; Yang, M. Mechanisms of Antifungal and Anti-Aflatoxicogenic Properties of Essential Oil Derived from Turmeric (*Curcuma Longa* L.) on *Aspergillus Flavus*. *Food Chem.* **2017**, *220*, 1–8, doi:10.1016/J.FOODCHEM.2016.09.179.
 44. Negi, P.S.; Jayaprakasha, G.K.; Rao, L.J.M.; Sakariah, K.K. Antibacterial Activity of Turmeric Oil: A Byproduct from Curcumin Manufacture. *J. Agric. Food Chem.* **1999**, *47*, 4297–4300, doi:10.1021/JF990308D.
 45. Ali, A.; Wang, Y.H.; Khan, I.A. Larvicidal and Biting Deterrent Activity of Essential Oils of *Curcuma Longa*, Ar-Turmerone, and Curcuminoids Against *Aedes Aegypti* and *Anopheles Quadrimaculatus* (Culicidae: Diptera). *J. Med. Entomol.* **2015**, *52*, 979–986, doi:10.1093/JME/TJV072.
 46. Ferreira, L.A.F.; Henriques, O.B.; Andreoni, A.A.S.; Vital, G.R.F.; Campos, M.M.C.; Habermehl, G.G.; de Moraes, V.L.G. Antivenom and Biological Effects of Ar-Turmerone Isolated from *Curcuma Longa* (Zingiberaceae). *Toxicon* **1992**, *30*, 1211–1218, doi:10.1016/0041-0101(92)90437-A.
 47. Lee, H.S. Antiplatelet Property of *Curcuma Longa* L. Rhizome-Derived Ar-Turmerone. *Bioresour. Technol.* **2006**, *97*, 1372–1376, doi:10.1016/j.biortech.2005.07.006.
 48. Prakash, P.; Misra, A.; Surin, W.R.; Jain, M.; Bhatta, R.S.; Pal, R.; Raj, K.; Barthwal, M.K.; Dikshit, M. Anti-Platelet Effects of *Curcuma* Oil in Experimental Models of Myocardial Ischemia-Reperfusion and Thrombosis. *Thromb. Res.* **2011**, *127*, 111–118, doi:10.1016/j.thromres.2010.11.007.
 49. Funk, J.L.; Frye, J.B.; Oyarzo, J.N.; Zhang, H.; Timmermann, B.N. Anti-Arthritic Effects and Toxicity of the Essential Oils of Turmeric (*Curcuma Longa* L.). *J. Agric. Food Chem.* **2010**, *58*, 842, doi:10.1021/JF9027206.
 50. Lee, Y. Activation of Apoptotic Protein in U937 Cells by a Component of Turmeric Oil. 1–5.
 51. Wahlström, B.; Blennow, G. A Study on the Fate of Curcumin in the Rat. *Acta Pharmacol. Toxicol. (Copenh)*. **1978**, *43*, 86–92, doi:10.1111/J.1600-0773.1978.TB02240.X.
 52. Shobal, G.; Joseph, T.; Majeed, M.; Rajendran, R.; Srinivas, P.S.S.R. Influence of Piperine on the Pharmacokinetics of Curcumin in Animals and Human Volunteers. **2000**, 353–356.
 53. Rasyid, A.; Rashid, A.; Rahman, A.; Jaalam, K. Effect of Different Curcumin Dosages on Human Gall Bladder. **2002**, *11*, 314–318.

54. Rasyid, A.; Lelo, A. The Effect of Curcumin and Placebo on Human Gall-Bladder Function: An Ultrasound Study. *Aliment. Pharmacol. Ther.* **1999**, *13*, 245–249, doi:10.1046/J.1365-2036.1999.00464.X.
55. Bundy, R.; Walker, A.F.; Middleton, R.W.; Booth, J. Turmeric Extract May Improve Irritable Bowel Syndrome Symptomology in Otherwise Healthy Adults : A Pilot Study. *J. Altern. Complement. Med.* **2004**, *10*, 1015–1018, doi:10.1089/acm.2004.10.1015.
56. James, J.S. Curcumin: Clinical Trial Finds No Antiviral Effect. *AIDS Treat News* **1996**, *242*, 1–2.
57. Seetharam, K.A.; Pasricha, J.S. Condiments and Contact Dermatitis of the Finger - Tips. *Indian J. Dermatol. Venereol. Leprol.* **1987**, *53*, 325.
58. Goh, C.L.; Ng, S.K. Allergic Contact Dermatitis to Curcuma Longa (Turmeric). *Contact Dermatitis* **1987**, *17*, 186–186, doi:10.1111/J.1600-0536.1987.TB02706.X.
59. Hata, M.; Sasaki, E.; Ota, M.; Fujimoto, K.; Yajima, J.; Shichida, T.; Honda, M. Allergic Contact Dermatitis from Curcumin (Turmeric). *Contact Dermatitis* **1997**, *36*, 107–108, doi:10.1111/J.1600-0536.1997.TB00426.X.
60. Souza, C.R.A.; Glória, M.B.A. Chemical Analysis of Turmeric from Minas Gerais, Brazil and Comparison of Methods for Flavour Free Oleoresin. *Brazilian Arch. Biol. Technol.* **1998**, *41*, 218–224, doi:10.1590/S1516-89131998000200008.
61. Braga, M.E.M.; Leal, P.F.; Carvalho, J.E.; Meireles, M.A.A. Comparison of Yield, Composition, and Antioxidant Activity of Turmeric (*Curcuma Longa* L.) Extracts Obtained Using Various Techniques. *J. Agric. Food Chem.* **2003**, *51*, 6604–6611, doi:10.1021/JF0345550/ASSET/IMAGES/LARGE/JF0345550F00003.JPEG.
62. Dandekar, D. V.; Gaikar, V.G. Microwave Assisted Extraction of Curcuminoids from *Curcuma Longa*. *Sep. Sci. Technol.* **2002**, *37*, 2669–2690, doi:10.1081/SS-120004458.
63. Wakte, P.S.; Sachin, B.S.; Patil, A.A.; Mohato, D.M.; Band, T.H.; Shinde, D.B. Optimization of Microwave, Ultra-Sonic and Supercritical Carbon Dioxide Assisted Extraction Techniques for Curcumin from *Curcuma Longa*. *Sep. Purif. Technol.* **2011**, *79*, 50–55, doi:10.1016/J.SEPPUR.2011.03.010.
64. Tran, T.H.; Nguyen, P.T.N.; Pham, T.N.; Nguyen, D.C.; Dao, T.P.; Nguyen, T.D.; Nguyen, D.H.; Vo, D.V.N.; Le, X.T.; Le, N.T.H.; et al. Green Technology to Optimize the Extraction Process of Turmeric (*Curcuma Longa* L.) Oils. *IOP Conf. Ser. Mater. Sci. Eng.* **2019**, *479*, doi:10.1088/1757-899X/479/1/012002.
65. Ibáñez, M.D.; Blázquez, M.A. *Curcuma Longa* L. Rhizome Essential Oil from Extraction to Its Agri-Food Applications. A Review. *Plants* **2020**, *10*, 44, doi:10.3390/PLANTS10010044.
66. Began, G.; Goto, M.; Kodama, A.; Hirose, T. Response Surfaces of Total Oil Yield of Turmeric (*Curcuma Longa*) in Supercritical Carbon Dioxide. *Food Res. Int.* **2000**, *33*, 341–345, doi:10.1016/S0963-9969(00)00053-3.
67. Patil, S.S.; Bhasarkar, S.; Rathod, V.K. Extraction of Curcuminoids from *Curcuma Longa*: Comparative Study between Batch Extraction and Novel Three Phase Partitioning. *Prep. Biochem. Biotechnol.* **2019**, *49*, 407–418,

doi:10.1080/10826068.2019.1575859.

68. Kurmudle, N.N.; Bankar, S.B.; Bajaj, I.B.; Bule, M. V.; Singhal, R.S. Enzyme-Assisted Three Phase Partitioning: A Novel Approach for Extraction of Turmeric Oleoresin. *Process Biochem.* **2011**, *46*, 423–426, doi:10.1016/j.procbio.2010.09.010.
69. Dennison, C.; Lovrien, R. Three Phase Partitioning: Concentration and Purification of Proteins. *Protein Expr. Purif.* **1997**, *11*, 149–161, doi:10.1006/prep.1997.0779.
70. Lateh, L.; Yuenyongsawad, S.; Chen, H.; Panichayupakaranant, P. A Green Method for Preparation of Curcuminoid-Rich Curcuma Longa Extract and Evaluation of Its Anticancer Activity. *Pharmacogn. Mag.* **2019**, *15*, 730–735, doi:10.4103/pm.pm_162_19.
71. Chemat, F.; Vian, M.A.; Cravotto, G. Green Extraction of Natural Products: Concept and Principles. *Int. J. Mol. Sci* **2012**, *13*, 8615–8627, doi:10.3390/ijms13078615.
72. Nagavekar, N.; Singhal, R.S. Supercritical Fluid Extraction of Curcuma Longa and Curcuma Amada Oleoresin: Optimization of Extraction Conditions, Extract Profiling, and Comparison of Bioactivities. *Ind. Crops Prod.* **2019**, *134*, 134–145, doi:10.1016/j.indcrop.2019.03.061.
73. Stahl, E.; Quirin, K.-W.; Gerard, D. II. Grundlagen Der Extraktion Mit Verdichteten Gasen. In *Verdichtete Gase zur Extraktion und Raffination*; Springer Berlin Heidelberg, 1987; pp. 10–36 ISBN 3-540-16937-7.
74. Cagniard de la Tour, C. le B. Exposé de Quelques Résultats Obtenus Par l'action Combinée de La Chaleur et de La Compression Sur Certains Liquides, Tels Que l'eau, l'alcool, L'éther Sulfurique et l'essence de Pétrole Rectifiée. *Ann. Chim. Phys.* **1822**, *2*, 127–132.
75. Gouw, T.H.; Jentoft, R.E. Supercritical Fluid Chromatography. *J. Chromatogr. A* **1972**, *68*, 303–323, doi:10.1016/S0021-9673(00)85722-2.
76. Phelps, C.L.; Smart, N.G.; Wai, C.M. Chemistry Everday for Everyone Past, Present, and Possible Future Applications of Supercritical Fluid Extraction Technology. *J. Chem. Educ.* **1996**, *73*, 1163–1168, doi:10.1021/ED073P1163.
77. Span, R.; Wagner, W. A New Equation of State for Carbon Dioxide Covering the Fluid Region from the Triple-Point Temperature to 1100 K at Pressures up to 800 MPa. *J. Phys. Chem. Ref. Data* **1996**, *25*, 1509–1596, doi:10.1063/1.555991.
78. King, J.W. Analytical Supercritical Fluid Extraction. In *Analytical Supercritical Fluid Chromatography and Extraction*; Lee, M.L., Markides, K.E., Eds.; Chromatography Conferences Inc.: Provo, Utah, 1990; pp. 311–362 ISBN 0-8425-2394-4.
79. Sihvonen, M.; Järvenpää, E.; Hietaniemi, V.; Huopalahti, R. Advances in Supercritical Carbon Dioxide Technologies. *Trends Food Sci. Technol.* **1999**, *10*, 217–222, doi:10.1016/S0924-2244(99)00049-7.
80. Randall, L.G. The Present Status of Dense (Supercritical) Gas Extraction and Dense Gas Chromatography: Impetus for DGC/MS Development. *Sep. Sci. Technol.* **1982**, *17*, 1–118, doi:10.1080/01496398208058142.

81. Joule, J.P.; Thomson, W. LXXVI. On the Thermal Effects Experienced by Air in Rushing through Small Apertures . *London, Edinburgh, Dublin Philos. Mag. J. Sci.* **1852**, *4*, 481–492, doi:10.1080/14786445208647169.
82. Joules, J.P. *Joint Scientific Papers of James Prescott Joule*; The Physical Society of London: London, 2004; Vol. 2; ISBN 3663537137.
83. SITEC-Sieber Engineering AG *User Manual Pilot Unit for Supercritical Fluid Extraction of Solids*; Maur, Switzerland, 1998;
84. Tyrer, D. LXII.-Solubilities Below and Above the Critical Temperature. *J. Chem. Soc., Trans.* **1910**, *97*, 621–632, doi:10.1039/CT9109700621.
85. Kumar, S.K.; Johnston, K.P. Modelling the Solubility of Solids in Supercritical Fluids with Density as the Independent Variable. *J. Supercrit. Fluids* **1988**, *1*, 15–22, doi:10.1016/0896-8446(88)90005-8.
86. Eckert, C.A.; Knutson, B.L.; Debenedetti, P.G. Supercritical Fluids as Solvents for Chemical and Materials Processing. *Nature* **1996**, *383*, 313–318, doi:10.1038/383313A0.
87. Kandiah, M.; Spiro, M. Extraction of Ginger Rhizome: Kinetic Studies with Supercritical Carbon Dioxide. *Int. J. Food Sci. Technol.* **1990**, *25*, 328–338, doi:10.1111/J.1365-2621.1990.TB01089.X.
88. Notej, B.; Bagheri, H.; Alsaikhan, F.; Hashemipour, H. Increasing Solubility of Phenytoin and Raloxifene Drugs: Application of Supercritical CO₂ Technology. *J. Mol. Liq.* **2023**, *373*, 121246, doi:10.1016/J.MOLLIQ.2023.121246.
89. Sparks, D.L.; Hernandez, R.; Estévez, L.A. Evaluation of Density-Based Models for the Solubility of Solids in Supercritical Carbon Dioxide and Formulation of a New Model. *Chem. Eng. Sci.* **2008**, *63*, 4292–4301, doi:10.1016/j.ces.2008.05.031.
90. Saitow, K.I.; Kajiya, D.; Nishikawa, K. Dynamics of Density Fluctuation of Supercritical Fluid Mapped on Phase Diagram. *J. Am. Chem. Soc.* **2004**, *126*, 422–423, doi:10.1021/JA038176Z/ASSET/IMAGES/MEDIUM/JA038176ZE00001.GIF.
91. Stahl, E.; Quirin, K.-W.; Gerard, D. IV. Anwendung Verdichteter Gase Zur Extraktion Und Raffination. In *Verdichtete Gase zur Extraktion und Raffination*; Springer Berlin Heidelberg, 1987; pp. 82–241 ISBN 3-540-16937-7.
92. Stahl, H.C.E.; Schilz, W. Extraktion Mit Überkritischen Gasen in Direkter Kopplung Mit Der Dünnschicht-Chromatographie. Anwendungsmöglichkeiten Auf Dem Naturstoffgebiet. *Chemie Ing. Tech.* **1976**, *48*, 773–778, doi:10.1002/CITE.330480908.
93. Stahl, E.; Quirin, K.-W.; Gerard, D. III. Methoden, Apparaturen, Anlagen. In *Verdichtete Gase zur Extraktion und Raffination*; Springer Berlin Heidelberg, 1987; pp. 38–81 ISBN 3-540-16937-7.
94. Bodkin, C.L.; Clarke, B.J.; Kavanagh, T.E.; Moulder, P.M.; Reitze, J.D. Preparation and Analysis of Liquid CO₂ Hop Extracts. *J. Am. Soc. Brew. Chem.* **1980**, *38*, doi:10.1094/asbcj-38-0137.
95. Stahl, E.; Schütz, E. Extraktion Der Kamillenblüten Mit Überkritischen Gasen. *Arch. Pharm. (Weinheim).* **1978**, *311*, 992–1001, doi:10.1002/ARDP.19783111204.

96. Kim, W.J.; Kim, J.D.; Kim, J.; Oh, S.G.; Lee, Y.W. Selective Caffeine Removal from Green Tea Using Supercritical Carbon Dioxide Extraction. *J. Food Eng.* **2008**, *89*, 303–309, doi:10.1016/j.jfoodeng.2008.05.018.
97. Tamkutė, L.; Pukalskas, A.; Syrpas, M.; Urbonavičienė, D.; Viškelis, P.; Venskutonis, P.R. Fractionation of Cranberry Pomace Lipids by Supercritical Carbon Dioxide Extraction and On-Line Separation of Extracts at Low Temperatures. *J. Supercrit. Fluids* **2020**, *163*, 104884, doi:10.1016/j.supflu.2020.104884.
98. Visentín, A.; Cismondi, M.; Maestri, D. Supercritical CO₂ Fractionation of Rosemary Ethanolic Oleoresins as a Method to Improve Carnosic Acid Recovery. *Innov. Food Sci. Emerg. Technol.* **2011**, *12*, 142–145, doi:10.1016/j.ifset.2011.01.004.
99. Zhang, Y.; Yang, J.; Yu, Y.X. Dielectric Constant and Density Dependence of the Structure of Supercritical Carbon Dioxide Using a New Modified Empirical Potential Model: A Monte Carlo Simulation Study. *J. Phys. Chem. B* **2005**, *109*, 13375–13382, doi:10.1021/JP045741R.
100. Hyatt, J.A. Liquid and Supercritical Carbon Dioxide as Organic Solvents. *J. Org. Chem.* **1985**, *50*, 3246, doi:10.1021/jo00217a602.
101. Kauffman, J.F. Quadrupolar Solvent Effects on Solvation and Reactivity of Solutes Dissolved in Supercritical CO₂. *J. Phys. Chem. A* **2001**, *105*, 3440–3442, doi:10.1021/JP004359L.
102. Reynolds, L.; Gardecki, J.A.; Frankland, S.J. V; Horng, M.L.; Maroncelli, M. Dipole Solvation in Nondipolar Solvents: Experimental Studies of Reorganization Energies and Solvation Dynamics †. *J. Phys. Chem. ABC* **1996**, *100*, 10337–10354, doi:10.1021/JP953110E.
103. Raveendran, P.; Wallen, S.L. Cooperative C-H₀ ... O Hydrogen Bonding in CO₂-Lewis Base Complexes: Implications for Solvation in Supercritical CO₂. *J. Am. Chem. Soc.* **2002**, *124*, 12590–12599, doi:10.1021/JA0174635.
104. Kazarian, S.G.; Vincent, F.M.; Bright, F. V.; Liotta, C.L.; Eckert*, C.A. Specific Intermolecular Interaction of Carbon Dioxide with Polymers. *J. Am. Chem. Soc.* **1996**, *118*, 1729–1736, doi:10.1021/JA950416Q.
105. Raveendran, P.; Ikushima, Y.; Wallen, S.L. Polar Attributes of Supercritical Carbon Dioxide. *Acc. Chem. Res.* **2005**, *38*, 478–485, doi:10.1021/AR040082M.
106. Meredith, J.C.; Johnston, K.P.; Seminario, J.M.; Kazarian, S.G.; Eckert, C.A. Quantitative Equilibrium Constants between CO₂ and Lewis Bases from FTIR Spectroscopy. *J. Phys. Chem.* **1996**, *100*, 10837–10848, doi:10.1021/JP953161B/SUPPL_FILE/JP10837.PDF.
107. Wahl, M. Supercritical Fluid Technology. *Handb. Pharm. Granulation Technol. Third Ed.* **2009**, 126–137, doi:doi:10.3109/9781616310035-7.
108. Ohgaki, K.; Katayama, T. Isothermal Vapor-Liquid Equilibrium Data for Binary Systems Containing Carbon Dioxide at High Pressures: Methanol–Carbon Dioxide, n-Hexane–Carbon Dioxide, and Benzene–Carbon Dioxide Systems. *J. Chem. Eng. Data* **1976**, *21*, 53–55, doi:10.1021/je60068a015.
109. Bitencourt, R.G.; Cabral, F.A.; Meirelles, A.J.A. Ferulic Acid Solubility in Supercritical Carbon Dioxide, Ethanol and Water Mixtures. *J. Chem. Thermodyn.*

- 2016**, 103, 285–291, doi:10.1016/j.jct.2016.08.025.
110. Monroy, Y.M.; Rodrigues, R.A.F.; Sartoratto, A.; Cabral, F.A. Influence of Ethanol, Water, and Their Mixtures as Co-Solvents of the Supercritical Carbon Dioxide in the Extraction of Phenolics from Purple Corn Cob (*Zea Mays* L.). *J. Supercrit. Fluids* **2016**, 118, 11–18, doi:10.1016/j.supflu.2016.07.019.
 111. Almeida, R.N.; Neto, R.G.; Barros, F.M.C.; Cassel, E.; von Poser, G.L.; Vargas, R.M.F. Supercritical Extraction of *Hypericum Caprifoliatum* Using Carbon Dioxide and Ethanol+water as Co-Solvent. *Chem. Eng. Process. Process Intensif.* **2013**, 70, 95–102, doi:10.1016/j.cep.2013.05.002.
 112. Iheozor-Ejiofor, P.; Dey, E.S. Extraction of Rosavin from *Rhodiola Rosea* Root Using Supercritical Carbon Dioxide with Water. *J. Supercrit. Fluids* **2009**, 50, 29–32, doi:10.1016/j.supflu.2009.04.011.
 113. Peker, H.; Srinivasan, M.P.; Smith, J.M.; McCoy, B.J. Caffeine Extraction Rates from Coffee Beans with Supercritical Carbon Dioxide. *AIChE J.* **1992**, 38, 761–770, doi:10.1002/AIC.690380513.
 114. De Lucas, A.; Gracia, I.; Rincón, J.; García, M.T. Solubility Determination and Model Prediction of Olive Husk Oil in Supercritical Carbon Dioxide and Cosolvents. *Ind. Eng. Chem. Res.* **2007**, 46, 5061–5066, doi:10.1021/ie061153j.
 115. Li, Q.; Zhang, Z.; Zhong, C.; Liu, Y.; Zhou, Q. Solubility of Solid Solutes in Supercritical Carbon Dioxide with and without Cosolvents. *Fluid Phase Equilib.* **2003**, 207, 183–192, doi:10.1016/S0378-3812(03)00022-0.
 116. Da Porto, C.; Decorti, D.; Natolino, A. Water and Ethanol as Co-Solvent in Supercritical Fluid Extraction of Proanthocyanidins from Grape Marc: A Comparison and a Proposal. *J. Supercrit. Fluids* **2014**, 87, 1–8, doi:10.1016/j.supflu.2013.12.019.
 117. Ivanovic, J.; Ristic, M.; Skala, D. Supercritical CO₂ Extraction of *Helichrysum Italicum*: Influence of CO₂ Density and Moisture Content of Plant Material. *J. Supercrit. Fluids* **2011**, 57, 129–136, doi:10.1016/j.supflu.2011.02.013.
 118. Balachandran, S.; Kentish, S.E.; Mawson, R. The Effects of Both Preparation Method and Season on the Supercritical Extraction of Ginger. *Sep. Purif. Technol.* **2006**, 48, 94–105, doi:10.1016/j.seppur.2005.07.008.
 119. Leeke, G.; Gaspar, F.; Santos, R. Influence of Water on the Extraction of Essential Oils from a Model Herb Using Supercritical Carbon Dioxide. *Ind. Eng. Chem. Res.* **2002**, 41, 2033–2039, doi:10.1021/ie010845z.
 120. Raps GmbH & Co. KG RAPS - Würzkraft Available online: <http://www.raps.com> (accessed on 21 March 2018).
 121. Zorić, M.; Banožić, M.; Aladić, K.; Vladimir-Knežević, S.; Jokić, S. Supercritical CO₂ Extracts in Cosmetic Industry: Current Status and Future Perspectives. *Sustain. Chem. Pharm.* **2022**, 27, 100688, doi:10.1016/J.SCP.2022.100688.
 122. Reverchon, E.; Donsi, G.; Osséo, L.S. Modeling of Supercritical Fluid Extraction from Herbaceous Matrices. *Ind. Eng. Chem. Res.* **1993**, 32, 2721–2726, doi:10.1021/IE00023A039.
 123. Qamar, S.; Torres, Y.J.M.; Parekh, H.S.; Falconer, J.R. Fractional Factorial Design Study for the Extraction of Cannabinoids from CBD-Dominant Cannabis Flowers by Supercritical Carbon Dioxide. **2022**, doi:10.3390/pr10010093.

124. Qamar, S.; Manrique, Y.J.; Parekh, H.S.; Falconer, J.R. Development and Optimization of Supercritical Fluid Extraction Setup Leading to Quantification of 11 Cannabinoids Derived from Medicinal Cannabis. *Biology (Basel)*. **2021**, *10*, 1–19, doi:10.3390/biology10060481.
125. Turner, C.; King, J.W.; Mathiasson, L. Supercritical Fluid Extraction and Chromatography for Fat-Soluble Vitamin Analysis. *J. Chromatogr. A* **2001**, *936*, 215–237, doi:10.1016/S0021-9673(01)01082-2.
126. Smirnova, I.; Türk, M.; Wischumerski, R.; Wahl, M.A. Comparison of Different Methods for Enhancing the Dissolution Rate of Poorly Soluble Drugs: Case of Griseofulvin. *Eng. Life Sci.* **2005**, *5*, 277–280, doi:10.1002/elsc.200500081.
127. Müllers, K.C.; Paisana, M.; Wahl, M.A. Simultaneous Formation and Micronization of Pharmaceutical Cocrystals by Rapid Expansion of Supercritical Solutions (RESS). *Pharm. Res.* **2015**, *32*, 702–713, doi:10.1007/s11095-014-1498-9.
128. Paisana, M.C.; Müllers, K.C.; Wahl, M.A.; Pinto, J.F. Production and Stabilization of Olanzapine Nanoparticles by Rapid Expansion of Supercritical Solutions (RESS). *J. Supercrit. Fluids* **2016**, *109*, 124–133, doi:10.1016/j.supflu.2015.11.012.
129. Armbruster, M.; Mönckedieck, M.; Scherließ, R.; Daniels, R.; Wahl, M.A. Birch Bark Dry Extract by Supercritical Fluid Technology: Extract Characterisation and Use for Stabilisation of Semisolid Systems. *Appl. Sci.* **2017**, *Vol. 7*, Page 292 **2017**, *7*, 292, doi:10.3390/APP7030292.
130. Akolade, J.O.; Nasir-Naeem, K.O.; Swanepoel, A.; Yusuf, A.A.; Balogun, M.; Labuschagne, P. CO₂-Assisted Production of Polyethylene Glycol / Lauric Acid Microparticles for Extended Release of Citrus Aurantifolia Essential Oil. *J. CO₂ Util.* **2020**, *38*, 375–384, doi:10.1016/j.jcou.2020.02.014.
131. Vega-González, A.; Subra-Paternault, P.; López-Periago, A.M.; García-González, C.A.; Domingo, C. Supercritical CO₂ Antisolvent Precipitation of Polymer Networks of L-PLA, PMMA and PMMA/PCL Blends for Biomedical Applications. *Eur. Polym. J.* **2008**, *44*, 1081–1094, doi:10.1016/j.eurpolymj.2008.01.009.
132. García-González, C.A.; Vega-González, A.; López-Periago, A.M.; Subra-Paternault, P.; Domingo, C. Composite Fibrous Biomaterials for Tissue Engineering Obtained Using a Supercritical CO₂ Antisolvent Process. *Acta Biomater.* **2009**, *5*, 1094–1103, doi:10.1016/j.actbio.2008.10.018.
133. Schmid, J.; Wahl, M.A.; Daniels, R. Supercritical Fluid Technology for the Development of 3d Printed Controlled Drug Release Dosage Forms. *Pharmaceutics* **2021**, *13*, doi:10.3390/PHARMACEUTICS13040543.
134. Hussein, K.; Türk, M.; Wahl, M.A. Comparative Evaluation of Ibuprofen/ β -Cyclodextrin Complexes Obtained by Supercritical Carbon Dioxide and Other Conventional Methods. *Pharmaceutical Res.* **2007**, *24*, 585–592, doi:10.1007/s11095-006-9177-0.
135. Hussein, K.; Türk, M.; Wahl, M.A. Drug Loading into β -Cyclodextrin Granules Using a Supercritical Fluid Process for Improved Drug Dissolution. *Eur. J. Pharm. Sci.* **2008**, *33*, 306–312, doi:10.1016/j.ejps.2008.01.003.
136. Ragna S. Wischumerski, Michael Türk; Wahl, M.A. Direct Drug Loading into

- Preformed Porous Solid Dosage Units by the Controlled Particle Deposition (CPD), a New Concept for Improved Dissolution Using SCF-Technology. *J. Pharm. Sci.* **2008**, *97*, 4416–4424, doi:10.1002/jps.
137. Lukic, I.; Pajnik, J.; Nisavic, J.; Tadic, V.; Vági, E.; Szekely, E.; Zizovic, I. Application of the Integrated Supercritical Fluid Extraction–Impregnation Process (SFE-SSI) for Development of Materials with Antiviral Properties. *Processes* **2022**, *10*, doi:10.3390/pr10040680.
 138. Ishikawa, M.; Hashimoto, Y. Improvement in Aqueous Solubility in Small Molecule Drug Discovery Programs by Disruption of Molecular Planarity and Symmetry. *J. Med. Chem.* **2011**, *54*, 1539–1554, doi:10.1021/JM101356P/ASSET/IMAGES/MEDIUM/JM-2010-01356P_0011.GIF.
 139. Raza, K.; Kumar, P.; Ratan, S.; Malik, R.; Arora, S. Polymorphism: The Phenomenon Affecting the Performance of Drugs. *SOJ Pharm. Pharm. Sci.* **2014**, *1*, 10.
 140. Qian, K.K.; Wurster, D.E.; Bogner, R.H. Spontaneous Crystalline-to-Amorphous Phase Transformation of Organic or Medicinal Compounds in the Presence of Porous Media, Part 3: Effect of Moisture. *Pharm. Res.* **2012**, *29*, 2698–2709, doi:10.1007/s11095-012-0734-4.
 141. Wegiel, L.A.; Zhao, Y.; Mauer, L.J.; Edgar, K.J.; Taylor, L.S. Curcumin Amorphous Solid Dispersions: The Influence of Intra and Intermolecular Bonding on Physical Stability. *Pharm. Dev. Technol.* **2014**, *19*, 976–986, doi:10.3109/10837450.2013.846374.
 142. Niebergall, P.J.; Milosovich, G.; Goyan, J.E. Dissolution Rate Studies II Dissolution of Particles Under Conditions of Rapid Agitation. *J. Pharm. Sci.* **1963**, *52*, 236–241, doi:doi:10.1002/jps.2600520310.
 143. Mosharraf, M.; Nyström, C. The Effect of Particle Size and Shape on the Surface Specific Dissolution Rate of Microsized Practically Insoluble Drugs. *Int. J. Pharm.* **1995**, *122*, 35–47, doi:10.1016/0378-5173(95)00033-F.
 144. Nernst, W. Theorie Der Reaktionsgeschwindigkeit in Heterogenen Systemen . *Zeitschrift für Phys. Chemie* **1904**, *47U*, doi:10.1515/ZPCH-1904-4704.
 145. Francis, A.P.; Murthy, P.B.; Devasena, T. Bis-Demethoxy Curcumin Analog Nanoparticles: Synthesis, Characterization, and Anticancer Activity in Vitro. *J. Nanosci. Nanotechnol.* **2014**, *14*, 4865–4873, doi:10.1166/jnn.2014.9219.
 146. Dr. Loges + Co. GmbH Curcumin-Loges® | Dr. Loges Available online: <https://www.loges.de/p/curcumin-loges> (accessed on 21 May 2023).
 147. Xiao, Y.; Chen, X.; Yang, L.; Zhu, X.; Zou, L.; Meng, F.; Ping, Q. Preparation and Oral Bioavailability Study of Curcuminoid-Loaded Microemulsion. *J. Agric. Food Chem.* **2013**, *61*, 3654–3660, doi:10.1021/JF400002X/ASSET/IMAGES/MEDIUM/JF-2013-00002X_0007.GIF.
 148. Kazi, M.; Shahba, A.A.; Alrashoud, S.; Alwadei, M.; Sherif, A.Y.; Alanazi, F.K. Bioactive Self-Nanoemulsifying Drug Delivery Systems (Bio-SNEDDS) for Combined Oral Delivery of Curcumin and Piperine. *Mol.* **2020**, *25*, 1703, doi:10.3390/MOLECULES25071703.

149. Porter, C.J.H.; Trevaskis, N.L.; Charman, W.N. Lipids and Lipid-Based Formulations: Optimizing the Oral Delivery of Lipophilic Drugs. *Nat. Rev. Drug Discov.* **2007**, *6*, 231–248, doi:10.1038/nrd2197.
150. Porter, C.J.H.; Charman, W.N. In Vitro Assessment of Oral Lipid Based Formulations. *Adv. Drug Deliv. Rev.* **2001**, *50*, 127–147, doi:10.1016/S0169-409X(01)00182-X.
151. Chakraborty, S.; Shukla, D.; Mishra, B.; Singh, S. Lipid - An Emerging Platform for Oral Delivery of Drugs with Poor Bioavailability. *Eur. J. Pharm. Biopharm.* **2009**, *73*, 1–15, doi:10.1016/j.ejpb.2009.06.001.
152. Aquanova AG NovaSOL® CURCUMIN Available online: <https://aquanova.de/health-solutions/novasol-curcumin> (accessed on 21 May 2023).
153. Botanicy Curcuma Forte 800 Mit Novasol Curcumin Available online: https://www.feelgood-shop.com/produkte/curcuma-forte-800-mit-novasol-curcumin/?trc_gcmp_id=17788348024&gclid=CjwKCAjwgqejBhBAEiwAuWHioCf5W1I25vH6_LqGeRqMSP0JbZpXsF0kHCaRxRHEe2eLpQINC4t5choCsjYQAvD_BwE (accessed on 21 May 2023).
154. Perrigo Abtei NATURE & SCIENCE Curcuma Available online: <https://www.abtei.de/produkte/abtei-nature-science/abtei-nature-science-curcuma/> (accessed on 21 May 2023).
155. Queisser Pharma Doppelherz Curcuma 750 Mit Curcumin Kapseln Available online: <https://www.doppelherz.de/produkte/doppelherz-curcuma-750> (accessed on 21 May 2023).
156. dm-drogerie markt GmbH + Co. KG Mivolis Premium Curcuma Kapseln Available online: https://www.dm.de/mivolis-premium-curcuma-kapseln-30-st-p4066447219432.html?wt_mc=shopping.google.lia.Gesundheit&storeId=DE-0070 (accessed on 21 May 2023).
157. Yixuan, L.; Qaria, M.A.; Sivasamy, S.; Jianzhong, S.; Daochen, Z. Curcumin Production and Bioavailability: A Comprehensive Review of Curcumin Extraction, Synthesis, Biotransformation and Delivery Systems. *Ind. Crops Prod.* **2021**, *172*, 114050, doi:10.1016/J.INDCROP.2021.114050.
158. Cole, E.T.; Cadé, D.; Benameur, H. Challenges and Opportunities in the Encapsulation of Liquid and Semi-Solid Formulations into Capsules for Oral Administration. *Adv. Drug Deliv. Rev.* **2008**, *60*, 747–756, doi:10.1016/j.addr.2007.09.009.
159. Hosny, E.A.; Al-shora, H.I.; Elmazar, M.M.A. Oral Delivery of Insulin from Enteric-Coated Capsules Containing Sodium Salicylate: Effect on Relative Hypoglycemia of Diabetic Beagle Dogs. *Int. J. Pharm.* **2002**, *237*, 71–76, doi:10.1016/S0378-5173(02)00024-8.
160. Feeney, O.M.; Crum, M.F.; Mcevoy, C.L.; Trevaskis, N.L.; Williams, H.D.; Pouton, C.W.; Charman, W.N.; Bergström, C.A.S.; Porter, C.J.H. 50 Years of Oral Lipid-Based Formulations: Provenance, Progress and Future Perspectives ☆. *Adv. Drug Deliv. Rev.* **2016**, *101*, 167–194, doi:10.1016/j.addr.2016.04.007.
161. Ramesh, V.; Meenakshi, S.; Jyothirmayee, N.; Bullebbai, M.; Noorjahan, S.K.; Rajeswari, G.; Babu, G.N.; Madhavi, D. Enhancement of Solubility, Dissolution

- Rate and Bioavailability of BCS Class II Drugs. *Int. J. Pharma Chem. Res.* **2016**, 2, 2395–3411.
162. IOI Oleo GmbH *Safety Data Sheet Witepsol® S58*; 2020;
 163. IOI Oleo GmbH *Safety Data Sheet Witepsol® W45*; 2020;
 164. Caesar & Loretz GmbH *Produktdatenblatt Macrogol 4000 Pulver*; 2022;
 165. Evonic Industries *SAFETY DATA SHEET AEROPERL® 300 Pharma* ; 2016;
 166. Capsugel *Coni-Snap Hard Gelatin Capsules*; 2011;
 167. DAC/NRF (2020) 1.9 Kapseln. In *Deutscher Arzneimittel-Codex/ Neues Rezeptur-Formularium*; Mediengruppe Deutscher Apotheker GmbH, Eschbom, 2021; pp. 1–30 ISBN 978-3-7741-1608-5.
 168. Gullapalli, R.P.; Mazzitelli, C.L. *Gelatin and Non-Gelatin Capsule Dosage Forms*; Elsevier Inc., 2017; Vol. 106; ISBN 9143164935.
 169. Kontny, M.J.; Mulski, C.A. Gelatin Capsule Brittleness as a Function of Relative Humidity at Room Temperature. *Int. J. Pharm.* **1989**, 54, 79–85, doi:10.1016/0378-5173(89)90168-3.
 170. Marques, M.; Kruep, D.; Gray, V.; Murachanian, D.; Brown, W.; Giancaspro, G. Liquid-Filled Gelatin Capsules. *Pharmacopeial Forum* **2009**, 35, 1029–1041.
 171. Diegenis, G.A.; Gold, T.B.; Shah, V.P. Cross-Linking of Gelatin Capsules and Its Relevance to Their in Vitro-in Vivo Performance. *J. Pharm. Sci.* **1994**, 83, 915–921, doi:10.1002/jps.2600830702.
 172. Cole, E.T. Liquid Filled and Sealed Hard Gelatin Capsules. *Gattefossé Bull.* **1999**, 92, 1–12.
 173. Cadé, D.; Cole, E.T.; Mayer, J.P.; Wittwer, F. Liquid Filled and Sealed Hard Gelatin Capsules. *Drug Dev. Ind. Pharm.* **1986**, 12, 2289–2300, doi:10.3109/03639048609042636.
 174. Armstrong, N.A.; James, K.C.; Pugh, W.K.L. Drug Migration into Soft Gelatin Capsule Shells and Its Effect on In-Vitro Availability. *J. Pharm. Pharmacol.* **2011**, 36, 361–365, doi:10.1111/J.2042-7158.1984.TB04399.X.
 175. Hom, F.S.; Veresh, S.A.; Ebert, W.R. Soft Gelatin Capsules II: Oxygen Permeability Study of Capsule Shells. *J. Pharm. Sci.* **1975**, 64, 851–857, doi:10.1002/JPS.2600640528.
 176. Pohl-Boskamp GeloMyrtol® Forte - Anwendungsgebiete & Wirkungsweise Available online: <https://www.gelomyrtol-forte.de/gelomyrtol-forte> (accessed on 10 June 2023).
 177. Aristo Sedariston - Mit Johanniskraut Und Baldrian Zu Innerer Stärke Finden Available online: <https://sedariston.de/produktinformation/> (accessed on 10 June 2023).
 178. IOI Oleo GmbH *Witepsol*; Hamburg;
 179. Radomska-Soukharev, A. Stability of Lipid Excipients in Solid Lipid Nanoparticles. *Adv. Drug Deliv. Rev.* **2007**, 59, 411–418, doi:10.1016/j.addr.2007.04.004.
 180. Nicholson, R.A.; Marangoni, A.G. Food Structure Development in Oil and Fat Systems. In *Handbook of Food Structure Development*; Spyropoulos, F., Lazidis,

- A., Norton, I., Eds.; Royal Society of Chemistry: Cambridge, 2020; pp. 115–133 ISBN 978-1-78801-216-4.
181. DAC/NRF (2018) Dronabinol-Kapseln 2,5 Mg / 5 Mg /10 Mg (NRF 22. 7.). In *Deutscher Arzneimittel-Codex/ Neues Rezeptur-Formularium*; AVOXA-Mediengruppe Deutscher Apotheker GmbH, Eschborn, 2018; pp. 1–12 ISBN 978-3-7741-1278-0.
 182. Jensen, L.H.; Mabis, A.J. Refinement of the Structure of 13-Tricaprin. *Acta Crystallogr.* **1966**, *21*, 770–781, doi:10.1107/S0365110X66003839.
 183. Acevedo, N.C.; Marangoni, A.G. Nanostructured Fat Crystal Systems. *Annu. Rev. Food Sci. Technol.* **2015**, *6*, 71–96, doi:10.1201/b12883-8.
 184. Ramel, P.R.; Co, E.D.; Acevedo, N.C.; Marangoni, A.G. Structure and Functionality of Nanostructured Triacylglycerol Crystal Networks. *Prog. Lipid Res.* **2016**, *64*, 231–242, doi:10.1016/j.plipres.2016.09.004.
 185. Acevedo, N.C.; Block, J.M.; Marangoni, A.G. Critical Laminar Shear-Temperature Effects on the Nano- and Mesoscale Structure of a Model Fat and Its Relationship to Oil Binding and Rheological Properties. *Faraday Discuss.* **2012**, *158*, 171–194, doi:10.1039/C2FD20008B.
 186. Dibildox-Alvarado, E.; Rodrigues, J.N.; Gioielli, L.A.; Toro-Vazquez, J.F.; Marangoni, A.G. Effects of Crystalline Microstructure on Oil Migration in a Semisolid Fat Matrix. *Cryst. Growth Des.* **2004**, *4*, 731–736, doi:10.1021/CG049933N/ASSET/IMAGES/MEDIUM/CG049933NE00003.GIF.
 187. Sato, K. Crystallization Behaviour of Fats and Lipids - a Review. *Chem. Eng. Sci.* **2001**, *56*, 2255–2265, doi:10.1016/S0009-2509(00)00458-9.
 188. Sato, K.; Wang, T.A.Z.H.; Ojima, K.; Sagi, N.; Mori, H. Polymorphism of POP and SOS . I . Occurrence and Polymorphic Transformation '. *J. Am. Oil Chem. Soc.* **1989**, *66*, 664–674, doi:10.1007/BF02669949.
 189. Larsson, K. Classification of Glyceride Crystal Forms. *Acta Chem. Scand.* **1966**, *20*, 2255–2260, doi:10.3891/ACTA.CHEM.SCAND.20-2255.
 190. Oliveira, G.M. de; Ribeiro, A.P.B.; Santo, A.O. dos; Cardoso, L.P.; Kieckbusch, T.G. Hard Fats as Additives in Palm Oil and Its Relationships to Crystallization Process and Polymorphism. *LWT - Food Sci. Technol.* **2015**, *63*, 1163–1170, doi:10.1016/j.lwt.2015.04.036.
 191. Acevedo, N.C.; Marangoni, A.G. Engineering the Functionality of Blends of Fully Hydrogenated and Non-Hydrogenated Soybean Oil by Addition of Emulsifiers. *Food Biophys.* **2014**, *9*, 368–379, doi:10.1007/s11483-014-9340-9.
 192. Acevedo, N.C.; Marangoni, A.G. Toward Nanoscale Engineering of Triacylglycerol Crystal Networks. **2010**, *10*, 3334–3339, doi:10.1021/cg100469x.
 193. Marty, S.; Marangoni, A.G. Effects of Cocoa Butter Origin, Tempering Procedure, and Structure on Oil Migration Kinetics. *Cryst. Growth Des.* **2009**, *9*, 4415–4423, doi:10.1021/cg9004505.
 194. MacDougall, C.J.; Razul, M.S.; Papp-Szabo, E.; Peyronel, F.; Hanna, C.B.; Marangoni, A.G.; Pink, D.A. Nanoscale Characteristics of Triacylglycerol Oils: Phase Separation and Binding Energies of Two-Component Oils to Crystalline Nanoplatelets. *Faraday Discuss.* **2012**, *158*, 425–433, doi:10.1039/C2FD20039B.

195. Heertje, I. Microstructural Studies in Fat Research. *Food Struct.* **1993**, *12*, 77–94.
196. IOI Oleo GmbH *Product List*, Hamburg;
197. Mor, N.; Raghav, N. Curcumin, the Panacea: A Review on Advancement to Solve Pharmaco-Kinetic Problems. *Chem. Biol. Interface* **2021**, *11*, 94–108.
198. Knop, K.; Hoogenboom, R.; Fischer, D.; Schubert, U.S. Poly(Ethylene Glycol) in Drug Delivery: Pros and Cons as Well as Potential Alternatives. *Angew. Chemie Int. Ed.* **2010**, *49*, 6288–6308, doi:10.1002/ANIE.200902672.
199. Craig, D.Q.M. A Review of Thermal Methods Used for the Analysis of the Crystal Form, Solution Thermodynamics and Glass Transition Behaviour of Polyethylene Glycols. *Thermochim. Acta* **1995**, *248*, 189–203, doi:10.1016/0040-6031(94)01886-L.
200. Baird, J.A.; Olayo-Valles, R.; Rinaldi, C.; Taylor, L.S. Effect of Molecular Weight, Temperature, and Additives on the Moisture Sorption Properties of Polyethylene Glycol. *J. Pharm. Sci.* **2010**, *99*, 154–168, doi:10.1002/JPS.21808.
201. CARBOWAX™ SENTRY™ | Polyethylene Glycol Supplier | Dow Inc. Available online: <https://www.dow.com/en-us/brand/carbowax-sentry.html> (accessed on 30 November 2022).
202. D'souza, A.A.; Shegokar, R. Polyethylene Glycol (PEG): A Versatile Polymer for Pharmaceutical Applications. *Expert Opin. Drug Deliv.* **2016**, *13*, 1257–1275, doi:10.1080/17425247.2016.1182485.
203. DAC/NRF (2013) Thalidomid-Kapseln 50 Mg / 100 Mg / 150 Mg /200 Mg (NRF 32.2). In *Deutscher Arzneimittel-Codex/ Neues Rezeptur-Formularium*; AMediengruppe Deutscher Apotheker GmbH, Eschborn, 2013; pp. 1–12 ISBN 978-3-7741-0044-2.
204. Stein, D.; Bindra, D.S. Stabilization of Hard Gelatin Capsule Shells Filled with Polyethylene Glycol Matrices. *Pharm. Dev. Technol.* **2007**, *12*, 71–77, doi:10.1080/10837450601166627.
205. Lloyd, W.G. Inhibition of Polyglycol Autoxidation. *J. Chem. Eng. Data* **1961**, *6*, 541–547, doi:10.1021/jc60011a019.
206. Gullapalli, R.P.; Mazzitelli, C.L. Polyethylene Glycols in Oral and Parenteral Formulations - A Critical Review. *Int. J. Pharm.* **2015**, *496*, 219–239, doi:10.1016/j.ijpharm.2015.11.015.
207. Persaud, S.; Eid, S.; Swiderski, N.; Serris, I.; Cho, H. Preparations of Rectal Suppositories Containing Artesunate. **2020**.
208. WHO INCHEM - Internationally Peer Reviewed Chemical Safety Information Available online: <https://incem.org/documents/jecfa/jecmono/v14je19.htm> (accessed on 30 November 2022).
209. Fisher, A.A. Immediate and Delayed Allergic Contact Reactions to Polyethylene Glycol. *Contact Dermatitis* **1978**, *4*, 135–138, doi:10.1111/J.1600-0536.1978.TB03759.X.
210. Yang, X.; Zhong, Z.; Huang, Y. The Effect of PEG Molecular Weights on the Thermal Stability and Dissolution Behaviors of Griseofulvin-PEG Crystalline Inclusion Complexes. *Int. J. Pharm.* **2016**, *508*, 51–60,

doi:10.1016/j.ijpharm.2016.05.014.

211. Vasa, D.M.; Dalal, N.; Katz, J.M.; Roopwani, R.; Nevrekar, A.; Patel, H.; Buckner, I.S.; Wildfong, P.L.D. Physical Characterization of Drug:Polymer Dispersion Behavior in Polyethylene Glycol 4000 Solid Dispersions Using a Suite of Complementary Analytical Techniques. *Pharm Sci* **2014**, *103*, 2911–2923, doi:10.1002/jps.24008.
212. Abd Ellah, N.H.; Shaltout, A.S.; Abd El Aziz, S.M.M.; Abbas, A.M.; Abd El Moneem, H.G.; Youness, E.M.; Arief, A.F.; Ali, M.F.; Abd El-hamid, B.N. Vaginal Suppositories of Cumin Seeds Essential Oil for Treatment of Vaginal Candidiasis: Formulation, in Vitro, in Vivo, and Clinical Evaluation. *Eur. J. Pharm. Sci.* **2021**, *157*, 105602, doi:10.1016/j.ejps.2020.105602.
213. Varona, S.; Kareth, S.; Martín, Á.; Cocero, M.J. Formulation of Lavandin Essential Oil with Biopolymers by PGSS for Application as Biocide in Ecological Agriculture. *J. Supercrit. Fluids* **2010**, *54*, 369–377, doi:10.1016/j.supflu.2010.05.019.
214. Werdin González, J.O.; Gutiérrez, M.M.; Ferrero, A.A.; Fernández Band, B. Essential Oils Nanoformulations for Stored-Product Pest Control - Characterization and Biological Properties. *Chemosphere* **2014**, *100*, 130–138, doi:10.1016/j.chemosphere.2013.11.056.
215. Kumar, P.; Sharma, U. PEG Supported Nano Formulations of Essential Oils for Agricultural Applications. *NVEO - Nat. Volatiles Essent. Oils J.* **2021**, *8*, 9367–9374.
216. Kumar, P.; Mishra, S.; Malik, A.; Satya, S. Preparation and Characterization of PEG-Mentha Oil Nanoparticles for Housefly Control. *Colloids Surfaces B Biointerfaces* **2014**, *116*, 707–713, doi:10.1016/j.colsurfb.2013.11.012.
217. Fernández, M.; Margarit, M.V.; Rodríguez, I.C.; Cerezo, A. Dissolution Kinetics of Piroxicam in Solid Dispersions with Polyethylene Glycol 4000. *Int. J. Pharm.* **1993**, *98*, 29–35, doi:10.1016/0378-5173(93)90037-G.
218. Margarit, M.V.; Rodríguez, I.C.; Cerezo, A. Physical Characteristics and Dissolution Kinetics of Solid Dispersions of Ketoprofen and Polyethylene Glycol 6000. *Int. J. Pharm.* **1994**, *108*, 101–107, doi:10.1016/0378-5173(94)90320-4.
219. Vélaz, I.; Sánchez, M.; Martín, C.; Martínez-Ohárriz, M.C. Effect of PEG 4000 on the Dissolution Rate of Naproxen. *Eur. J. Drug Metab. Pharmacokinet.* **1998**, *23*, 103–108, doi:10.1007/BF03189323/METRICS.
220. Mccarthy, C.A.; Ahern, R.J.; Dontireddy, R.; Ryan, K.B.; Crean, A.M. Mesoporous Silica Formulation Strategies for Drug Dissolution Enhancement A Review. *Expert Opin. Drug Deliv.* **2016**, *13*, 93–108, doi:10.1517/17425247.2016.1100165.
221. Trzeciak, K.; Chotera-Ouda, A.; Bak-Sypien, I.I.; Potrzebowski, M.J. Mesoporous Silica Particles as Drug Delivery Systems-The State of the Art in Loading Methods and the Recent Progress in Analytical Techniques for Monitoring These Processes. *Pharmaceutics* **2021**, *13*, 950, doi:10.3390/pharmaceutics13070950.
222. Meyer, J.; Oswald, M.; Deller, K. Granules Based on Pyrogenically Prepared Silicon Dioxide, Method for Their Preparation and Use Thereof 2006, 39.

223. Buyuktimkin, T.; Wurster, D.E. The Influence of the Adsorption of Metoclopramide on the Surface Ionization of Fumed Silica. *Int. J. Pharm.* **2015**, *478*, 164–171, doi:10.1016/j.ijpharm.2014.11.028.
224. Evionik Industries AG Aeroperl 300 Pharma - Technical Information.
225. Prasertsri, S.; Rattanasom, N. Fumed and Precipitated Silica Reinforced Natural Rubber Composites Prepared from Latex System: Mechanical and Dynamic Properties. *Polym. Test.* **2012**, *31*, 593–605, doi:10.1016/j.polymertesting.2012.03.003.
226. Sing, K.S.W. Reporting Physisorption Data for Gas/Solid Systems with Special Reference to the Determination of Surface Area and Porosity (Recommendations 1984). *Pure Appl. Chem.* **1985**, *57*, 603–619, doi:10.1351/pac198557040603.
227. Söpper, U. Development of Mucoadhesive Carrier Systems for Flavoring Agents and Cannabidiol, Eberhard Karls Universität Tübingen, 2022.
228. Seljak, K.B.; Kocbek, P.; Gašperlin, M. Mesoporous Silica Nanoparticles as Delivery Carriers: An Overview of Drug Loading Techniques. *J. Drug Deliv. Sci. Technol.* **2020**, *59*, 101906, doi:10.1016/j.jddst.2020.101906.
229. Chaudhari, S.; Gupte, A. Mesoporous Silica as a Carrier for Amorphous Solid Dispersion. *Br. J. Pharm. Res.* **2017**, *16*, 1–19, doi:10.9734/BJPR/2017/33553.
230. Spireas, S.S.; Jarowski, C.I.; Rohera, B.D. *Powdered Solution Technology: Principles and Mechanism*; 1992; Vol. 9;.
231. Hentzschel, C.M.; Sakmann, A.; Leopold, C.S. Suitability of Various Excipients as Carrier and Coating Materials for Liquisolid Compacts. *Drug Dev. Ind. Pharm.* **2011**, *37*, 1200–1207, doi:10.3109/03639045.2011.564184.
232. Adler, C.; Teleki, A.; Kuentz, M. Multifractal and Mechanical Analysis of Amorphous Solid Dispersions. *Int. J. Pharm.* **2017**, *523*, 91–101, doi:10.1016/j.ijpharm.2017.03.014.
233. Shah, D.S.; Jha, D.K.; Gurram, S.; Suñé-Pou, M.; Garcia-Montoya, E.; Amin, P.D. A New SeDeM-SLA Expert System for Screening of Solid Carriers for the Preparation of Solidified Liquids: A Case of Citronella Oil. *Powder Technol.* **2021**, *382*, 605–618, doi:10.1016/j.powtec.2021.01.019.
234. Choudhari, Y.; Reddy, U.; Monsuur, F.; Pauly, T.; Hofer, H.; McCarthy, W. Comparative Evaluation of Porous Silica Based Carriers for Lipids and Liquid Drug Formulations. *Gruyter Open Mater. Sci.* **2014**, *1*, 64–74, doi:10.2478/MESBI-2014-0004.
235. Albert, K.; Huang, X.; Hsu, H. Bio-Templated Silica Composites for next-Generation Biomedical Applications. *Adv. Colloid Interface Sci.* **2017**, *249*, 272–289, doi:10.1016/j.cis.2017.04.011.
236. Greenspan, L. Humidity Fixed Points of Binary Saturated Aqueous Solutions. *J. Res. Natl. Bur. Stand. Phys. Chem.* **1977**, *81A*, 89–96, doi:10.6028/jres.081A.011.
237. Lorenz, P.; Berger, M.; Bertrams, J.; Wende, K.; Wenzel, K.; Lindequist, U.; Meyer, U.; Stintzing, F.C. Natural Wax Constituents of a Supercritical Fluid CO₂ Extract from Quince (*Cydonia Oblonga* Mill.) Pomace. *Anal. Bioanal. Chem.* **2008**, *391*, 633–646, doi:10.1007/S00216-008-2000-5/FIGURES/8.

238. Council of Europe 2.5.12. Water: Semi-Micro Determination. In *European Pharmacopoeia 10.8*; EDQM: Strasbourg, France, 2022; pp. 171–172.
239. Thoma, K.; Simon, G.; Kräutle, T. Untersuchungen Zur Bestimmung Der Ölzahl von Vaselinen. Available online: https://dacnrf.pharmazeutische-zeitung.de/suche?searchword=Thoma%2C+K.%2C+Simon%2C+G.%2C+Kräutle%2C+T.%2C+Untersuchungen+zur+Bestimmung+der+Ölzahl+von+Vaseline n.+2.+Mitteilung%3A+Vorschlag+einer+Bestimmungsmethode+für+das+Deutsche+Arzneibuch%2C+Pharm.+Ind.+52+%281990%29+622+-+626.&init=1&suche_optionen=0 (accessed on 9 July 2022).
240. Gillespie, T. The Capillary Rise of a Liquid in a Vertical Strip of Filter Paper. *J. Colloid Sci.* **1959**, *14*, 123–130, doi:10.1016/0095-8522(59)90036-4.
241. Council of Europe Pharmaceutical Preparations. In *European Pharmacopoeia 10.8*; EDQM: Strasbourg, France, 2022; pp. 880–882 ISBN 978-3-7692-7515-5.
242. Council of Europe Capsules. In *European Pharmacopoeia 10.8*; EDQM: Strasbourg, France, 2022; pp. 906–907 ISBN 978-3-7692-7515-5.
243. Council of Europe 2.9.40 Uniformity of Dosage Units. In *European Pharmacopoeia 10.8*; EDQM: Strasbourg, France, 2022; pp. 398–400 ISBN 978-3-7692-7515-5.
244. Herebian, D.; Choi, J.-H.; Abd El-Aty, † A M; Shim, J.-H.; Spitteller, M. Metabolite Analysis in Curcuma Domestica Using Various GC-MS and LC-MS Separation and Detection Techniques. *Biomed. Chromatogr.* **2009**, *23*, 951–965, doi:10.1002/bmc.1207.
245. Jiang, H.; Somogyi, Á.; Jacobsen, N.E.; Timmermann, B.N.; Gang, D.R. Analysis of Curcuminoids by Positive and Negative Electrospray Ionization and Tandem Mass Spectrometry. *Rapid Commun. Mass Spectrom.* **2006**, *20*, 1001–1012, doi:10.1002/RCM.2401.
246. Cao, Y.; Xu, R.X.; Liu, Z. A High-Throughput Quantification Method of Curcuminoids and Curcumin Metabolites in Human Plasma via High-Performance Liquid Chromatography/Tandem Mass Spectrometry. *J. Chromatogr. B* **2014**, *949–950*, 70–78, doi:10.1016/J.JCHROMB.2013.12.039.
247. Gören, A.C.; Çikrikçi, S.; Çergel, M.; Bilsel, G. Rapid Quantitation of Curcumin in Turmeric via NMR and LC–Tandem Mass Spectrometry. *Food Chem.* **2009**, *113*, 1239–1242, doi:10.1016/J.FOODCHEM.2008.08.014.
248. Allen, F.; Greiner, R.; Wishart, D. Competitive Fragmentation Modeling of ESI-MS/MS Spectra for Putative Metabolite Identification. *Metabolomics* **2015**, *11*, 98–110, doi:10.1007/S11306-014-0676-4.
249. Matsumura, S.; Murata, K.; Zaima, N.; Yoshioka, Y.; Morimoto, M.; Kugo, H.; Yamamoto, A.; Moriyama, T.; Matsuda, H. Inhibitory Activities of Essential Oil Obtained from Turmeric and Its Constituents against β -Secretase. *Nat. Prod. Commun.* **2016**, *11*, 1785–1788, doi:10.1177/1934578X1601101203.
250. Iwamoto, K.; Matsumura, S.; Yoshioka, Y.; Yamamoto, A.; Makino, S.; Moriyama, T.; Zaima, N. Using Turmeric Oil as a Solvent Improves the Distribution of Sesamin-Sesamol in the Serum and Brain of Mice. *Lipids* **2019**, *54*, 311–320, doi:10.1002/LIPD.12147.
251. Chang, L.H.; Jong, T.T.; Huang, H.S.; Nien, Y.F.; Chang, C.M.J. Supercritical

- Carbon Dioxide Extraction of Turmeric Oil from *Curcuma Longa* Linn and Purification of Turmerones. *Sep. Purif. Technol.* **2006**, *47*, 119–125, doi:10.1016/j.seppur.2005.06.018.
252. Gopalan, B.; Goto, M.; Kodama, A.; Hirose, T. Supercritical Carbon Dioxide Extraction of Turmeric (*Curcuma Longa*). *J. Agric. Food Chem.* **2000**, *48*, 2189–2192, doi:10.1021/jf9908594.
 253. Galano, A.; Álvarez-Diduk, R.; Ramírez-Silva, M.T.; Alarcón-Ángeles, G.; Rojas-Hernández, A. Role of the Reacting Free Radicals on the Antioxidant Mechanism of Curcumin. *Chem. Phys.* **2009**, *363*, 13–23, doi:10.1016/j.chemphys.2009.07.003.
 254. Kharat, M.; Du, Z.; Zhang, G.; McClements, D.J. Physical and Chemical Stability of Curcumin in Aqueous Solutions and Emulsions: Impact of PH, Temperature, and Molecular Environment. *J. Agric. Food Chem.* **2016**, *65*, 1525–1532, doi:10.1021/acs.jafc.6b04815.
 255. Pandey, K.U.; Dalvi, S.V. Understanding Stability Relationships among Three Curcumin Polymorphs. *Adv. Powder Technol.* **2019**, *30*, 266–276, doi:10.1016/j.apt.2018.11.002.
 256. Litwinienko, G.; Ingold, K.U. Abnormal Solvent Effects on Hydrogen Atom Abstraction. 2. Resolution of the Curcumin Antioxidant Controversy. The Role of Sequential Proton Loss Electron Transfer. *J. Org. Chem.* **2004**, *69*, doi:10.1021/jo049254j.
 257. Gordon, O.N.; Schneider, C. Vanillin and Ferulic Acid: Not the Major Degradation Products of Curcumin. *Trends Mol. Med.* **2012**, *18*, 361–363, doi:10.1016/J.MOLMED.2012.04.011.
 258. Malasoni, R.; Naqvi, A.; Srivastava, A.; Pandey, R.R.; Singh, A.; Chaudhary, M.; Paliwal, S.K.; Dwivedi, A.K. An Improved HPLC Method for Simultaneous Estimation of Isocurcumenol, Ar-Turmerone and α,β -Turmerone in Hexane Soluble Fraction of *Curcuma Longa* and Its Formulations. *J. Biomater. Tissue Eng.* **2014**, *4*, 405–410, doi:10.1166/JBT.2014.1175.
 259. van 'T Hoff, J.H. L'équilibre Chimique Dans Les Systèmes Gazeux ou Dissous à l'état Dilué. *Recl. des Trav. Chim. des Pays-Bas* **1885**, *4*, 424–427, doi:10.1002/RECL.18850041207.
 260. Lv, R.; Zhang, X.; Xing, R.; Shi, W.; Zhao, H.; Li, W.; Jouyban, A.; Acree, W.E. Comprehensive Understanding on Solubility and Solvation Performance of Curcumin (Form I) in Aqueous Co-Solvent Blends. *J. Chem. Thermodyn.* **2022**, *167*, 106718, doi:10.1016/J.JCT.2021.106718.
 261. Jagannathan, R.; Abraham, P.M.; Poddar, P. Temperature-Dependent Spectroscopic Evidences of Curcumin in Aqueous Medium: A Mechanistic Study of Its Solubility and Stability. *J. Phys. Chem. B* **2012**, *116*, 14533–14540, doi:10.1021/JP3050516/SUPPL_FILE/JP3050516_SI_001.PDF.
 262. Chiwele, I.; Jones, B.E.; Podczek, F. The Shell Dissolution of Various Empty Hard Capsules. *Chem. Pharm. Bull.* **2000**, *48*, 951–956, doi:10.1248/cpb.48.951.
 263. van Dalen, G.; van Velzen, E.J.J.; Heussen, P.C.M.; Sovago, M.; van Malssen, K.F.; van Duynhoven, J.P.M. Raman Hyperspectral Imaging and Analysis of Fat Spreads. *J. Raman Spectrosc.* **2017**, *48*, 1075–1084, doi:10.1002/JRS.5171.

264. Vemula, V.R.; Lagishetty, V.; Lingala, S. Solubility Enhancement Techniques. *Int. J. Pharm. Sci. Rev. Res.* **2010**, *5*, 41–51.
265. Zhong, Z.; Guo, C.; Chen, L.; Xu, J.; Huang, Y. Co-Crystal Formation between Poly(Ethylene Glycol) and a Small Molecular Drug Griseofulvin. *Chem. Commun.* **2014**, *50*, 6375–6378, doi:10.1039/c4cc00159a.
266. Lonza Capsules & Health Ingredients What Is the Difference between Gelatin Capsules and Capsugel® Vcaps® Plus Capsules Related to Moisture and Storage Conditions? Available online: <https://www.capsugel.com/knowledge-center/vcapsplus-faq-moisture-and-storage-conditions> (accessed on 9 August 2022).
267. Wang, Z.; Ye, B.-N.; Zhang, Y.-T.; Xie, J.-X.; Li, W.-S.; Zhang, H.-T.; Liu, Y.; Feng, N.-P. Exploring the Potential of Mesoporous Silica as a Carrier for Puerarin: Characterization, Physical Stability, and In Vivo Pharmacokinetics. *Am. Assoc. Pharm. Sci. PharmSciTech* **2019**, *20*, doi:10.1208/s12249-019-1502-0.
268. Cadé, D.; Madit, N. Liquid Filling in Hard Gelatin Capsules - Preliminary Steps. *Bull. Tech. Gattefossé* **1996**, *89*, 15–20.
269. Hailu, S.A.; Bogner, R.H. Complex Effects of Drug/Silicate Ratio, Solid-State Equivalent PH, and Moisture on Chemical Stability of Amorphous Quinapril Hydrochloride Coground with Silicates. *J. Pharm. Sci.* **2012**, *100*, 1503–1515, doi:10.1002/jps.22387.
270. Mellaerts, R.; Roeffaers, M.B.J.; Houthoofd, K.; Van Speybroeck, M.; De Cremer, G.; Jammaer, J.A.G.; Van Den Mooter, G.; Augustijns, P.; Hofkens, J.; Martens, J.A. Molecular Organization of Hydrophobic Molecules and Co-Adsorbed Water in SBA-15 Ordered Mesoporous Silica Material. *Phys. Chem. Chem. Phys.* **2011**, *13*, 2706–2713, doi:10.1039/C0CP01640C.
271. McGinity, J.W.; Hill, J.A.; La Via, A.L. Influence of Peroxide Impurities in Polyethylene Glycols on Drug Stability. *J. Pharm. Sci.* **1975**, *64*, 356–357, doi:10.1002/jps.2600640243.
272. Mantzavinos, D.; Livingston, A.G.; Hellenbrand, R.; Metcalfe, I.S. Wet Air Oxidation of Polyethylene Glycols; Mechanisms, Intermediates and Implications for Integrated Chemical Biological Wastewater Treatment. *Chem. Eng. Sci.* **1996**, *51*, 4219–4235, doi:10.1016/0009-2509(96)00272-2.
273. Zuidam, N.J.; Velikov, K.P. The Development of Food Structures for the Encapsulation and Delivery of Bioactive Compounds. In *Handbook of Food Structure Development*; Spyropoulos, F., Lazidis, A., Norton, I., Eds.; Royal Society of Chemistry: Cambridge, 2020; pp. 259–283 ISBN 978-1-78801-216-4.
274. Kinnari, P.; Mäkilä, E.; Heikkilä, T.; Salonen, J.; Hirvonen, J.; Santos, H.A. Comparison of Mesoporous Silicon and Non-Ordered Mesoporous Silica Materials as Drug Carriers for Itraconazole. *Int. J. Pharm.* **2011**, *414*, 148–156, doi:10.1016/j.ijpharm.2011.05.021.
275. O'Reilly Beringhs, A.; Minatovicz, B.C.; Zhang, G.G.Z.; Chaudhuri, B.; Lu, X. Impact of Porous Excipients on the Manufacturability and Product Performance of Solid Self-Emulsifying Drug Delivery Systems. *Am. Assoc. Pharm. Sci. PharmSciTech* **2018**, *19*, 3298–3310, doi:10.1208/s12249-018-1178-x.
276. Turek, C.; Stintzing, F.C. Stability of Essential Oils: A Review. *Compr. Rev. Food*

- Sci. Food Saf.* **2013**, *12*, 40–53, doi:10.1111/1541-4337.12006.
277. Singh, G.; Kapoor, I.P.S.; Singh, P.; De Heluani, C.S.; De Lampasona, M.P.; Catalan, C.A.N. Comparative Study of Chemical Composition and Antioxidant Activity of Fresh and Dry Rhizomes of Turmeric (*Curcuma Longa* Linn.). *Food Chem. Toxicol.* **2010**, *48*, 1026–1031, doi:10.1016/j.fct.2010.01.015.
278. Ray, A.; Mohanty, S.; Jena, S.; Sahoo, A.; Acharya, L.; Chandra Panda, P.; Sial, P.; Duraisamy, P.; Nayak, S. Drying Methods Affects Physicochemical Characteristics, Essential Oil Yield and Volatile Composition of Turmeric (*Curcuma Longa* L.) Micropropagation of Zingiberaceous Plants View Project Turmeric Production in Odisha-It's Quality and Curcumin Content. *Vie. Artic. J. Appl. Res. Med. Aromat. Plants* **2021**, *26*, 100357, doi:10.1016/j.jarmap.2021.100357.
279. Schneider, C.; Gordon, O.N.; Edwards, R.L.; Luis, P.B. Degradation of Curcumin: From Mechanism to Biological Implications. *J. Agric. Food Chem.* **2015**, *63*, 7606–7614, doi:10.1021/acs.jafc.5b00244.
280. Han, S.; Kim, C.; Kwon, D. Thermal Degradation of Poly(Ethyleneglycol). *Polym. Degrad. Stab.* **1995**, *47*, 203–208, doi:10.1016/0141-3910(94)00109-L.
281. Staub, S.; Stobaugh, J. Quantification of Trace Levels of Active Oxygen in Pharmaceutical Excipients, University of Kansas, 2017.

6. APPENDIX

6.1. SUPERCRITICAL FLUID EXTRACTION ACCORDING TO EXPERIMENTAL DESIGN

Table 18 Results of all experiments of the experimental design according to 2.2.4.

Experiment	Pressure [bar]	Temperature [°C]	Yield [% in drug]	Curcumin [% in drug]	DMC [% in drug]	BDMC [% in drug]	ar-turmerone [% in drug]	α -turmerone [% in drug]	β -turmerone [% in drug]
1	75	35	2.417265	0.002044	0.00059	8.21E-05	0.637935	0.588113	0.707002
2	250	35	2.800337	0.017392	0.002592	0.000264	0.670031	0.674495	0.723597
3	425	35	2.878798	0.042305	0.008031	0.001136	0.660217	0.661386	0.703081
4	250	55	2.78069	0.028098	0.00456	0.000726	0.662264	0.645919	0.66605
5	125	55	2.796018	0.007667	0.001537	0.000229	0.687297	0.690653	0.74639
6	425	55	3.07078	0.071183	0.013168	0.001903	0.681323	0.687092	0.742684
7	425	75	3.25747	0.110534	0.00735	0.004168	0.687706	0.710135	0.735801
8	250	75	3.089204	0.048384	0.008629	0.001945	0.680561	0.701421	0.726409
9	150	75	2.953685	0.038539	0.020671	0.001243	0.683749	0.713557	0.746192
10	125	55	2.722008	0.004356	0.001026	0.00016	0.679335	0.681964	0.734027
11	425	35	2.969611	0.036418	0.007673	0.001085	0.695315	0.697389	0.748299
12	425	75	3.318505	0.176213	0.000002	0.003635	0.690706	0.712326	0.735966
13	250	35	2.818799	0.027968	0.005036	0.000786	0.679745	0.689764	0.750681
14	250	75	3.127157	0.04389	0.008594	0.00178	0.690131	0.721643	0.758902
15	425	55	3.173377	0.07339	0.015662	0.002651	0.703177	0.699834	0.749111
16	75	35	2.176826	0.008256	0.001858	0.000263	0.601221	0.55725	0.668831
17	150	75	2.940767	0.011753	0.003259	0.000581	0.653463	0.678608	0.70471
18	250	55	2.981798	0.025892	0.004486	0.00074	0.699888	0.705379	0.766028
19	425	35	2.786166	0.038615	0.007612	0.001524	0.648489	0.636285	0.659294
20	250	55	2.898227	0.030321	0.005491	0.001202	0.674327	0.663481	0.696668
21	250	35	2.82752	0.021716	0.004	0.000686	0.683022	0.690791	0.752513

22	250	75	3.094446	0.034879	0.006787	0.001799	0.671498	0.701924	0.737097
23	75	35	2.081753	0.009311	0.001445	0.000248	0.612422	0.579067	0.631229
24	150	75	3.091664	0.024613	0.006174	0.001282	0.685656	0.682481	0.690137
25	425	75	3.335776	0.109022	0.018898	0.003634	0.672872	0.698953	0.730622
26	425	55	3.020453	0.07702	0.015005	0.002427	0.660641	0.65725	0.697222
27	125	55	2.863854	0.014895	0.003696	0.000636	0.680142	0.685824	0.74581
28	250	55	3.111807	0.024758	0.004007	0.000626	0.739802	0.71204	0.732582
29	250	55	2.89733	0.025183	0.004612	0.000631	0.688007	0.689083	0.739548
30	250	55	3.075139	0.034322	0.006678	0.001069	0.720951	0.693354	0.710449
31	250	55	2.975207	0.027243	0.004745	0.000751	0.70349	0.692927	0.732656
32	250	55	2.945566	0.02825	0.00534	0.000942	0.697478	0.689135	0.731082
33	250	55	3.302627	0.033833	0.00637	0.001251	0.701836	0.705419	0.769639

6.2. COMPOSITIONS OF CAPSULE FORMULATIONS

Table 19 Composition of capsule formulations for stability study according to 0.

Matrix	Extract Concentration in %	Extract Concentration [mg per capsule]	Freeze-Dried Extract [g]	Matrix Material [g]
			For 30 capsules incl. overage of 4 capsules	
Witepsol S58B	16.1	71	2.845	14.835
Witepsol W45	21.2	93	3.742	13.938
PEG 4000	21.2	109	3.958	14.742
Aeroperl 300 Pharma	57.3	127	5.845	4.355